HDL-TR-1915
December 1980

Damage Characterization of Semiconductor Devices for the AN/TRC-145 EMP Study

by Bruno M. Kalab

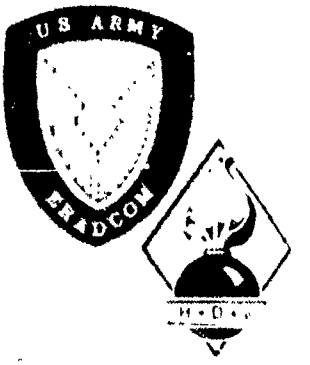

U.S. Army Electronics Research
and Development Command
Harry Diamond Laboratories
Adelphi, MD 20783

The findings in this report are not to be construed as an official Department of the Army position unless so designated by other authorized documents.

Citation of manufacturers' or trade names does not constitute an official indorsement or approval of the use thereof.

Destroy this report when it is no longer needed. Do not return it to the originator.

UNCLASSIFIED

SECURITY CLASSIFICATION OF THIS PAGE (When Data Entered)

14

REPORT DOCUMENTATION PAGE

READ INSTRUCTIONS BEFORE COMPLETING FORM

1. REPORT NUMBER	2. GOVT ACCESSION NO.	3. RECIPIENT'S CATALOG NUMBER
HDL-TR-1915	AD-A095021	9

4. TITLE (and Subtitle) — 6
Damage Characterization of Semiconductor Devices for the AN/TRC-145 EMP Study.

5. TYPE OF REPORT & PERIOD COVERED
Technical Report.

6. PERFORMING ORG. REPORT NUMBER

7. AUTHOR(s) — 10
Bruno M. Kalab

8. CONTRACT OR GRANT NUMBER(s)

9. PERFORMING ORGANIZATION NAME AND ADDRESS
Harry Diamond Laboratories
2800 Powder Mill Road
Adelphi, MD 20783

10. PROGRAM ELEMENT, PROJECT, TASK AREA & WORK UNIT NUMBERS
Prog. El.: 6.21.20.A

11. CONTROLLING OFFICE NAME AND ADDRESS — 11
U.S. Army Materiel Development and Readiness Command
Alexandria, VA 22333

12. REPORT DATE
December 1980

13. NUMBER OF PAGES
110

14. MONITORING AGENCY NAME & ADDRESS (if different from Controlling Office) — 12 110

15. SECURITY CLASS. (of this report)
UNCLASSIFIED

15a. DECLASSIFICATION/DOWNGRADING SCHEDULE

16. DISTRIBUTION STATEMENT (of this Report)
Approved for public release; distribution unlimited.

17. DISTRIBUTION STATEMENT (of the abstract entered in Block 20, if different from Report)

18. SUPPLEMENTARY NOTES
HDL Project: X758E0
DRCMS Code: 8-612120.H250011
DA: 1L162120AH25 02 — 10 — 11 12

19. KEY WORDS (Continue on reverse side if necessary and identify by block number)
Nuclear survivability
EMP analysis
Pulse damage to semiconductor devices
Second breakdown
AN/TRC-145

20. ABSTRACT (Continue on reverse side if necessary and identify by block number)
Seventeen types of diodes and 22 types of transistors of the AN/TRC-145 radio terminal set were damage tested, and the damage characteristics of the devices are provided. Damage testing consisted of stepstressing of individual junctions of the devices with voltage square pulses of 0.1- to 10-μs widths, both forward and reverse biasing the junctions. The damage characteristics consist of (1) the pulse power for failure or second breakdown as a function of pulse width, and (2) the pulse voltage and device

DD FORM 1 JAN 73 1473, EDITION OF 1 NOV 65 IS OBSOLETE

UNCLASSIFIED

SECURITY CLASSIFICATION OF THIS PAGE (When Data Entered)

16305

20. Abstract (Cont'd)

impedance at the failure threshold. The pulse power for failure data are least-square fitted to theoretical relationships between failure power and pulse width. The damage constants of the thermal failure model are then obtained. Comparisons are made between experimental device failure powers and the failure powers predicted by theoretical models. Anomalous responses of low-voltage bipolar transistors are discussed. The introductory sections of the report also contain a condensed review of the state of the practical knowledge of discrete junction device failure from voltage transients.

FOREWORD

This work was part of the electromagnetic pulse (EMP) vulnerability assessment of the AN/TRC-145 radio terminal set, conducted under the Multiple Systems Evaluation Program at the Harry Diamond Laboratories (HDL). The device damage characterization contributed to the vulnerability study of the AN/TRC-145 in two ways: (1) it provided electrical characteristics of critical devices in system critical circuits, so that these devices could be modeled in the DAMTRAC circuit-analysis code, and (2) it provided a failure criterion of the device types, so that system vulnerability could be determined.

The device testing from which this damage characterization resulted was performed by Asa Williams, whose effectiveness and dedication made it possible to provide this information in a fraction of the time previously expended on a comparable task. Mr. Williams, together with Loren Dillingham, also provided the computer calculations of the damage constants. Charles Ruzik calculated the device damage constants based on the junction capacitance model.

Device damage testing and associated data reduction for the system study were begun in September 1974 and completed in November 1975. In condensed form, the device damage characterizations are contained in George Gornak et al, EMP Assessment for Army Tactical Communications Systems: Transmission Systems Series No. 1, Radio Terminal Set AN/TRC-145 (U), HDL-TR-1746, February 1976 (SECRET RESTRICTED DATA). However, because of the continuing effort to improve present methods of predicting failure of semiconductor devices in circuits, a more extensive discussion and an analysis of the device responses observed in damage testing are provided here and made accessible, in an unclassified document, to a wider audience. The manuscript for this report was completed in October 1977.

The author would like to thank the technical reviewers of this report, especially for suggestions concerning the presentation of data.

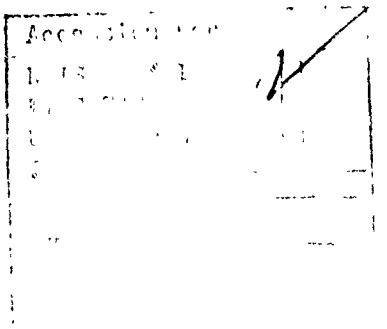

CONTENTS

FIGURES

TABLES

1. INTRODUCTION

For very short periods of time, such as the duration of an electromagnetic pulse (EMP) induced signal, electronic network components can withstand voltage and current levels and can safely dissipate powers that are significantly larger than the ratings for voltage, current, and power for continuous operation. In nuclear weapons effects analyses, it is important to know exactly what transient signal level a component can withstand without degradation in performance. Unfortunately, there is no obvious relationship between those transient threshold signals that cause a component to fail and the design of the component (for instance, as reflected in the ratings and characteristics provided by manufacturers for circuit design purposes).

To obtain information on the threshold signal for failure, components are stepstressed with voltage pulses. This method, which was used in the work reported here, is extensively described in the literature.[1] Efforts have been made also to predict the damage thresholds of semiconductor junction devices (considered to be the circuit components most susceptible to failure from electrical transients) on the basis of theoretical failure models.[2,3] In these theories, plausible assumptions were made about the failure mechanism (heating of the semiconductor material to a certain temperature) and formulated analytically. As a result, these thermal models suggest a defined pulse power for failure which depends on pulse width and certain device characteristics such as junction area[2] or the volume of a defect region;[3] however, these characteristics of a device are not directly measurable. Subsequently, a link was recognized between the junction area and device characteristics which are obtainable from nondestructive terminal measurements and which may even be provided by the device manufacturer (such as junction capacitance). This link, then, led to expressions of the pulse power for failure in terms of these characteristics.[4,5]

---

[1] *B. Kalab, Analysis of Failure of Electronic Circuits from EMP-Induced Signals--Review and Contribution, Harry Diamond Laboratories, HDL-TR-1615 (August 1973).*

[2] *D. C. Wunsch and R. R. Bell, Determination of Threshold Failure Levels of Semiconductor Diodes and Transistors Due to Pulse Voltages, IEEE Trans. Nucl. Sci., NS-15 (December 1968), 244-259.*

[3] *D. M. Tasca, Pulsed Power Failure Modes in Semiconductors, IEEE Trans. Nucl. Sci., NS-17 (December 1968), 364-372.*

[4] *D. C. Wunsch, R. L. Cline, and G. R. Case, Theoretical Estimates of Failure Levels of Selected Semiconductor Diodes and Transistors, Braddock, Dunn and McDonald, Inc., for Air Force Special Weapons Center, BDM/A-42-69-R (December 1969).*

[5] *DNA EMP (Electromagnetic Pulse) Handbook, Defense Nuclear Agency 2114H-2 (September 1975).*

This way of finding the power for failure has been available since 1969, but it is not extensively used in weapons effects analyses. To meet the requirement for system survivability without excessive and therefore costly hardening, we should know component damage levels with a degree of accuracy that is not achievable with this method, as comparisons with experimental results show. (However, in preliminary screening, where accuracy requirements can be relaxed, device damage information based on this method may be sufficient.) Besides predicting the power for failure with only modest accuracy, the thermal failure models do not furnish the device impedance near the failure level, which is also essential to circuit failure analysis. Damage testing readily discloses this impedance. However, experiments have shown[6] that device damage testing as it is done now (that is, stepstressing with either forward- or reverse-biasing pulses) does not furnish a complete characterization of the susceptibility of a device to damage from EMP-induced transients. These experiments also revealed previously unsuspected basic limitations of the range of applicability of the thermal failure models. Still, stepstressing with unipolar pulses is the state-of-the-art technique for obtaining component damage characterizations in most systems studies presently conducted.

Theoretical as well as experimental development work continues[7-9,*] whose goals are to clarify the failure mechanisms in semiconductor devices and to identify the device parameters or the experimental procedures that can lead to a complete quantitative description of the pulse hardness of a device. To such efforts, detailed information on device responses observed in damage testing should be useful and is therefore provided in this report.

During the testing effort reported here, device responses were observed which are difficult to interpret in terms of the thermal failure model. A further purpose of this report is to discuss these responses, as they will be a subject of continued research at the Harry Diamond Laboratories (HDL) and may also be of interest to the community. Nevertheless, in support of present systems analyses, the results of this testing effort are also reported in conventional terms; that is, all failure thresholds are least-square fitted to the functional relationships between power for failure and pulse width as

---

[6] *B. Kalab, Second Breakdown and Damage in 1N4148 from Oscillating Electrical Transients, IEEE Trans. Nucl. Sci., NS-22 (August 1975), 2006-2009.*

[7] *R. H. Dickhaut, Electromagnetic Pulse Damage to Bipolar Devices, IEEE Circuits and Systems, 10 (April 1976), 8-21.*

[8] *A. L. Ward, An Electro-thermal Model of Second Breakdown, IEEE Trans. Nucl. Sci., NS-23 (December 1976), 1679-1684.*

[9] *A. L. Ward, Studies of Second Breakdown in Silicon Diodes, IEEE Trans. Parts, Hybrids, and Packaging, PHP-13 (December 1977), 361-368.*

** A. Mathews, U.S. Army Missile Command, Redstone Arsenal, AL, private communication.*

they result from the thermal failure model, and "damage constants" are derived from these regression analyses. In these terms, device damage characteristics are being collected in data bases.[10,11] The device damage information reported here (especially the tables of app A) may also augment the data base from which engineering models of device pulse damage are being developed.[12] These engineering models are mathematical expressions (resulting from regression analyses of experimental damage data) of the power or current for failure and the device impedance in terms of pulse width and general electrical device parameters. An advantage of this kind of modeling is that the regression equations can be developed independent of any conjecture about the failure mechanism.

Section 2 explains how the damage characteristics were obtained, reduced, and operated on (such as by regression analysis). Section 3 discusses anomalous device responses which are considered significant enough to warrant further investigation. Section 4 describes the AN/TRC-145 devices selected for damage testing, summarizes the damage test results, and compares experimental failure powers (or damage constants) with failure powers (or damage constants) predicted by theoretical models (tables 6 and 7). Appendix A gives the detailed test results (such as powers for failure and impedance at the failure level of the individual test specimens) and the plots of failure power versus pulse width.

2. TEST PROCEDURE AND DEVICE CHARACTERIZATION

2.1 Background and Definitions

Damage testing by stepstressing is the state-of-the-art procedure for obtaining information on the pulse-handling capability of semiconductor junction devices. This method was used for the damage characterization of the AN/TRC-145 devices reported here. The procedure consists of applying a series of voltage pulses of a certain waveform to the device terminals and increasing the voltage from pulse to pulse by a certain amount. The pulses are produced by a high-power pulse generator with single-shot capability. At each pulse application, the oscilloscope traces of both the voltage across the device and the current through the device are recorded. Before the first pulse is applied,

[10] *J. L. Cooke et al, Users Manual for SUPERSAP2, Boeing Aerospace Co., Seattle, WA, and BDM Corp., Air Force Weapons Laboratory, AFWL-TR-75-70 (March 1976).*

[11] *T. V. Noon, Implementation of the Device Data Bank on the HDL IBM Computer, Harry Diamond Laboratories, HDL-TR-1819 (October 1977).*

[12] *D. M. Tasca and S. J. Stokes, III, EMP Response and Damage Modeling of Diodes, Junction Field Effect Transistor Damage Testing and Semiconductor Device Failure Analysis, General Electric Co., for Harry Diamond Laboratories, HDL-CR-76-090-1 (April 1976).*

certain electrical characteristics of the test specimen are measured; these are remeasured after each pulse of the series to detect degradation. It is then possible to relate the characteristics of the applied pulse to the degree of device degradation which results. According to the thermal failure model, only the duration and the average power of the applied pulse are of interest, but, in principle, other pulse characteristics (such as peak values of voltage or current) also may be considered. This method and related questions are discussed in more detail by Kalab.[1]

Where the assumptions of the thermal failure model apply, the waveform of the pulses used in damage testing should not be critical. For thermal systems such as are assumed in the thermal failure model of junction devices, the temperature rise due to heat production at an arbitrary rate (complex waveform), P(t), can be expressed as the superposition integral of P(t) and the temperature rise of the system due to heat production at a constant rate (the step or square-pulse response of the system). This principle (Duhamel's theorem) can be applied to predicting the power for failure of a junction device from, say, a triangular pulse, on the basis of the measured power for failure from a square pulse of the same duration.

An application of this principle (using 1N4148 diodes) showed[13] that the failure powers for these widely differing waveforms (in either forward or reverse biasing of the junction) differ by about a factor of two over a wide range of pulse widths. This difference was found to be in fair agreement with measurements of the failure power (of the 1N4148) from triangular pulses.[13] Such a variation of the failure power due to differing unipolar waveforms is much smaller than the variations usually observed in damage testing of a sample of devices with the same waveform (square pulse) and pulse width and attributed to physical differences between the specimens of the sample. Therefore, we can ignore the effect that the waveform of a unipolar pulse has on the mean power for failure or for second breakdown of a sample of devices. However, in spite of this result, we should not lightly dismiss the question of what pulse waveform is to be used in damage testing to insure that the resulting device damage characterization is relevant to EMP effects analyses. The thermal failure model is, after all, only a conjecture; as will be discussed, significant waveform effects, unpredicted by this model, have been observed in diodes subjected to an oscillating electrical transient.

---

[1] *B. Kalab, Analysis of Failure of Electronic Circuits from EMP-Induced Signals--Review and Contribution, Harry Diamond Laboratories, HDL-TR-1615, (August 1973).*

[13] *D. M. Tasca et al, Theoretical and Experimental Studies of Semiconductor Device Degradation Due to High Power Electrical Transients, General Electric Co., 73SD4289 (December 1973).*

It is widely recognized now[5] that many types of discrete semiconductor junction devices do not obey the thermal model. More severely, it has yet to be demonstrated that there are indeed devices whose mechanism for failure or second breakdown from short-duration, reverse-biasing electrical transients is as postulated by this model. The thermal failure model was considered proven, and its applicability to predicting failure or second breakdown in a junction device established, when damage testing with reverse-biasing square pulses showed that the power for failure or second breakdown, P, varied with pulse width, t, over some range of t (see sect. 2.2.4) according to $P = kt^{-1/2}$. This is the relationship between P and t which follows from the thermal failure model for this excitation. However, in all the damage testing done to date, such a dependence of P on t rarely emerged unambiguously. Wunsch and Marzitelli,[14] Singletary et al,[15] and many others, as well as the data in this report, give examples of what is generally observed in damage testing. The best that can be said is that the power for failure or second breakdown of most of the devices tested to date may or may not vary according to $P = kt^{-1/2}$ (the exponent of t is not at all critical in this context). The reasons commonly given for a lack of agreement with $P = kt^{-1/2}$ are small sample size and a considerable variation of failure power between the individual specimens of a sample (which, in turn, is attributed to manufacturing inhomogeneities of one kind or another). Indeed, these factors can contribute to a generally poor conformance of experimental failure powers to $P = kt^{-1/2}$, but they are not necessarily the only reasons for such discrepancies. (Besides, the variation of junction area in a population of planar devices of a given design can only be very small.)

However, even if damage testing of any device type with unipolar square pulses showed a close dependence according to $P = kt^{-1/2}$, this would not prove the validity of the thermal failure model for that device. A very small number of device types have been damage tested with reverse-biasing square pulses under conditions (as regards sample size, uniformity of devices, and other factors) that were more rigorous than usually observed in routine damage testing. In one of these types, the 1N4148, the pre-second-breakdown power varied over a

---

[5] *DNA EMP (Electromagnetic Pulse) Handbook, Defense Nuclear Agency 2114H-2 (September 1975).*

[14] *D. C. Wunsch and L. Marzitelli, BDM Final Report, 1, Semiconductor and Nonsemiconductor Damage Study, Braddock, Dunn and McDonald, Inc., for U.S. Army Mobility Equipment Research and Development Center, BDM-375-69-F-0168 (April 1969).*

[15] *J. B. Singletary, W. O. Collier, and J. A. Myers, Experimental Threshold Failure Levels of Selected Diodes and Transistors, II, Braddock, Dunn and McDonald, Inc. for Air Force Weapons Laboratory, AFWL-TR-73-119 (July 1973).*

certain range of t very closely[16] according to $P = kt^{-1/2}$, and this diode is considered an excellent example[12] of a device whose failure mechanism is as postulated in the thermal failure model. Yet, when this device had been subjected to a full-cycle square pulse, providing a forward bias before the reverse-biasing half cycle, the device response was very different from that the thermal failure model would predict for this excitation.[6,17] (The application of Duhamel's theorem to this excitation fails completely to yield the observed response.) In other words, a variation of the power for failure from square-pulse excitation according to $P = kt^{-1/2}$ is only one of several aspects of a device response predicted by the thermal failure model, and all these aspects, not just $P = kt^{-1/2}$, must be observable if the model applies.

Furthermore, there are reports[18,19] on significant variations of the pre-second-breakdown power of certain types of junction devices with the rise time of the excitation; on the basis of the thermal failure model, pulse rise time should not be critical. Other "anomalous" responses (relative to the predictions of the thermal failure model) of diodes and transistor junctions of low breakdown voltage are discussed in section 3. The manner in which details of the transient excitation affect second breakdown and reverse failure in junction devices is far from understood.

For practical reasons (ease of generation, measurement of pulse duration, and data reduction), square pulses of voltage have come to be used in routine damage testing. Efforts are usually made (such as

---

[6] *B. Kalab, Second Breakdown and Damage in 1N4148 from Oscillating Electrical Transients, IEEE Trans. Nucl. Sci., NS-22 (August 1975), 2006-2009.*

[12] *D. M. Tasca and S. J. Stokes, III, EMP Response and Damage Modeling of Diodes, Junction Field Effect Transistor Damage Testing and Semiconductor Device Failure Analysis, General Electric Co., for Harry Diamond Laboratories, HDL-CR-76-090-1 (April 1976).*

[16] *D. M. Tasca and J. C. Peden, Feasibility Study of Developing a Nondestructive Screening Procedure for Thermal Second Breakdown, General Electric Co. (July 1971).*

[17] *B. Kalab, On the Necessary and Sufficient Conditions (Thresholds) for Damage of Semiconductor Junctions from Electrical Transients, Proc. Joint EMP Technical Meeting, First Annual Nuclear EMP Meeting, Albuquerque, NM, V, Hardening Technology (September 1973), 249-260.*

[18] *K. Hübner et al, Uniform Turn-on in Four-Layer Diodes, IEEE Trans. Electron Devices, ED-8 (November 1964), 1372-1373.*

[19] *T. Agatsuma et al, An Aspect of Second Breakdown in Transistors, Proc. IEEE (Correspondence), 52 (November 1961), 461-464.*

through current limitation by a series resistor) to prevent large variations of current during the pulse. It is then possible to determine the pulse power averaged over pulse width, with acceptable accuracy, from the average values of voltage and current; these, in turn, can be found by transformation of the area under the curve into rectangles. In addition, if the pulse shape is nearly rectangular, this area transformation can often be estimated with acceptable accuracy, usually with the aid of a mechanical device such as a caliper. (Before the introduction of digital techniques in 1971,[1] all device damage data taken in the wider EMP community were reduced in this manner.) In practice, the varying impedance exibited by the specimen during pulsing is a major limitation to achieving square pulses of both voltage and current at longer pulse widths (1 to 10 μs). At pulse widths below about 0.2 μs, the device waveforms deviate even more from a square pulse, because of the rather large rise and fall times of the output of typical hard-tube pulsers.

The thermal failure model suggests that the threshold for failure from electrical pulses should be expressed in terms of pulse power. This is acceptable, irrespective of any failure model, if increasing degradation of an electrical device characteristic requires the application of pulses of increasing average power. In forward stepstressing of semiconductor junctions, such a relationship is indeed generally observed (at constant pulse width).

It is necessary to arbitrarily define the degree of degradation to be called failure. Then the threshold power for failure can be said to lie between the powers of two consecutive pulses, one causing degradation before the point of failure (or no degradation at all) and the other causing degradation beyond the point of failure. The arithmetic mean of the two pulse powers is usually taken to be the threshold for failure, although a more elaborate method of interpolation can be considered. If a pulse degrades a device exactly to the point of failure, the power of that pulse is equal to the failure threshold. These definitions also tell how the failure threshold can be determined practically. The error associated with the threshold power for failure depends largely on the increase in pulse power from one pulse to the next (step size).

Although the threshold power for failure depends on how failure is defined, in most situations this dependence is of little practical concern. When the point of beginning degradation is reached, most junctions tested required only a small increase in pulse power for degradation beyond the point of failure, no matter how it was defined (within a reasonable range). However, exceptions have been observed.

---

[1] *B. Kalab, Analysis of Failure of Electronic Circuits from EMP-Induced Signals--Review and Contribution, Harry Diamond Laboratories, HDL-TR-1615 (August 1973).*

In routine damage testing of devices, in either forward or reverse bias, it has been observed that the current gain of a few types of devices, mostly of germanium, begins to be affected at a pulse power substantially lower (up to two orders of magnitude) than the power that caused failure by the commonly used definition. Such an initial effect on the current gain is usually slight and may even be an increase of h_{FE}. We cannot rule out the possibility that this effect on the current gain is associated with a much larger change (deterioration) in other electrical characteristics that are not measured in routine damage testing, such as the noise performance of microwave devices. Therefore, when defining failure and determining the threshold power for pulse failure, we should take into account the specific function of a device in a system.

In reverse pulsing of junctions, second breakdown may or may not occur before junction failure. Low-voltage Zener diodes rarely exhibit second breakdown, and a threshold for reverse failure for devices like these can be defined as previously for forward pulsing. If second breakdown occurs, the definition of a threshold for failure in terms of pulse power can encounter a conceptual difficulty.[17] (Briefly, it can happen that the power of a pulse that does not trigger second breakdown and does not degrade a specimen is higher than that of a subsequent pulse that does cause second breakdown and degradation; it does not appear that cumulative effects are involved.) To avoid such a difficulty, and also for easier data reduction, the following rule appears to have been widely adopted.[20,21]

> When, before device failure, second breakdown occurs for the first time during stepstressing, the averaged pre-second-breakdown power is taken to be the failure threshold at a pulse width equal to the delay time. This holds regardless of whether or not the device is degraded after application of the pulse that caused second breakdown and regardless of whether or not multiple breakdown occurs. (For a review of multiple breakdown in single junctions, see Kalab,[1] p 53.)

---

[1] *B. Kalab, Analysis of Failure of Electronic Circuits from EMP-Induced Signals--Review and Contribution, Harry Diamond Laboratories, HDL-TR-1615 (August 1973).*

[17] *B. Kalab, On the Necessary and Sufficient Conditions (Thresholds) for Damage of Semiconductor Junctions from Electrical Transients, Proc. Joint EMP Technical Meeting, First Annual Nuclear EMP Meeting, Albuquerque, NM, V, Hardening Technology (September 1973), 249-260.*

[20] *L. W. Ricketts, J. E. Bridges, and J. Miletta, EMP Radiation and Protective Techniques, John Wiley & Sons, Inc., New York (1976).*

[21] *J. R. Miletta, Component Damage from Electromagnetic Pulse (EMP) Induced Transients, Harry Diamond Laboratories, HDL-TM-77-22 (November 1977).*

This rule is based on the assumption that, as soon as a junction enters second breakdown, any additional energy that may be required to cause failure will be small compared to the pre-second-breakdown energy.[20,21] Many observations made in routine damage testing of devices support this assumption. However, damage testing of quite common devices (low-voltage, bipolar transistors) at short pulse widths has shown that this rule can lead to a value of the damage threshold that is up to an order of magnitude smaller than the pulse power necessary and sufficient for device failure. Situations of this kind were observed in the present testing effort (sect. 3).

Besides a measure (such as pulse power) of the condition for failure, a circuit model of a semiconductor device is needed for carrying out a circuit failure analysis. This circuit model must be able to represent the device especially for excitations approaching the threshold signals for damage. An important element of such a circuit model will be the resistance of the device where electrical energy is converted to heat. In present circuit models,[22] this resistance appears in the form of the so-called surge impedance, which is derived from the impedance that the device exhibits when pulsed with the threshold pulse for failure or second breakdown. The device impedance is the quotient of average voltage across the device over average current through the device; the averages are taken either over the entire pulse width or over the time to failure or second breakdown, whenever such a time can be identified. When the threshold of device failure must be determined from two consecutive pulses, the device voltage, current, and impedance (as well as power) at the threshold for failure are usually taken to be the arithmetic means of the respective magnitudes of the consecutive pulses. As for pulse power as the sole criterion for device failure, the device impedance (or the surge impedance derived from it) is only a first approximation of a device circuit model for EMP analysis. The applicability of this device damage characterization (by threshold power for failure and surge impedance) is a separate topic in itself.

2.2 Procedure

2.2.1 General

The damage characterizations (power for failure versus pulse width, device impedance) of the AN/TRC-145 semiconductor devices were obtained by stepstressing with unipolar pulses. A hard-tube pulser

[20] *L. W. Ricketts, J. E. Bridges, and J. Miletta, EMP Radiation and Protective Techniques, John Wiley & Sons, Inc., New York (1976).*

[21] *J. R. Miletta, Component Damage from Electromagnetic Pulse (EMP) Induced Transients, Harry Diamond Laboratories, HDL-TM-77-22 (November 1977).*

[22] *G. H. Baker et al, Damage Analysis Modified TRAC Computer Program (DAMTRAC), Harry Diamond Laboratories, HDL-TM-75-6 (May 1975).*

provided a maximum power output of 20 kW at impedance levels ranging from 0.2 to 2000 ohms. Whenever possible, the pulser (plug-in output transformer) was terminated with its internal impedance for optimum output waveform (square pulse with little undershoot or overshoot), and a resistor was put in series with the test specimen for current limitation. However, these techniques significantly reduced the power available to the test specimen and were avoided when the full power of the pulser was needed to reach the damage level of a device. The rise and fall times of the voltage pulses across a specimen varied from about 20 to 150 ns, depending on pulser impedance and pulse width (type of output transformer). The voltage and the associated current waveform of the pulse applied to the test specimen were measured with a dual-beam oscilloscope and photographically recorded.

Testing of a device was begun at the longest pulse width (10 μs). The responses of the junctions were routinely obtained in both reverse and forward pulsing. A type of junction which did not fail in forward pulsing at a 10-μs pulse width and the full output power of the pulser (no additional termination or series resistor) did not have to be tested at a shorter pulse width, because forward failure levels are not expected to be lower at shorter pulse widths. The nominal pulse widths used were 10, 1.0, and 0.1 μs; if it appeared that the maximum available power at 0.1 μs was slightly too low for failure, the pulse width was increased up to 0.3 μs so that damage information could still be obtained in that range of pulse width. In reverse pulsing of junctions, second breakdown could occur at any time (delay time) during the pulse. Both the emitter-base (E-B) and collector-base (C-B) junctions of junction transistors were tested with the third terminal open; of the field effect transistor (2N4092), the gate-source (G-S) junction and the drain-source (D-S) section were pulsed with the third terminal open.

In stepstressing, the open-circuit pulse voltage was increased from one pulse to the next by about 15 percent. The associated increase in power dissipated in the device (step size) depended on the voltage-current characteristics of the device, as well as on the impedances of the pulser and the external circuit; this increase was found to be typically 30 percent. (It rarely exceeded 50 percent.)

For the EMP analysis of the AN/TRC-145, damage characterizations of 17 types of diodes and 22 types of transistors were required by the system analysts. Approximately 1100 devices were damage tested in this effort. On the average, only three devices could be tested in any combination of pulse width, junction, and pulse polarity.

2.2.2 Failure Criterion

In the present damage testing program, failure of a diode was defined to be a reduction of the breakdown voltage (voltage at 10-μA reverse current) to 50 percent or less of the original value. For transistors, failure was defined to be a reduction of the dc current gain (at a chosen operating point) to 50 percent or less of the original value. These definitions applied if no second breakdown occurred. If second breakdown did occur the device was considered to have failed regardless of whether or not a degradation was associated with the second breakdown (sect. 2.1).

A definition of diode failure in terms of a 50-percent reduction of the junction breakdown voltage may not be appropriate for special-purpose diodes in critical applications. One could, for instance, be concerned about the deterioration of the noise characteristics of microwave diodes due to electrical overstress. It is conceivable that such deterioration occurs long before there are significant changes in breakdown voltage and before second breakdown. As far as transistors are concerned, it is not advisable to define failure in terms of the breakdown voltage of the junction being stepstressed. It was observed that the E-B junction can fail during stepstressing of the C-B junction at power levels that do not affect the breakdown voltage of the C-B junction.

2.2.3 Data Reduction

The information that we wished to obtain from the test photographs is the following: (1) time to failure or second breakdown, (2) pulse power averaged over the time to failure or second breakdown, and (3) average impedance of the device at the failure level. Section 2.1 discusses how these magnitudes can be defined and determined in the various situations that present themselves in damage testing of semiconductor junction devices. In particular, where the threshold power for junction failure must be determined through interpolation of the powers of two consecutive pulses, the arithmetic mean of these powers was taken to be the failure threshold. Furthermore, if the first pulse that caused any measurable device degradation at all reduced the junction breakdown voltage or current gain to a value between 1.2 and 0.8 F (F being the failure criterion for the specimen as defined in sect. 2.2.2), the power of that pulse was taken to be the power for failure (failure threshold). Also, the rule given in section 2.1 was always followed.

The numerical values of pulse power and device impedance were not determined with any great accuracy. The average pulse power, $1/t \int iv\ dt$ (i and v are the instantaneous current and voltage, respectively), was approximated by the product of average current times average voltage. In the case of ideal square pulses of voltage and

current, this product is identical to the average power; in general, however, it is not. The average values of voltage and current were obtained as discussed in section 2.1, that is, by approximate transformation of the area under the curve. No elaborate error analysis of the power or impedance data obtained in this effort was performed. Previous experience (in which the scope traces were digitized and the average power was computed[1]) suggests that, if the procedure discussed above is performed by skilled personnel, the error of power and impedance is typically between ±30 and ±50 percent, the smaller error being associated with the 10-μs data. For applications in present systems analyses, this accuracy of the failure power or the impedance at the failure level of an individual test specimen is considered adequate. There are significant variations of these values over a sample of devices, due to various kinds of physical differences among specimens, which must be taken into account in applications (sect. 2.2.4) and do not justify obtaining measurements of increased accuracy on individual specimens.

2.2.4 Least-Square Fitting

In applications of experimental device damage data obtained at selected pulse widths to EMP systems studies, extrapolation or interpolation of these data to other pulse widths is usually required. Also, the generally large scatter of failure powers requires the determination of a mean (nominal) value for applications to systems studies. To obtain such a mean value for any pulse width, it has become the custom to least-square fit the experimental failure powers (or pre-second-breakdown powers) to relationships between failure power (P) and pulse width (t) resulting from the thermal failure model. These relationships are the following.[23,24]

Forward pulsing	$P = k_1 t^{-1}$	$0 < t < t_1$	(1)
Reverse pulsing	$P = k_2 t^{-1}$	$0 < t \leq t_2$	(2)
	$P = k_3 t^{-1/2}$	$t_2 < t < t_3$	(3)

The constants k_i (i = 1, 2, 3) involve the material and geometry of the device. In particular, in equations (2) and (3) the geometry appears as junction area, A, and k_2 and k_3 contain A as a factor. The constant k_3 is commonly called the damage constant or Wunsch constant.

[1] *B. Kalab, Analysis of Failure of Electronic Circuits from EMP-Induced Signals--Review and Contribution, Harry Diamond Laboratories, HDL-TR-1615 (August 1973).*

[23] *D. C. Wunsch, Semiconductor Device Damage in an EMP Environment, Proc. Conference on Component Degradation from Transient Inputs, U.S. Army Mobility Equipment Research and Development Center, Ft. Belvoir, VA (April 1970), 6-50.*

[24] *J. B. Singletary and D. C. Wunsch, Final Summary Report on Semiconductor Damage Study, Phase II, Braddock, Dunn and McDonald, Inc., BDM/A-84-70-TR (February 1971).*

As indicated, these relationships are not expected to hold for all pulse widths. Although equation (3) was originally believed[2] to apply over a range of five orders of magnitude of t, there is good indication that the range in which it might apply is considerably smaller. For instance, the graphic representations of experimental failure power versus pulse width ("damage plots") of appendix A show that for quite a few types of junctions the power for reverse failure, extrapolated to pulse widths greater than approximately 20 μs, would be higher than that for forward failure, if equations (1) and (3) would still apply in this range of pulse widths. Such a behavior would be incompatible with the assumptions of the thermal failure model. On theoretical grounds, it would be plausible to assume that t_1 and t_3 are of the order of the thermal time constant of a device. For t_2 (the lower limit of the range for eq (3)), it has not been possible to relate this time to physical device characteristics; however, on the basis of experimental results it has been concluded that the (gradual) transition from equation (2) to equation (3) begins for most devices between 0.1 to 10 μs.[25]

A computer program[26] permits least-square fits to equations (1) and (3) and an equation of the form

$$P = at^{-1/2} + bt^{-1} , \qquad 0 < t < t_3 , \qquad (4)$$

to be produced from the experimental failure powers; equation (4) follows from a more involved version of the thermal model for reverse junction failure.[3] The output of the computation is the values of k_1 (or k_2), k_3, a, and b, and a statement about which equation best fits the data. (The Gauss criterion as a measure of the goodness of fit is used.) In view of the final selection of least-square fits, only failure powers for pulse widths ≥50 ns were used for fitting reverse damage data. The least-square analyses showed that the forward failure data of most types of junctions are better represented by equation (3) or (4), whereas the reverse failure data of a few types of junctions are better represented by equation (1), rather than by the type of relationship that results for either polarity from the thermal model. Nevertheless, to follow a widely accepted practice, the fit of forward failure

---

[2] *D. C. Wunsch and R. R. Bell, Determination of Threshold Failure Levels of Semiconductor Diodes and Transistors Due to Pulse Voltages, IEEE Trans. Nucl. Sci., NS-15 (December 1968), 244-259.*

[3] *D. M. Tasca, Pulsed Power Failure Modes in Semiconductors, IEEE Trans. Nucl. Sci., NS-17 (December 1968), 364-372.*

[25] *J. Singletary and D. C. Wunsch, Final Report on Semiconductor Damage Study, Phase II, Braddock, Dunn and McDonald, Inc., BDM/A-66-70-TR (June 1970).*

[26] *J. M. Clodfelter, SEMCON: A Semiconductor Damage Data Reduction Computer Code, Harry Diamond Laboratories, HDL-TM-76-28 (December 1976).*

powers to equation (1) and that of reverse failure powers to equation (3) were accepted for a'l junctions and entered into the damage plots. The straight lines in the damage plots of appendix A show these least-square fits. These lines are drawn on the basis of k_1 and k_3 and the associated slope of -1 (forward) and -1/2 (reverse, $t \geq 50$ ns), respectively. To account for the change in the variation of failure power with pulse width which the thermal model predicts (eq (2) and (3)), the line providing the least-square fit of reverse failure powers is continued into the range of $t < 50$ ns by changing the slope of the line from -1/2 to -1. The experimental failure powers of the drain-source part of the 2N4092 junction field effect transistor (FET), for either pulse polarity, were fitted to equation (1).

3. ANOMALOUS RESPONSES

During the damage testing of several types of diodes and transistors of the AN/TRC-145 devices, responses were observed which were strikingly incompatible with present concepts of device failure. Two kinds of "anomalous" responses were observed (anomalous from the standpoint of present concepts, especially the thermal failure model). First, there is the peculiar response tentatively called instantaneous second breakdown, occurring as follows. A junction is stepstressed into reverse bias and draws a certain amount of avalanche current. The voltage and current traces may be as shown in figure 1 (pulse width of 10 μs). There is no measurable device degradation and no second breakdown. The next pulse, whose open-circuit voltage would be only about 15 percent higher than that of the pulse of figure 1, produces the response of figure 2. The voltage trace shows that the device instantly went into second breakdown, V_2 being the second breakdown sustaining voltage.

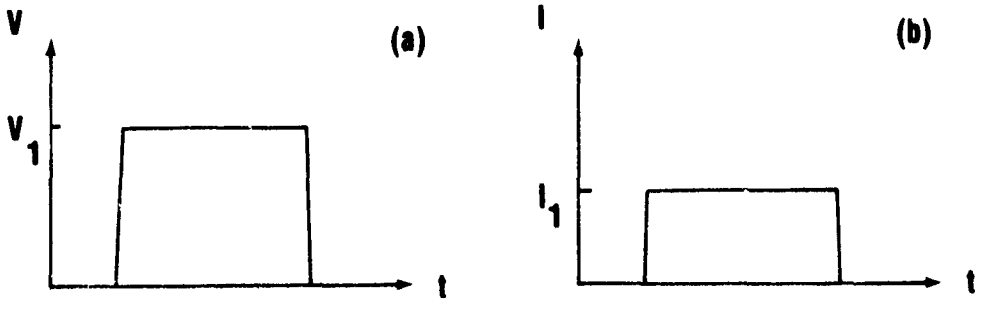

Figure 1. (a) Voltage and (b) current pulses before instantaneous second breakdown.

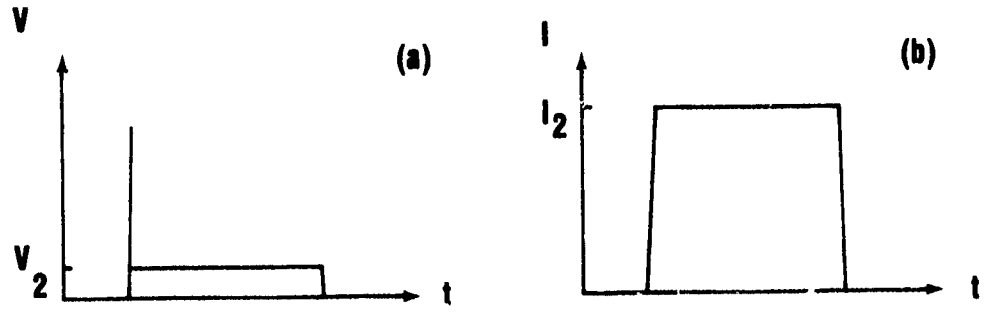

Figure 2. (a) Voltage and (b) current responses in instantaneous second breakdown.

When the oscilloscope is set up for proper recording of a 10-μs-wide pulse, the voltage spike and the leading edge of the current pulse in figure 2 are often not visible in the Polaroid photograph. Thus, many of these responses could not be properly evaluated, and an interpretation in terms of the thermal failure model may be possible. Also, some of the devices which responded in this manner were rectifiers of a rather high breakdown voltage, and the thermal failure model is not expected to apply.[5]

However, among the numerous cases showing this instantaneous second breakdown were many in which a definite evaluation of the oscilloscope traces could be made, and the devices involved were low-voltage bipolar transistors (even E-B junctions). The critical responses in such situations would be like those of figure 1 followed by those of figure 3 (10-μs pulse width). The leading edges of both the voltage and the current pulses are clearly visible; in particular, no initial current spike exceeds the value of I_3. The bright spot in the voltage and current traces indicates that V_3 and I_3 were assumed by the device for a short time (estimated to be between 50 and 100 ns). If one now assumes that

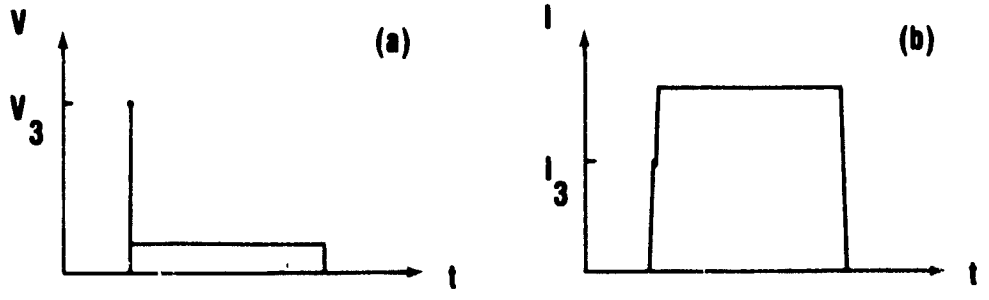

Figure 3. Other (a) voltage and (b) current responses in instantaneous second breakdown.

[5] *DNA EMP (Electromagnetic Pulse) Handbook, Defense Nuclear Agency 2114H-2 (September 1975).*

V_1I_1 (fig. 1) is the pre-second-breakdown power of the specimen for a delay time of 10 μs (worst case), the thermal failure model predicts a pre-second-breakdown power (V_3I_3) of at least $10V_1I_1$ for a delay time of 80 ns; however, V_3I_3 in responses like that of figure 3 was often found to be less than $2V_1I_1$. On a few occasions, responses like those of figure 2 or 3 were observed upon application of the very first pulse to a previously unpulsed specimen. This suggests that at least some of these responses are not due to an undetectable degradation of a device in previous pulse applications (cumulative effects). Devices were found to degrade (fail) or not to degrade in an event like that of figure 2 or 3, probably depending on the degree of current limitation while in second breakdown. According to the general rules of characterizing the conditions for device failure (sect. 2.1, 2.2.3), the damage information furnished by a device responding in the manner of figure 3 is a pre-second-breakdown power averaged over the delay time (of usually less than 100 ns) rather than a pre-second-breakdown power of V_1I_1 for a delay time of 10 μs; this accounts for many of the low power values around a 100-ns pulse width in the damage plots of the appendix.

This "instantaneous" form of second breakdown was observed also during damage testing at shorter pulse widths (1 and 0.1 μs). Here, second breakdown was seen to occur, at unexpectedly low power levels, from the leading edge of the pulse before the voltage leveled off significantly. At the higher sweep speeds used in this pulse-width range, the second-breakdown events are not perceived as instantaneous; nevertheless, for this report (sect. 4.2), the term "instantaneous" refers to second breakdown occurring during the rise phase of the pulse.

The kind of device response illustrated by figures 1 to 3 was observed in a damage characterizaton of the E-B junction of the 2N3858 transistor[1] and may also be the response of the C-B junction of the 2N3512 (BV_{cbo} = 60 V) that had been termed voltage-sensitive failure.[27] A systematic investigation of this effect is planned.

The second noteworthy response observed on certain types of devices was the apparent absence of second breakdown before failure at pulse widths of less than about 0.2 μs (reverse pulsing). On closer investigation of one of these devices (of the 2N1490), with stepstressing beginning at a very low pulse amplitude, it turned out that second breakdown did occur, but in a form quite different from that observed in longer pulse width testing. In fact, second breakdown first occurred at a very low pulse amplitude and associated power, very much lower than

[1] *B. Kalab, Analysis of Failure of Electronic Circuits from EMP-Induced Signals--Review and Contribution, Harry Diamond Laboratories, HDL-TR-1615 (August 1973).*

[27] *J. D. Holder and V. W. Ruwe, Statistical Component Damage Study, U.S. Army Missile Command, RG-TR-71-1 (January 1971).*

the level at which stepstressing is usually begun. (The pulse amplitude required for second breakdown or failure at the longest pulse width, at which stepstressing of a device type is begun, serves as a guideline for the start of stepstressing at shorter pulse widths. An experienced worker takes into consideration a certain increase in pulse power for failure as the pulse width is reduced and begins stepstressing at a shorter pulse width at a higher level, so that only a few more steps are required to cause device failure.)

The second breakdown at this low level is nondegrading; however, it does have the familiar appearance--that is, the voltage rapidly drops to a low second-breakdown sustaining level. According to the rule of section 2.1, the damage testing of a specimen is completed as soon as second breakdown is observed. However, the pre-second-breakdown power of this device was found to be more than an order of magnitude lower than the power for failure observed on other specimens of the same type (where no second breakdown had been seen). Therefore, stepstressing of this specimen was continued beyond the first occurrence of second breakdown.

By this procedure, it could be seen how the typical second-breakdown response of the device gradually disappears, as if it were overridden by the driving waveform. First, the delay times become shorter and shorter until second breakdown eventually begins from the rising edge of the pulse (as for instantaneous second breakdown, discussed previously). In addition, the second-breakdown sustaining voltage increases considerably in consecutive pulses. As one approaches the amplitude of the applied pulse at which stepstressing is usually begun, the pre-second-breakdown voltage appears only as a small overshoot on the rising edge of the pulse. Without having seen the development of such a response, beginning from the first occurrence of second breakdown, one would not recognize that the device is in second breakdown during almost the entire pulse duration. The only clue that this is the case might be the device impedance, which is conspicuously lower (in spite of the large second-breakdown sustaining voltage) than it is before second breakdown at delay times of about 1 μs.

This form of second breakdown at short pulse widths (nondegrading, high second-breakdown sustaining voltage) was seen to occur in several types of junctions. However, no attempt was made to ascertain whether it occurred in all devices of this testing program which failed to exhibit the familiar form of second breakdown before failure. Such a nondegrading and, presumably, nonthermal second breakdown at low power levels can result in a large spread of failure powers over a sample of devices, depending on whether or not the second breakdown is seen (which, in turn, depends on how stepstressing of each specimen of a sample is conducted) and whether or not the rule of section 2.1 is followed. From an applications point of view, it would seem important

to establish whether or not a device exhibiting this form of second breakdown can withstand a large post-second-breakdown power without damage under all possible conditions of circuit impedance and forms of excitation (of less than about a 0.2-μs duration). The observations made in this testing program show only the possibility of such an effect; they are much too limited to allow generalizations to be made.

The tables of the appendix list, for each specimen tested, the pulse voltage, the pulse current, the pulse power and the device impedance at the damage level, and the time to failure. The tables also indicate whether or not second breakdown was observed in a test specimen. Among the devices which failed in reverse pulsing without exhibiting second breakdown are those that were in second breakdown during most of the damaging pulse but not recognized as such. However, other devices, as well, are in this category; previously,[1] as well as in the present effort, it was found that reverse-pulsed junctions can degrade (and also fail, according to the definition of sect. 2.2.2) definitely without ever having entered second breakdown.

Still other aspects of observed device responses are unexpected on the basis of present concepts. The transistor types 2N1485, 2N1490, 2N3013, and 2N3439 exhibit a quite unusual relationship between the pre-second-breakdown power or power for reverse failure of the C-B junction (P_c) and that of the E-B junction (P_e). If the power for failure or for second breakdown is proportional to junction area, the ratio of P_c/P_e (at a given pulse width) of a discrete transistor would be expected to be between 1 and about 5 (the larger values applying to planar devices, for example). However, P_c/P_e for the transistors listed above (for pulse widths between about 5 and 10 μs) is between 0.05 and 0.6. The relationships of the damage constants of the C-B and E-B junctions of these transistors, although somewhat different from these values of P_c/P_e, reflect this unexpected observation. A value of P_c/P_e of 0.05 would suggest that the area of the C-B junction is only 1/20 that of the E-B junction. In spite of these relationships between P_c and P_e, both junctions of these transistors exhibit thermal second breakdown (long delay times), and the pre-second-breakdown power varies with the delay time according to $P = kt^{-1/2}$ to the same degree of approximation as it does for devices to which the thermal failure model is claimed to apply. This is another indication that the criterion ($P = kt^{-1/2}$) commonly applied to identify the failure mode and to establish the validity of the thermal failure model is insufficient.

[1] *B. Kalab, Analysis of Failure of Electronic Circuits from EMP-Induced Signals--Review and Contribution, Harry Diamond Laboratories, HDL-TR-1615 (August 1973).*

Recently, general relationships between device impedance and failure current of p-n junctions were developed.[12] According to these relationships, the forward device impedance at the failure level would decrease with pulse width because of conductivity modulation. The present damage data show a practically constant forward impedance at the damage level in the 10- to 0.1-μs range of pulse width for most types of junctions, with a few exceptions (1N277, PC115, 2N393) that have a statistically (and perhaps also practically) significant increase.

4. DAMAGE CHARACTERISTICS

4.1 Devices

The types of devices that were damage tested in the present effort, along with electrical characteristics and other identifying information, are listed in tables 1 and 2. Most of the devices were obtained from the Defense Electronic Supply Center. To relate the damage data of individual specimens to the predictions of a general failure theory (as is attempted with the least-square fits to relationships of the form $P = kt^{-1/2}$, etc), the specimens of a given device type should be of the same design and manufactured under identical conditions. There is no guarantee that this is true of the devices tested in this effort, although for most of the types tested it probably is. It can be assumed that the packaging of devices of a certain type which comprise different designs or manufacturing processes is not identical in all aspects. Therefore, the devices of any given type were closely inspected, and the number in column 2 (Packaging) of tables 1 and 2 indicates how many different kinds of packaging could be distinguished. Distinguishing characteristics were the material, color, and shape of the can or the encapsulation, and the complete alphanumeric designation appearing on the exterior of the devices. As can be seen from tables 1 and 2, most types of devices came in only one kind of packaging; thus, these devices were probably of the same design.

The manufacturer is identified in the tables by the manufacturer's designation or the D.A.T.A. manufacturer's code, both of which are listed in the D.A.T.A. books of Derivation and Tabulation Associates, Inc.[28,29] The designation appeared on the packaging of most device types, but the manufacturer meant could not be identified in all cases.

[12] *D. M. Tasca and S. J. Stokes, III EMP Response and Damage Modeling of Diodes, Junction Field Effect Transistor Damage Testing and Semiconductor Device Failure Analysis, General Electric Co., for Harry Diamond Laboratories, HDL-CR-76-090-1 (April 1976).*

[28] *Semiconductor Diode D.A.T.A. Book, 37th Ed., D.A.T.A., Inc., Orange, NJ (Spring 1976).*

[29] *Transistors, 42nd Ed., 1, D.A.T.A., Inc., Pine Brook, NJ (1977).*

TABLE 1. AN/TRC-145 DIODES SELECTED FOR DAMAGE TESTING

Diode	Packaging	Manufacturer[a]	Material	Function	Peak inverse voltage (V)	Capacitance (pF)
1N227 JAN	1	CIT	Ge	Diode (D)	125	--
1N485B JAN	1	--	Si	D	200	1.2
1N538 JAN	1	CDKF	Si	Rectifier (R)	240	10
1N645 JAN	1	CIT	Si	R	270	4
1N746A JAN	1	CCAB	Si	Ref diode (REF)	3.3	460
1N751A JAN	1	CDAQ	Si	REF	5.1	300
1N980B JAN	1	CCZL	Si	REF	62	31
1N1202RA JAN	1	CCSR	Si	R	200	57
1N1731A JAN	1	CAKK	Si	R	1800	14
1N2580	1	SSDI	Si	R	400	120
1N2991B JAN	1	CCSR	Si	REF	36	240
1N3025B JAN	1	CCZL	Si	REF	16	100
1N4385 JAN	1	CIT	Si	R	600	10
IR-69-6735	1	--	Si	REF	6.8	100
MO1054	1	Micro-optics	Ge	Varactor diode	--	--
MS1040	1	CMC	Ge	Microwave diode	--	--
PC115	2	CCNL	Si	Varactor diode	100	6.5

[a] *CAKK: General Instrument Corp.*
CCAB: Transitron Electronic Corp.
CCNL: TRW Semiconductors, Inc.
CCSR: NAE, Inc.
CCZL: Dickson Electronic Corp.
CDAQ: Teledyne Semiconductor Corp.
CDKF: Semicon, Inc.
CIT: ITT Semiconductors
CMC: Not identified
SSDI: Solid State Devices, Inc.

TABLE 2. AN/TRC-145 TRANSISTORS SELECTED FOR DAMAGE TESTING

Transistor	Packaging	Manufacturer[a]	Material	Function	BV_{cbo} (V)	C_{ob} (pF)
2N393 JAN	1	CSF	Ge, PNP	Low-power transistor (L)	10	4
2N396A	1	SES	Ge, PNP	L, switching transistor (S)	30	20
2N428M JAN	1	CGO	Ge, PNP	L, S	30	20
2N466M JAN	1	CAKK	Ge, PNP	L	35	60
2N501A JAN	1	CSF	Ge, PNP	L, S	15	3
2N705 JAN	1	CGG	Ge, PNP	L, S	15	8
2N706 JAN	3	CCXP, CDAQ	Si, NPN	L, S	25	6
2N1042 JAN	1	CCSX	Ge, PNP	High-power transistor (H)	40	--
2N1485 JAN	1	CQN	Si, NPN	H	60	50
2N1490 JAN	1	CRC	Si, NPN	H	100	100
2N1613 JAN	1	CDAQ	Si, NPN	L	75	25
2N1711 JAN	1	CDAQ	Si, NPN	L, S	75	25
2N2857 JAN	1	CDAQ	Si, NPN	L	30	1
2N2894	1	CCAB	Si, PNP	L, S	12	6
2N3013 JAN	2	CCAB, CIT	Si, PNP	L, S	40	5
2N3375 JAN	2	CRC, CGG	Si, NPN	H, S	65	10
2N3439	1	CRC	Si, NPN	H	450	10
2N3584	2	CEO, CGO	Si, NPN	H, S	375	120
2N4092	1	CAY	Si, nFET	--	--	--
2N5829	1	CGG	Si, PNP	L	30	0.8
CA 3018	1	CRC	Si, NPN	Integr. circuit trans. array	30	0.6
SMB526517	1	SES	Si, NPN	Integr. circuit trans. array	--	--

[a] *CAKK: General Instrument Corp.*
CAY: Westinghouse Electric Corp.
CCAB: Transitron Electronic Corp.
CCSX: Silicon Transistor Corp.
CCXP: National Semiconductor Corp.
CDAQ: Teledyne Semiconductor Corp.
CEO: Not identified
CGG: Motorola Semiconductor Products
CGO: Texas Instruments, Inc.
CIT: ITT Semiconductors
CQN: Sensitron Semiconductors
CRC: RCA Corporation, RCA Solid State Div.
CSF: Sprague Electric Co.
SES: Semitronics Corporation

The maximum reverse voltages of the junctions (peak inverse voltage of table 1, BV_{cbo} of table 2) are the values listed in the D.A.T.A. books.[28,29] The values in the Capacitance column of table 1 are the junction capacitances at 7 V reverse bias or at one half of the Zener voltage, whichever is lower, as measured with a capacitance bridge (mean value of three devices). The values in the C_{ob} column of table 2 are the common base open-circuit output capacitances as listed in the D.A.T.A. book[29] or manufacturers' data sheets. These values of breakdown voltage (peak inverse voltage, BV_{cbo}) and capacitances are used later to calculate theoretical values of the device damage constants.

4.2 Damage Characteristics

This section summarizes certain aspects of the conditions for failure of the damage-tested device types. Tables 3 and 4 show the rather frequent occurrence of special failure modes, including instantaneous second breakdown, even in low-voltage bipolar devices. Table 5 lists the damage constants of these device types (times certain powers of 10), produced by least-square analyses of the failure powers of the individual test specimens. The failure powers of individual specimens, the associated pulse width, and the device impedances at the failure level are presented in the tables and figures of the appendix.

In table 5, the constants k_1 and k_3 are those of equations (1) and (3), respectively (sect. 2.2.4). With the values of k_1 and k_3 as they result from table 5, the failure power is obtained in watts from equations (1) and (3) if the pulse duration is measured in seconds; therefore, the unit of k_1 is the watt-second and the unit of k_3 is the watt-second$^{1/2}$. The powers of 10, as factors of k_1 and k_3 in table 5, are chosen so that the number in the column for k_1 is numerically equal to the power in kilowatts for forward failure at a pulse width of 1 μs, and the number in the column for k_3 is numerically equal to the power in watts for reverse failure at a pulse width of 1 μs.

---

[28] *Semiconductor Diode D.A.T.A. Book, 37th Ed., D.A.T.A., Inc., Orange, NJ (Spring 1976).*

[29] *Transistors, 42nd Ed., 1, D.A.T.A., Inc., Pine Brook, NJ (1977).*

TABLE 3. FAILURE MODES AND SECOND BREAKDOWN IN DIODES OF AN/TRC-145[a]

Diode	Width of applied pulse (forward)						Width of applied pulse (reverse)											
	10 μs		1.0 μs		<0.5 μs		10, 1.0 μs						<0.5 μs					
	N	Sp	N	Sp	N	Sp	Fail no SB	SB no degr	SB degr	SB fail	Inst SB no degr	Inst SB D/F	Fail no SB	SB no degr	SB degr	SB fail	Inst SB no degr	Inst SB D/F
1N277 JAN	x	-	x	-	x	-	-	-	-	x	-	x	-	-	-	-	-	-
1N485B JAN	x	-	x	-	-	-	x	-	-	x	-	-	x	-	-	-	-	-
1N538 JAN	-	-	-	-	-	-	x	-	-	-	-	-	-	-	-	-	-	-
1N645 JAN	x	-	-	-	-	-	-	-	-	x	-	x	-	-	-	x	-	-
1N746A JAN	x	x	-	-	-	-	x	-	-	-	-	-	-	-	-	-	-	-
1N751A JAN	x	-	x	-	-	-	x	-	-	-	-	-	x	-	-	-	-	-
1N980B JAN	x	-	-	-	-	-	x	-	-	x	-	-	-	-	-	-	-	-
1N1202RA JAN	-	-	-	-	-	-	-	-	-	x	-	-	-	-	-	x	-	-
1N1731A JAN	x	-	-	-	-	-	x	x	-	x	-	-	x	-	-	x	-	-
1N2580	-	-	-	-	-	-	x	-	-	-	-	-	-	-	-	-	-	-
1N2991B JAN	-	-	-	-	-	-	x	-	-	-	-	-	-	-	-	-	-	-
1N3025B JAN	x	-	-	-	-	-	x	-	-	-	-	-	-	-	-	-	-	-
1N4385 JAN	-	-	-	-	-	-	-	-	x	x	-	x	-	-	-	x	-	-
IR-69-6735	x	-	x	-	-	-	x	-	-	-	-	-	-	-	-	-	-	-
MO1054	x	-	x	-	-	-	x	x	-	x	-	x	-	x	-	x	-	x
MS1040	x	-	x	-	x	-	x	-	-	-	-	-	x	-	-	-	-	-
PC115	x	-	x	-	-	-	x	-	-	x	-	-	x	-	-	x	-	-

[a]Symbols are defined as follows.

N: Normal failure mode in forward pulsing, that is, junction breakdown voltage or current gain reduced to values constituting failure; no indication of moment of failure in voltage or current trace
Sp: Any special failure mode (like open-circuiting) also indicating moment of failure
Fail no SB: No indication of moment of failure, especially no transition to second breakdown
SB no degr: Second breakdown without measurable degradation device characteristics
Inst SB D/F: Instantaneous second breakdown (sect. 3) associated with device degradation or failure
x: Applicable failure mode

TABLE 4. FAILURE MODES AND SECOND BREAKDOWN IN TRANSISTORS OF AN/TRC-145[a]

Transistor	Junction	Width of applied pulse (forward)						Width of applied pulse (reverse)											
		10 μs		1.0 μs		<0.5 μs		10, 1.0 μs						<0.5 μs					
		N	Sp	N	Sp	N	Sp	Fail no SB	SB no degr	SB degr	SB fail	Inst SB no degr	Inst SB D/F	Fail no SB	SB no degr	SB degr	SB fail	Inst SB no degr	Inst SB D/F
2N393 JAN	E-B	x	-	x	-	x	-	x	-	-	x	-	-	x	-	-	-	-	-
	C-B	x	-	x	-	x	-	x	-	-	-	-	-	x	-	-	-	-	-
2N396A	E-B	x	-	x	-	-	-	-	x	-	-	x	-	-	x	x	-	x	-
	C-B	x	-	x	-	-	-	-	x	-	-	x	-	-	x	-	-	x	-
2N428M JAN	E-B	x	-	x	-	-	-	-	x	-	-	-	-	-	x	-	-	x	x
	C-B	x	-	x	-	-	-	-	x	-	-	x	-	-	x	-	-	x	-
2N466M JAN	E-B	x	x	x	-	-	-	-	x	x	x	-	x	-	-	-	-	-	x
	C-B	x	-	x	-	-	-	-	x	-	x	-	-	-	x	-	x	x	x
2N501A JAN	E-B	x	x	x	x	x	-	x	x	x	x	-	-	x	-	-	-	-	-
	C-B	x	-	x	-	x	-	-	x	x	x	-	-	x	-	-	-	-	-
2N705 JAN	E-B	x	-	x	x	x	-	-	x	-	-	-	x	-	x	-	x	x	-
	C-B	x	-	x	-	x	-	-	x	-	x	-	x	-	-	-	-	x	x
2N706 JAN	E-B	x	x	x	-	x	-	x	-	-	x	-	-	x	-	-	-	-	-
	C-B	-	x	x	x	-	x	-	x	x	x	-	-	x	x	-	x	-	-
2N1042 JAN	E-B	x	-	-	-	-	-	-	x	-	x	-	-	-	-	-	-	-	-
	C-B	x	-	-	-	-	-	-	x	x	x	x	x	-	x	-	-	x	-
2N1485 JAN	E-B	x	-	-	-	-	-	x	-	x	-	-	-	-	-	-	-	-	-
	C-B	-	-	-	-	-	-	-	x	-	-	x	x	x	x	-	x	x	-
2N1490 JAN	E-B	-	-	-	-	-	-	x	x	x	x	-	-	x	-	-	-	-	-
	C-B	-	-	-	-	-	-	x	x	x	-	x	-	-	x	-	-	-	-
2N1613 JAN	E-B	x	-	x	-	-	-	x	-	-	x	-	-	x	-	-	-	-	-
	C-B	x	-	x	-	-	-	x	x	-	x	-	x	-	-	-	-	-	x
2N1711 JAN	E-B	x	-	x	-	-	-	-	-	-	x	-	-	x	-	-	-	-	-
	C-B	x	-	x	-	-	-	-	x	x	x	-	-	x	-	-	x	-	-
2N2857 JAN	E-B	-	x	-	x	-	-	x	-	-	x	-	-	x	-	-	-	-	-
	C-B	-	x	-	x	-	x	-	-	-	x	-	x	-	x	-	-	-	-
2N2894	E-B	-	x	-	x	-	-	x	-	-	x	-	-	x	-	-	-	-	-
	C-B	-	x	x	x	-	x	x	x	-	x	-	-	-	-	-	x	-	-
2N3013 JAN	E-B	-	x	-	x	x	x	x	-	-	x	-	-	x	-	-	-	-	-
	C-B	-	x	-	x	-	x	-	x	x	x	-	x	-	x	-	-	x	-
2N3375 JAN	E-B	x	x	x	-	x	-	x	-	-	x	-	-	x	-	-	-	-	-
	C-B	x	-	x	-	x	-	-	x	x	x	-	-	-	x	x	x	-	-
2N3439	E-B	x	-	x	-	-	-	x	-	-	x	-	-	x	-	-	-	-	-
	C-B	x	-	-	-	-	-	-	x	-	-	-	-	-	-	-	x	-	-
2N3584	E-B	x	-	-	-	-	-	x	-	-	x	-	-	x	-	-	-	-	-
	C-B	x	-	-	-	-	-	-	x	-	-	-	-	-	x	-	-	-	-
2N4092	G-S	-	x	-	x	-	x	-	x	x	x	-	-	x	x	-	-	-	-
	D-S	-	x	-	x	-	x	-	x	-	x	-	x	x	-	-	-	-	-
2N5829	E-B	-	x	x	x	x	x	x	-	-	x	-	-	-	-	-	-	-	x
	C-B	-	x	-	x	-	x	-	x	x	x	-	x	-	-	x	-	-	x
CA3018	E-B	-	x	-	x	x	-	-	-	-	x	-		x	-	-	-	-	-
	C-B	-	x	-	x	x	-	-	-	-	-	x	x	x	-	-	-	x	-
SMB526517	E-B	x	x	x	-	x	-	x	-	-	x	-	-	-	-	-	-	-	x
	C-B	x	x	x	-	-	-	-	x	-	x		-	-	x	-	-	x	-

[a] *Symbols as defined in table 3, p. 29.*

TABLE 5. DAMAGE CONSTANTS OF AN/TRC-145 DIODES AND TRANSISTORS

Diode	$10^3 k_1$ (Ws)	$10^3 k_3$ ($Ws^{1/2}$)	Transistor	Junction	$10^3 k_1$ (Ws)	$10^3 k_3$ ($Ws^{1/2}$)	Transistor	Junction	$10^3 k_1$ (Ws)	$10^3 k_3$ ($Ws^{1/2}$)
1N277 JAN	0.34[a]	12	2N393 JAN	E-B C-B	0.61[b] 0.82[b]	140 850	2N1711 JAN	E-B C-B	3.8[b] 15[b]	270 1,500
1N485B JAN	9.4[b]	460								
1N538 JAN	-	10,000	2N396A	E-B C-B	2.5[b] 16[b]	41 49	2N2857 JAN	E-B C-B	0.012[a] 0.024[a]	2.5 5.6
1N645 JAN	72	270								
1N746A JAN	20[a]	8,800	2N428M JAN	E-B C-B	3.8 13[b]	140 160	2N2894	E-B C-B	0.021[b] 0.019[b]	17 34
1N751A JAN	8.4[b]	2,100[c]	2N466M JAN	E-B C-B	2.7 15[b]	820 600	2N3013 JAN	E-B C-B	0.084[c] 0.068[b]	24 4.5
1N980B JAN	69[a]	3,600								
1N1202RA JAN	-	840	2N501A JAN	E-B C-B	0.12[a] 0.39[b]	15 15	2N3375 JAN	E-B C-B	1.8[b] 4.1[b]	450 670
1N1731A JAN	160	1,900	2N705 JAN	E-B C-B	0.033[a] 0.080[a]	2.9 7.7	2N3439	E-B C-B	13[a] 37	580 26
1N2580	-	54,000								
1N2991B JAN	-	30,000	2N706 JAN	E-B C-B	0.090 0.035[b]	18 17	2N3584	E-B C-B	34 160	1,800 470
1N3025B JAN	45	3,900	2N1042 JAN	E-B C-B	140 155	1,200 770	2N4092	G-S D-S	0.21[b] 0.001[a]	110 -
1N4385 JAN	-	190								
IR-69-6735	7.9	4,600[c]	2N1485 JAN	E-B C-B	50 -	4,500[c] 230	2N5829	E-B C-B	0.014[a] 0.034[b]	7.9 5.7
MO1054	6.7[b]	78	2N1490 JAN	E-B C-B	- -	3,300 330	CA 3018	E-B C-B	0.048[b] 0.17[b]	8.7 2.3
MS1040	0.002[b]	0.27								
PC115	20[a]	1,200	2N1613 JAN	E-B C-B	3.0[b] 17[b]	280 1,200	SMB526517	E-B C-B	0.40[b] 5.0[b]	52 35

[a] *Fitting the forward failure data to an equation of the type $P = k^{-1/2}$ would provide a better goodness of fit (P = power for damage, k = constant, t = time to damage).*
[b] *Fitting the forward failure data to an equation of the type $P = at^{-1/2} + by^{-1}$ would provide a better goodness of fit.*
[c] *Fitting the reverse failure data to an equation of the type $P = kt^{-1}$ would provide a better goodness of fit.*

4.3 Comparison between Experimental and Theoretical Failure Powers

There is a continuing interest in the community in obtaining a relevant device damage characterization without resorting to extensive damage testing. The relationships between failure power (or damage constant) and general device characteristics referred to in the introduction[4,5] furnish a device failure power (although not the device impedance) without damage testing. To show how accurate the damage constants based on these relationships are in typical cases, the experimental damage constants obtained from the present testing effort are compared with the theoretical values. Only the more accurate junction capacitance model[4] is used here. To find the damage constant of a silicon diode for reverse pulsing, the following equation is suggested:[5]

$$k_3 = 4.97 \times 10^{-3} \, CV_{BD}^{0.57} \quad , \tag{5}$$

where C is the junction capacitance at 5- to 10-V reverse voltage, and V_{BD} is the bias voltage at a 10-μA reverse current (or the minimum breakdown voltage for the device type as specified by the manufacturer).[4] For transistors, the method requires[5] the use of equation (5) for nonplanar silicon transistors and

$$k_3 = 1.66 \times 10^{-4} \, CV_{BD}^{0.99} \tag{6}$$

for mesa and planar silicon transistors. C is the common base open-circuit output capacitance (C_{ob}) and BV_{cbomax} is to be used for V_{BD} in equations (5) and (6). With these magnitudes, k_3 is the damage constant of the E-B junction. No relationships of this kind are recommended for germanium diodes or transistors.

For the AN/TRC-145 silicon diodes and for the silicon transistors for which specification values of C_{ob} were available (table 2), the theoretical damage constants, k_{3th}, were calculated and compared with the experimental values, k_{3exp}. Table 6 shows the quotients k_{3exp}/k_{3th}. For quite a few devices, this quotient is acceptably close to 1, but differences up to more than an order of magnitude do occur in a number of device types.

---

[4] *D. C. Wunsch, R. L. Cline, and G. R. Case, Theoretical Estimates of Failure Levels of Selected Semiconductor Diodes and Transistors, Braddock, Dunn and McDonald, Inc., for Air Force Special Weapons Center, BDM/A-42-69-R (December 1969).*

[5] *DNA EMP (Electromagnetic Pulse) Handbook, Defense Nuclear Agency 2114H-2 (September 1975).*

TABLE 6. COMPARISON OF EXPERIMENTAL AND THEORETICAL (JUNCTION CAPACITANCE MODEL) DAMAGE CONSTANTS OF SELECTED AN/TRC-145 DIODES AND TRANSISTORS (E-B JUNCTIONS)

Diode	k_{3exp}/k_{3th}	Transistor	k_{3exp}/k_{3th}
1N485B JAN	3.8	2N706 JAN	0.74
1N538 JAN	9.6	2N1485 JAN	9.8
1N645 JAN	0.67	2N1490 JAN	2.5
1N746A JAN	2.1	2N1613 JAN	0.93
1N751A JAN	0.62	2N1711 JAN	0.90
1N980B JAN	2.7	2N2857 JAN	0.52
1N1202RA JAN	0.16	2N2894	1.4
1N1731 JAN	0.47	2N3013 JAN	0.80
1N2580	3.2	2N3375 JAN	4.5
1N2991B JAN	3.1	2N3439	0.77
1N3025B JAN	1.8	2N3584	0.26
1N4385 JAN	0.05	2N5829	18
IR-69-6735	3.7	CA 3018	23
PC115	2.5		

Besides the use of the junction capacitance model or similar models,[4] obtaining powers for failure of a device type can also be simplified by damage testing with only one pulse width. This restriction would make it economically feasible to use a larger sample size for obtaining better statistics and would also greatly simplify the automation of instrumentation for damage testing. The pulse width to be used in testing would best be the longest one for which device damage information is needed, because testing and data reduction are easier at longer pulse widths. The power for failure at other pulse widths would be extrapolated on the basis of equation (3).

[4] *D. C. Wunsch, R. L. Cline, and G. R. Case, Theoretical Estimates of Failure Levels of Selected Semiconductor Diodes and Transistors, Braddock, Dunn and McDonald, Inc., for Air Force Special Weapons Center, BDM/A-42-69-R (December 1969).*

Table 7 shows how the failure powers of selected AN/TRC-145 devices for a 0.1-μs pulse width, extrapolated on this basis, compared with experimental values. $P_{0.1th}$ is the power for reverse failure (or second breakdown) for a 0.1-μs pulse width extrapolated on the basis of equation (3) from the experimental failure power at a 10-μs pulse width, P_{10exp} ($P_{0.1th} = 10P_{10exp}$); $P_{0.1exp}$ is the experimental failure power at a 0.1-μs pulse width. To obtain P_{10exp} and $P_{0.1exp}$ (which are mean values of a sample of devices), extrapolation, by use of equation (3), of experimental data points near the 10- and 0.1-μs pulse widths is required because many pulse widths and delay times are not exactly 10 or 0.1 μs. Not all devices of the present testing program furnished experimental failure powers near the 10- and 0.1-μs pulse widths; therefore, the list of devices (or junctions) of table 7 is not complete. If equation (3) indeed expresses the variation of reverse failure power (or pre-second-breakdown power) of a semiconductor junction device with the pulse width, $P_{0.1th}$ should compare well with $P_{0.1exp}$ for such a device. However, many types of junctions, especially E-B junctions, of table 7 exhibit a difference of a factor of 10 between $P_{0.1th}$ and $P_{0.1exp}$; for most of these junctions, this difference would be even greater if equation (4) were used to extrapolate from P_{10exp} to $P_{0.1th}$. The values in column $P_{0.1exp}$ of table 7 are the smallest experimental failure powers observed at a 0.1-μs pulse width on the small samples used in damage testing, and these values are often smaller by an order of magnitude than the experimental mean values ($P_{0.1exp}$). Therefore, a mean value of failure power at a 0.1-μs pulse width, extrapolated on the basis of the thermal model, equation (3), from an experimental mean value at 10 μs would have to be reduced by at least two orders of magnitude to obtain a "sure safe" value of failure power for a pulse width of 0.1 μs. In other words, device damage testing at a 10-μs pulse width and extrapolation of the experimental failure powers to shorter pulse widths on the basis of the thermal failure model can lead to very inaccurate results.

TABLE 7. COMPARISON OF THEORETICAL AND EXPERIMENTAL REVERSE FAILURE POWERS OF SELECTED AN/TRC-145 DIODES AND TRANSISTORS FOR 0.1-μs PULSE WIDTH

Device	Junction	$P_{0.1th}$ (W)	$P_{0.1exp}$ (W)	$P_{0.1exp}$ (W)
1N277 JAN	-	120	8.0	7.0
1N485B JAN	-	890	4,100	3,600
1N645 JAN	-	7,900	620	45
1N751A JAN	-	2,400	21,000	19,000
1N1202RA JAN	-	2,100	4,700	390
1N1731A JAN	-	12,000	6,300	4,200
1N4385	-	1,500	850	55
MO1054	-	440	240	100
PC115	-	4,500	2,600	1,200
2N393 JAN	E-B	340	1,400	650
	C-B	3,000	2,700	2,100
2N396A	E-B	910	110	19
	C-B	820	85	27
2N428M JAN	E-B	2,200	220	89
	C-B	1,400	190	64
2N466M JAN	E-B	6,600	530	410
	C-B	4,000	640	380
2N501A JAN	E-B	39	160	17
	C-B	63	95	5.0
2N705 JAN	E-B	40	4.5	1.5
	C-B	52	5.0	5.0
2N706 JAN	E-B	61	50	37
2N1042 JAN	E-B	9,100	4,200	4,200
2N1485 JAN	C-B	2,900	600	220
2N1490 JAN	E-B	13,000	7,000	6,000
	C-B	6,800	390	180
2N1613 JAN	E-B	1,100	480	430
	C-B	11,000	1,400	590
2N1711 JAN	E-B	1,100	490	310
	C-B	8,700	2,300	1,900
2N2857 JAN	E-B	8.0	7.8	2.5
	C-B	140	31	3.6
2N2894	E-B	93	26	25
	C-B	130	140	110
2N3013 JAN	E-B	120	48	30
2N3375 JAN	E-B	1,900	1,300	740
	C-B	4,300	860	430
2N3439	E-B	1,800	2,300	1,200
	C-B	85	92	19
2N3584	E-B	4,000	4,900	4,900
	C-B	4,400	660	410
2N4092	G-S	550	230	160
2N5829	E-B	44	11	10
	C-B	92	16	2.4
CA 3018	E-B	38	22	19
SMB526517	E-B	190	36	32
	C-B	280	31	5.0

LITERATURE CITED

(1) B. Kalab, Analysis of Failure of Electronic Circuits from EMP-Induced Signals--Review and Contribution, Harry Diamond Laboratories, HDL-TR-1615 (August 1973).

(2) D. C. Wunsch and R. R. Bell, Determination of Threshold Failure Levels of Semiconductor Diodes and Transistors Due to Pulse Voltages, IEEE Trans. Nucl. Sci., NS-15 (December 1968), 244-259.

(3) D. M. Tasca, Pulsed Power Failure Modes in Semiconductors, IEEE Trans. Nucl. Sci., NS-17 (December 1968), 364-372.

(4) D. C. Wunsch, R. L. Cline, and G. R. Case, Theoretical Estimates of Failure Levels of Selected Semiconductor Diodes and Transistors, Braddock, Dunn and McDonald, Inc., for Air Force Special Weapons Center, BDM/A-42-69-R (December 1969).

(5) DNA EMP (Electromagnetic Pulse) Handbook, Defense Nuclear Agency 2114H-2 (September 1975).

(6) B. Kalab, Second Breakdown and Damage in 1N4148 from Oscillating Electrical Transients, IEEE Trans. Nucl. Sci., NS-22 (August 1975), 2006-2009.

(7) R. H. Dickhaut, Electromagnetic Pulse Damage to Bipolar Devices, IEEE Circuits and Systems, 10 (April 1976), 8-21.

(8) A. L. Ward, An Electro-thermal Model of Second Breakdown, IEEE Trans. Nucl. Sci., NS-23 (December 1976), 1679-1684.

(9) A. L. Ward, Studies of Second Breakdown in Silicon Diodes, IEEE Trans. Parts, Hybrids, and Packaging, PHP-13 (December 1977), 361-368.

(10) J. L. Cooke et al, Users Manual for SUPERSAP2, Boeing Aerospace Co., Seattle, WA, and BDM Corp., Air Force Weapons Laboratory, AFWL-TR-75-70 (March 1976).

(11) T. V. Noon, Implementation of the Device Data Bank on the HDL IBM Computer, Harry Diamond Laboratories, HDL-TR-1819 (October 1977).

(12) D. M. Tasca and S. J. Stokes, III, EMP Response and Damage Modeling of Diodes, Junction Field Effect Transistor Damage Testing and Semiconductor Device Failure Analysis, General Electric Co., for Harry Diamond Laboratories, HDL-CR-76-090-1 (April 1976).

LITERATURE CITED (Cont'd)

(13) D. M. Tasca et al, Theoretical and Experimental Studies of Semiconductor Device Degradation Due to High Power Electrical Transients, General Electric Co., 73SD4289 (December 1973).

(14) D. C. Wunsch and L. Marzitelli, BDM Final Report, 1, Semiconductor and Nonsemiconductor Damage Study, Braddock, Dunn and McDonald, Inc., for U.S. Army Mobility Equipment Research and Development Center, BDM-375-69-F-0168 (April 1969).

(15) J. B. Singletary, W. O. Collier, and J. A. Myers, Experimental Threshold Failure Levels of Selected Diodes and Transistors, II, Braddock, Dunn and McDonald, Inc., for Air Force Weapons, Laboratory, AFWL-TR-73-119 (July 1973).

(16) D. M. Tasca and J. C. Peden, Feasibility Study of Developing a Nondestructive Screening Procedure for Thermal Second Breakdown, General Electric Co. (July 1971).

(17) B. Kalab, On the Necessary and Sufficient Conditions (Thresholds) for Damage of Semiconductor Junctions from Electrical Transients, Proc. Joint EMP Technical Meeting, First Annual Nuclear EMP Meeting, Albuquerque, NM, V, Hardening Technology (September 1973), 249-260.

(18) K. Hubner et al, Uniform Turn-on in Four-Layer Diodes, IEEE Trans. Electron Devices, ED-8 (November 1964), 1372-1373.

(19) T. Agatsuma et al, An Aspect of Second Breakdown in Transistors, Proc. IEEE (Correspondence), 52 (November 1961), 461-464.

(20) L. W. Ricketts, J. E. Bridges, and J. Miletta, EMP Radiation and Protective Techniques, John Wiley & Sons, Inc., New York (1976).

(21) J. R. Miletta, Component Damage from Electromagnetic Pulse (EMP) Induced Transients, Harry Diamond Laboratories, HDL-TM-77-22 (November 1977).

(22) G. H. Baker et al, Damage Analysis Modified TRAC Computer Program (DAMTRAC), Harry Diamond Laboratories, HDL-TM-75-6 (May 1975).

(23) D. C. Wunsch, Semiconductor Device Damage in an EMP Environment, Proc. Conference on Component Degradation from Transient Inputs, U.S. Army Mobility Equipment Research and Development Center, Ft. Belvoir, VA (April 1970), 6-50.

LITERATURE CITED (Cont'd)

(24) J. B. Singletary and D. C. Wunsch, Final Summary Report on Semiconductor Damage Study, Phase II, Braddock, Dunn and McDonald, Inc., BDM/A-84-70-TR (February 1971).

(25) J. Singletary and D. C. Wunsch, Final Report on Semiconductor Damage Study, Phase II, Braddock, Dunn and McDonald, Inc., BDM/A-66-70-TR (June 1970).

(26) J. M. Clodfelter, SEMCON: A Semiconductor Damage Data Reduction Computer Code, Harry Diamond Laboratories, HDL-TM-76-28 (December 1976).

(27) J. D. Holder and V. W. Ruwe, Statistical Component Damage Study, U.S. Army Missile Command, RG-TR-71-1 (January 1971).

(28) Semiconductor Diode D.A.T.A. Book, 37th Ed., D.A.T.A., Inc., Orange, NJ (Spring 1976).

(29) Transistors, 42nd Ed., 1, D.A.T.A., Inc., Pine Brook, NJ (1977).

APPENDIX A.--DAMAGE CHARACTERISTICS OF DIODES AND TRANSISTORS TESTED

CONTENTS

APPENDIX A

FIGURES AND TABLES (Cont'd)

APPENDIX A. DAMAGE CHARACTERISTICS OF DIODES AND TRANSISTORS TESTED

This appendix contains the data that characterize the selected devices of the AN/TRC-145 radio terminal set at the failure level under the conditions of testing discussed in section 2.2 in the body of this report. The damage characteristics of each specimen or junction tested are entered in tables A-1 to A-39 in one line, under either the Forward column or the Reverse column. The columns show the following:

t_o the width of the applied pulse

t the time to failure or second breakdown, wherever this time could be identified as being different from t_o (no entry means $t = t_o$)

P the pulse power for failure or second breakdown (sect. 2.1)

V the voltage (averaged over t_o or t) of the pulse producing failure (sect. 2.1) or the average pre-second-breakdown voltage

Z the device impedance at the failure level (as defined in sect. 2.1)

If the moment (t) of failure is identifiable from the voltage or current trace of the applied pulse, the nature of the event occurring at t is indicated in the Condition column of the tables. The most frequent event of this kind is second breakdown, with the variations discussed below. However, there can be other events, like the opening of a metallization; a brief comment is made after the tables in these other cases, explaining the symbol used in this column and the nature of the event to which it refers. Several variations of the symbol SB for second breakdown are used:

SB second breakdown without measurable device degradation

SBD second breakdown with degradation of electrical device characteristics

SBF second breakdown with changes in device characteristics defined to be failure (sect. 2.2.2)

ISB instantaneous second breakdown (sect. 3) without measurable degradation of device characteristics

ISBD instantaneous second breakdown with device degradation

ISBF instantaneous second breakdown with device failure

APPENDIX A

A dash in the Condition column means that neither second breakdown nor any other failure mode could be identified from the voltage or current trace; upon application of a pulse of width t_o, the device exhibited the reduction in breakdown voltage or current gain that had been defined as failure. It is possible that a terminal pair open-circuited in such a pulse. Several cases of this kind were identified; others may have gone undetected.

Plots of the failure power of the individual test specimens of each device type tested at the respective times to failure or second breakdown are provided in figures A-1 to A-39. In addition, these damage plots contain the least-square fits, as discussed in section 2.2.4, and an indication of the power limitation of the pulse generator, where applicable. If a specimen could not be damaged or second breakdown could not be induced at the maximum output of the pulse generator, the maximum power dissipated in the devices (upon averaging, if more than one specimen could not be damaged in a particular test condition) is indicated in the plots by a short horizontal bar ("L") centered over the corresponding pulse width. The kind of data point (dot or circle) above the bar, pointed at by an arrow, indicates whether the power limitation was reached in forward or reverse pulsing of the junction. Despite a maximum power output of 20 kW of the pulse generator used in testing, the maximum power dissipated in devices around a 0.1-μs pulse width was often quite low; this is due to an impedance mismatch between load and pulse generator.

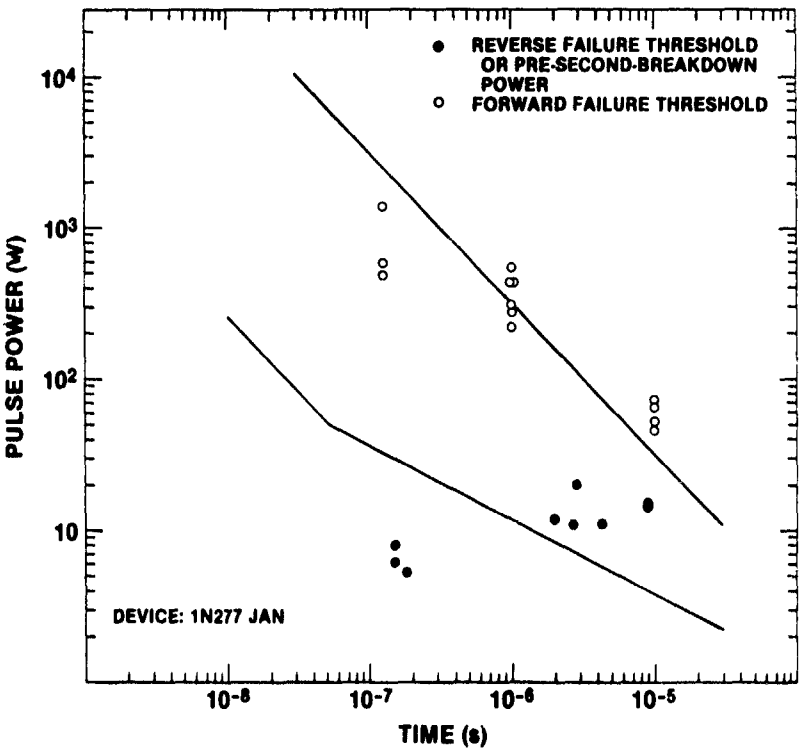

Figure A-1. Damage characteristics of 1N277 JAN.

TABLE A-1. DAMAGE CHARACTERISTICS OF 1N277 JAN

Forward						Reverse					
t_o(μs)	t(μs)	P(W)	V(V)	Z(Ω)	Condition	t_o(μs)	t(μs)	P(W)	V(V)	Z(Ω)	Condition
10	-	48	5.5	0.63	-	10	9.0	15	360	8500	SBF
10	-	52	5.3	0.54	-	10	8.8	15	360	8700	SBF
10	-	65	5.8	0.52	-	10	4.2	11	270	6400	SBF
10	-	75	5.7	0.43	-	10	2.8	20	360	6500	SBF
10	-	120	8.8	0.65	-	10	2.7	11	300	8300	SBF
1.0	-	220	12	0.59	-	10	2.0	12	320	8700	SBF
1.0	-	280	15	0.80	-	1.0	0.18	5.3	180	5800	ISBF
1.0	-	310	17	0.94	-	1.0	0.15	6.0	150	3800	ISBF
1.0	-	440	16	0.60	-	1.0	0.15	7.9	180	3900	ISBF
1.0	-	440	18	0.70	-						
1.0	-	550	17	0.53	-						
0.13	-	510	23	1.0	-						
0.13	-	610	28	1.3	-						
0.13	-	1400	41	1.2	-						

APPENDIX A

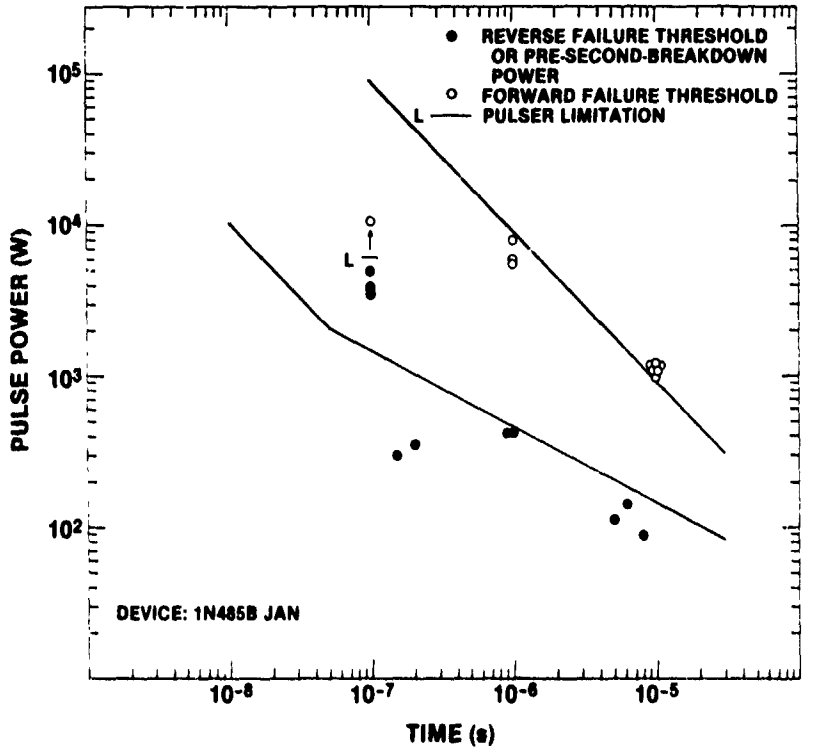

Figure A-2. Damage characteristics of 1N485B JAN.

TABLE A-2. DAMAGE CHARACTERISTICS OF 1N485B JAN

Forward						Reverse					
t_o(μs)	t(μs)	P(W)	V(V)	Z(Ω)	Condition	t_o(μs)	t(μs)	P(W)	V(V)	Z(Ω)	Condition
10	-	1000	16	0.25	-	10	8.0	90	200	440	SBF
10	-	1100	16	0.24	-	10	6.0	140	310	690	SBF
10	-	1100	17	0.25	-	10	5.0	110	200	360	SBF
10	-	1200	16	0.20	-	1.0	-	420	360	300	-
10	-	1200	17	0.23	-	1.0	0.90	420	220	120	SBF
10	-	1200	17	0.24	-	1.0	0.20	360	240	160	SBF
1.0	-	5500	41	0.31	-	1.0	0.15	300	850	2500	SBF
1.0	-	5800	41	0.29	-	0.10	-	3600	270	20	-
1.0	-	8000	50	0.31	-	0.10	-	3800	300	24	-
						0.10	-	3900	300	23	-
						0.10	-	4900	350	25	-

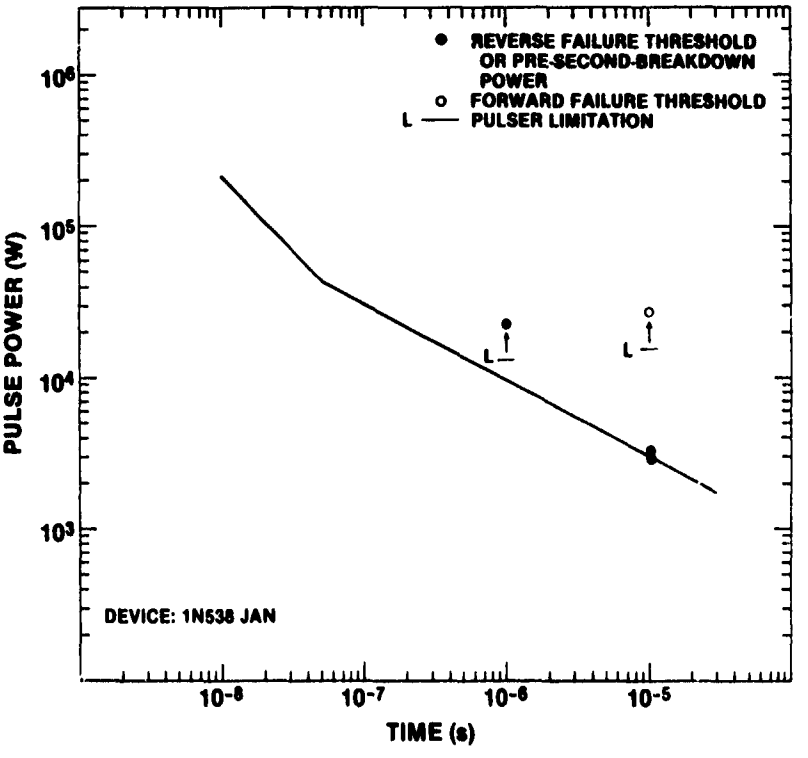

Figure A-3. Damage characteristics of 1N538 JAN.

TABLE A-3. DAMAGE CHARACTERISTICS OF 1N538 JAN

Forward						Reverse					
t_o(μs)	t(μs)	P(W)	V(V)	Z(Ω)	Condition	t_o(μs)	t(μs)	P(W)	V(V)	Z(Ω)	Condition
						10	-	3000	1100	370	-
						10	-	3400	1100	360	-

APPENDIX A

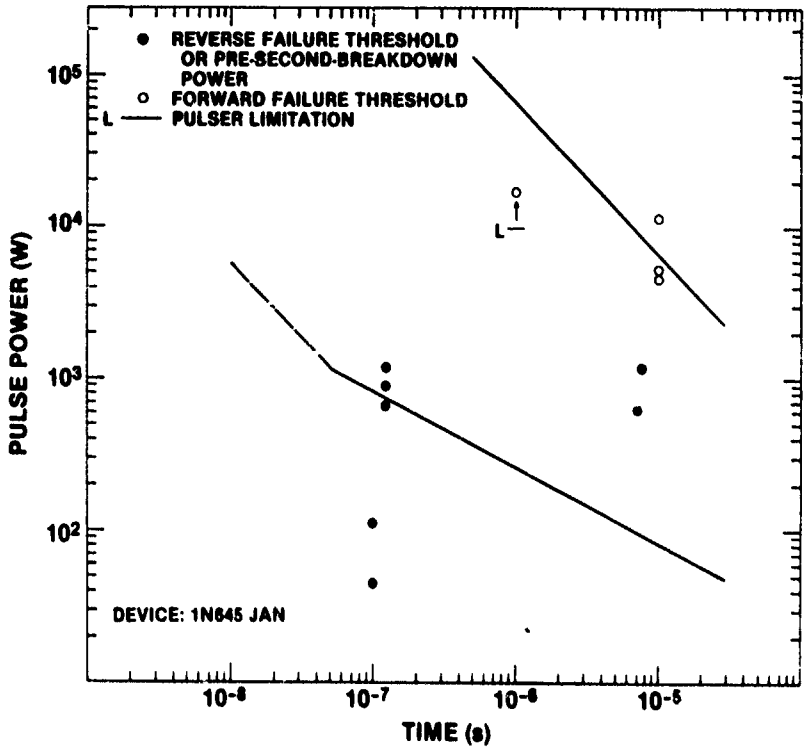

Figure A-4. Damage characteristics of 1N645 JAN.

TABLE A-4. DAMAGE CHARACTERISTICS OF 1N645 JAN

Forward						Reverse					
t_o(μs)	t(μs)	P(W)	V(V)	Z(Ω)	Condition	t_o(μs)	t(μs)	P(W)	V(V)	Z(Ω)	Condition
10	-	4,600	30	0.20	-	10	7.5	1200	1300	1,400	SBF
10	-	5,300	28	0.15	-	10	7.0	640	1100	2,000	SBF
10	-	12,000	50	0.21	-	10	0.10	110	710	4,700	ISBF
						1.0	0.12	900	1300	1,800	SBF
						1.0	0.10	45	740	12,000	SBF
						0.40	0.12	650	1400	3,200	SBF
						0.40	0.12	1200	1400	1,500	SBF

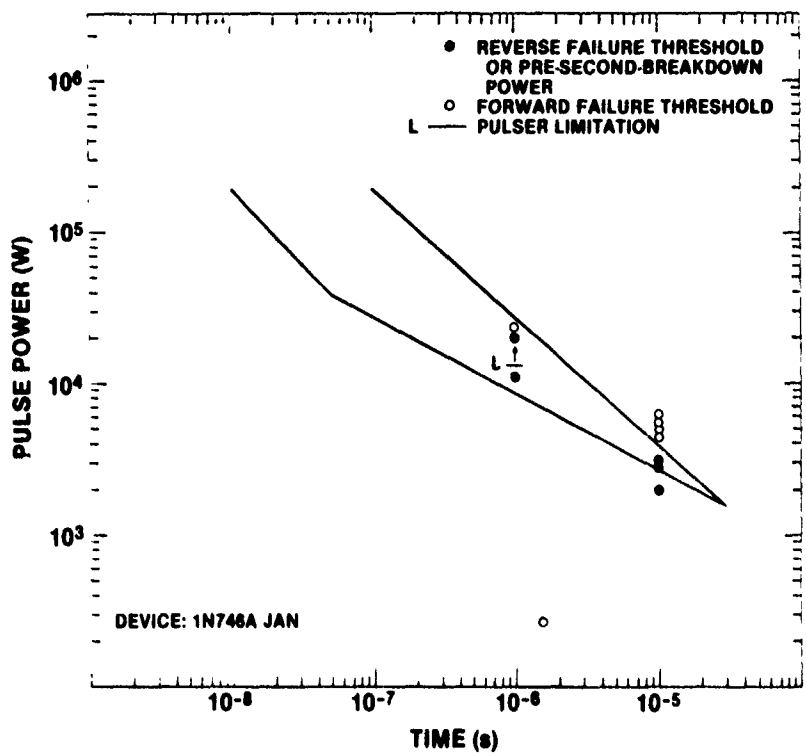

Figure A-5. Damage characteristics of 1N746A JAN.

TABLE A-5. DAMAGE CHARACTERISTICS OF 1N746A JAN

Forward						Reverse					
t_o(μs)	t(μs)	P(W)	V(V)	Z(Ω)	Condition	t_o(μs)	t(μs)	P(W)	V(V)	Z(Ω)	Condition
10	-	4500	32	0.23	-	10	-	2,000	27	0.36	-
10	-	5000	35	0.25	-	10	-	2,800	29	0.30	-
10	-	5700	36	0.23	-	10	-	3,200	30	0.28	-
10	-	6400	46	0.33	-	1.0	-	11,000	60	0.33	-
10	1.5	260	9.5	0.34	0						

Note: In forward pulsing, one device open-circuited ("O") at 1.5 μs at a low power level. Three of the other devices that were forward pulsed at 10 μs exhibited a sudden increase in impedance; after several microseconds, the current suddenly dropped to about half the previous value, while the voltage across the device slightly increased. There was no device degradation after the first occurrence of such an event. This event was also observed in reverse pulsing of one device (10-μs pulse width).

APPENDIX A

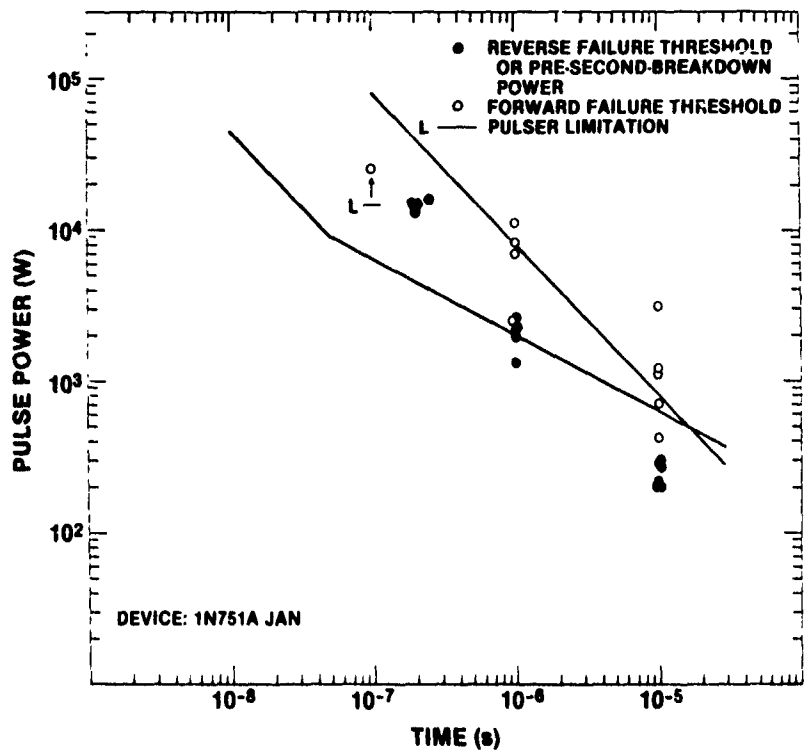

Figure A-6. Damage characteristics of 1N751A JAN.

TABLE A-6. DAMAGE CHARACTERISTICS OF 1N751A JAN

Forward						Reverse					
t_o(μs)	t(μs)	P(W)	V(V)	Z(Ω)	Condition	t_o(μs)	t(μs)	P(W)	V(V)	Z(Ω)	Condition
10	-	420	11	0.29	-	10	-	200	15	1.1	-
10	-	720	12	0.22	-	10	-	200	12	0.77	-
10	-	1,100	17	0.25	-	10	-	210	12	0.75	-
10	-	1,200	17	0.24	-	10	-	270	14	0.78	-
10	-	3,100	20	0.13	-	10	-	280	14	0.73	-
1.0	-	2,500	20	0.15	-	10	-	300	14	0.65	-
1.0	-	7,000	35	0.18	-	1.0	-	1,300	28	0.59	-
1.0	-	8,600	36	0.15	-	1.0	-	2,000	31	0.48	-
1.0	-	11,000	51	0.24	-	1.0	-	2,300	31	0.42	-
						1.0	-	2,400	34	0.48	-
						1.0	-	2,600	34	0.44	-
						0.25	-	16,000	100	0.63	-
						0.20	-	13,000	98	0.73	-
						0.20	-	15,000	100	0.75	-
						0.20	-	15,000	110	0.81	-
						0.20	-	15,000	110	0.77	-

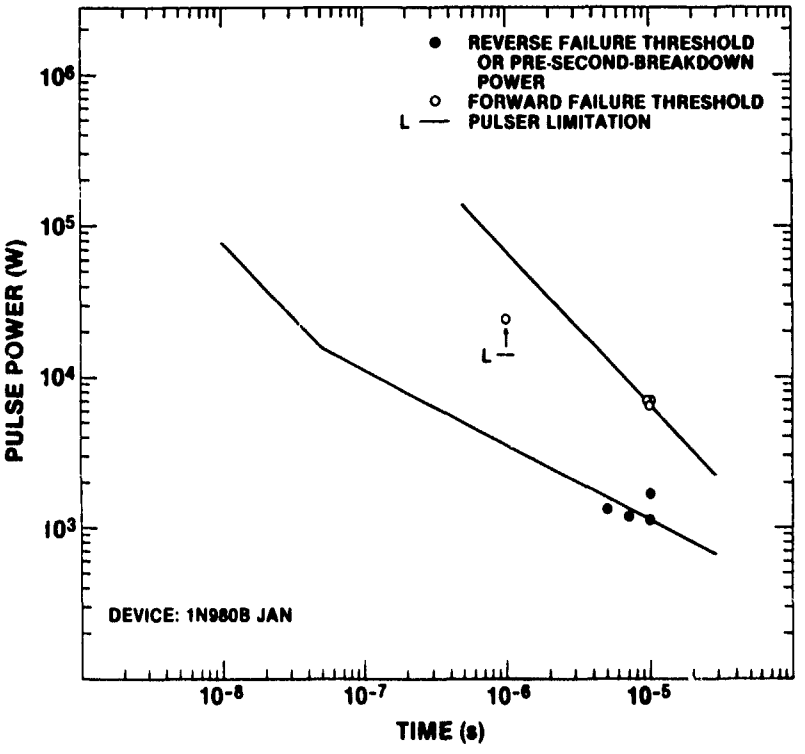

Figure A-7. Damage characteristics of 1N980B JAN.

TABLE A-7. DAMAGE CHARACTERISTICS OF 1N980B JAN

Forward						Reverse					
t_o(μs)	t(μs)	P(W)	V(V)	Z(Ω)	Condition	t_o(μs)	t(μs)	P(W)	V(V)	Z(Ω)	Condition
10	-	6800	29	0.12	-	10	-	1100	78	5.5	-
10	-	7000	31	0.14	-	10	-	1700	96	5.5	-
10	-	7000	32	0.15	-	10	7.0	1200	75	4.8	SBF
						10	5.0	1300	75	4.4	SBF

APPENDIX A

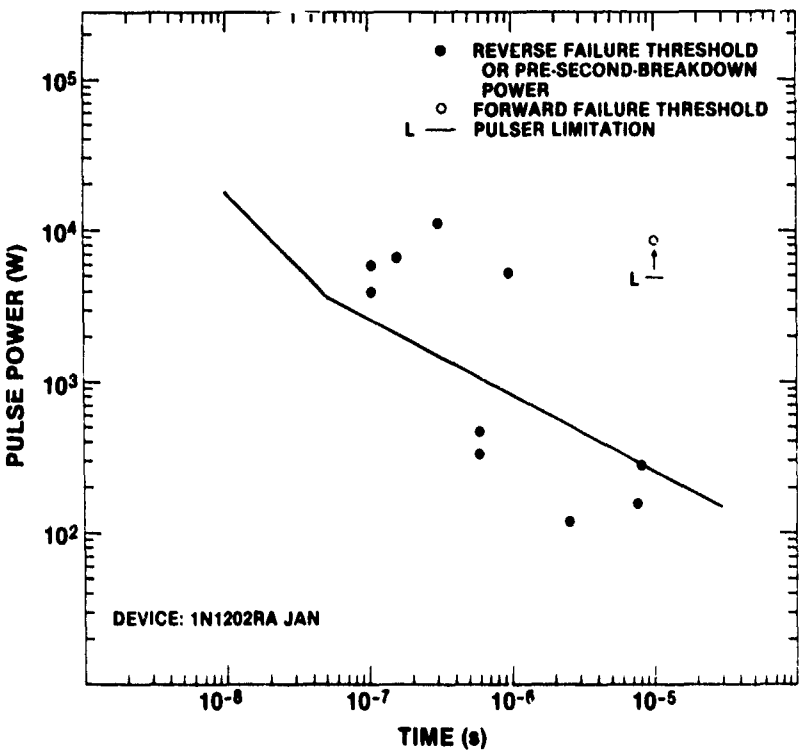

Figure A-8. Damage characteristics of 1N1202RA JAN.

TABLE A-8. DAMAGE CHARACTERISTICS OF 1N1202RA JAN

Forward						Reverse					
t_o(μs)	t(μs)	P(W)	V(V)	Z(Ω)	Condition	t_o(μs)	t(μs)	P(W)	V(V)	Z(Ω)	Condition
						10	8.0	290	910	2900	SBF
						10	7.5	160	600	2200	SBF
						10	2.5	120	660	3800	SBF
						1.0	0.95	5,400	540	54	SBF
						1.0	0.60	340	850	2100	SBF
						1.0	0.60	460	850	1600	SBF
						1.0	0.30	11,000	1300	160	SBF
						1.0	0.15	320	800	2000	SBF
						0.15	0.15	6,800	1000	160	SBF
						0.10	0.10	4,000	1000	250	SBF
						0.10	0.10	6,000	1100	200	SBF

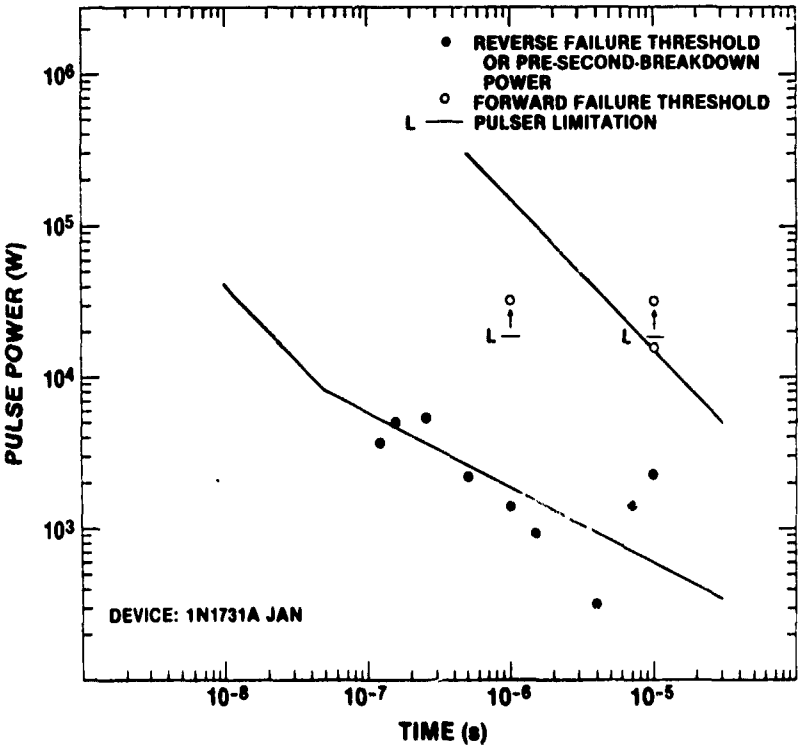

Figure A-9. Damage characteristics of 1N1731A JAN.

TABLE A-9. DAMAGE CHARACTERISTICS OF 1N1731A JAN

Forward						Reverse					
t_o(μs)	t(μs)	P(W)	V(V)	Z(Ω)	Condition	t_o(μs)	t(μs)	P(W)	V(V)	Z(Ω)	Condition
10	-	16,000	40	0.10	-	10	-	2200	1700	1300	-
						10	7.0	1400	1600	1900	SBF
						10	4.0	310	1700	9300	SBF
						10	1.5	960	1600	2700	SBF
						1.0	-	1400	1600	1800	-
						1.0	0.50	2300	2300	2300	SB
						1.0	0.25	5300	2100	830	SBF
						0.18	0.12	3800	1500	590	SBF
						0.15	-	5000	1700	580	-

APPENDIX A

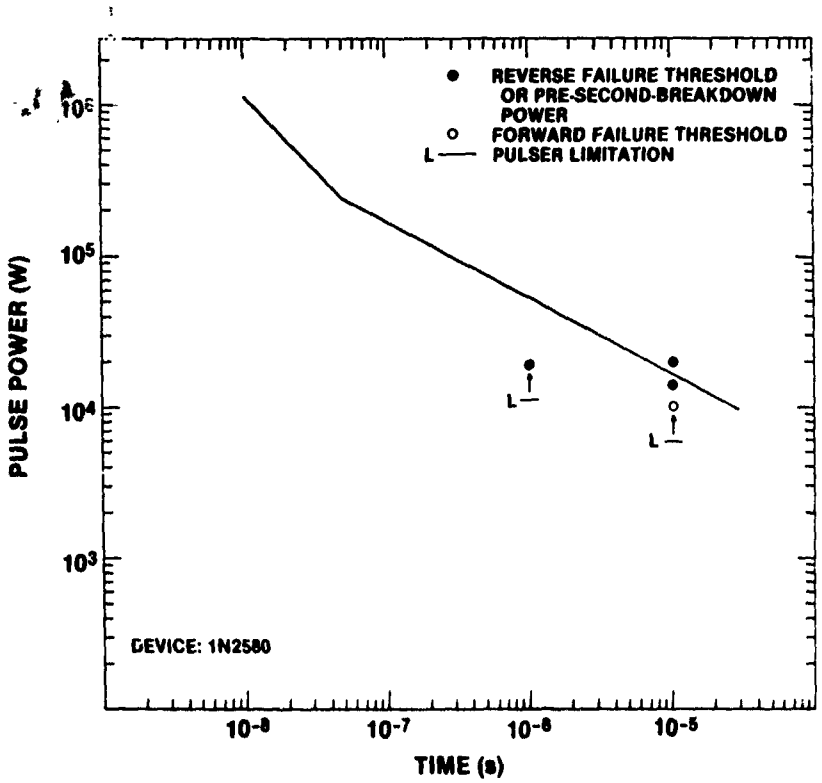

Figure A-10. Damage characteristics of 1N2580.

TABLE A-10. DAMAGE CHARACTERISTICS OF 1N2580

Forward						Reverse					
t_o(μs)	t(μs)	P(W)	V(V)	Z(Ω)	Condition	t_o(μs)	t(μs)	P(W)	V(V)	Z(Ω)	Condition
						10	-	14,000	800	45	-
						10	-	20,000	900	40	-

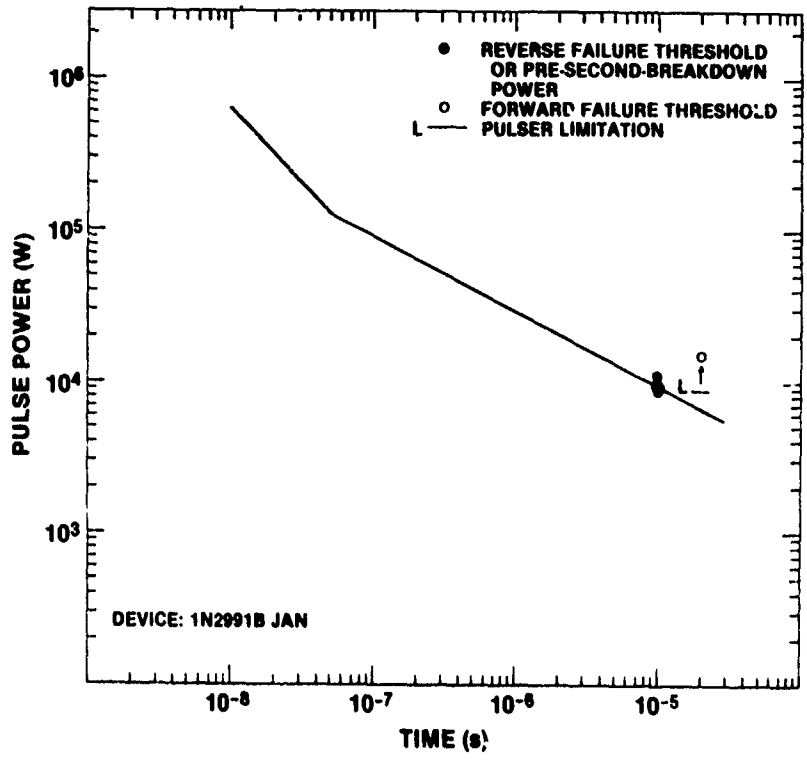

Figure A-11. Damage characteristics of 1N2991B JAN.

TABLE A-11. DAMAGE CHARACTERISTICS OF 1N2991B JAN

Forward						Reverse					
t_o(μs)	t(μs)	P(W)	V(V)	Z(Ω)	Condition	t_o(μs)	t(μs)	P(W)	V(V)	Z(Ω)	Condition
						10	-	9,000	58	0.37	-
						10	-	9,600	57	0.34	
						10	-	9,700	61	0.38	-
						10	-	9,900	58	0.34	-
						10	-	11,000	62	0.36	-
						10	-	11,000	59	0.32	-

APPENDIX A

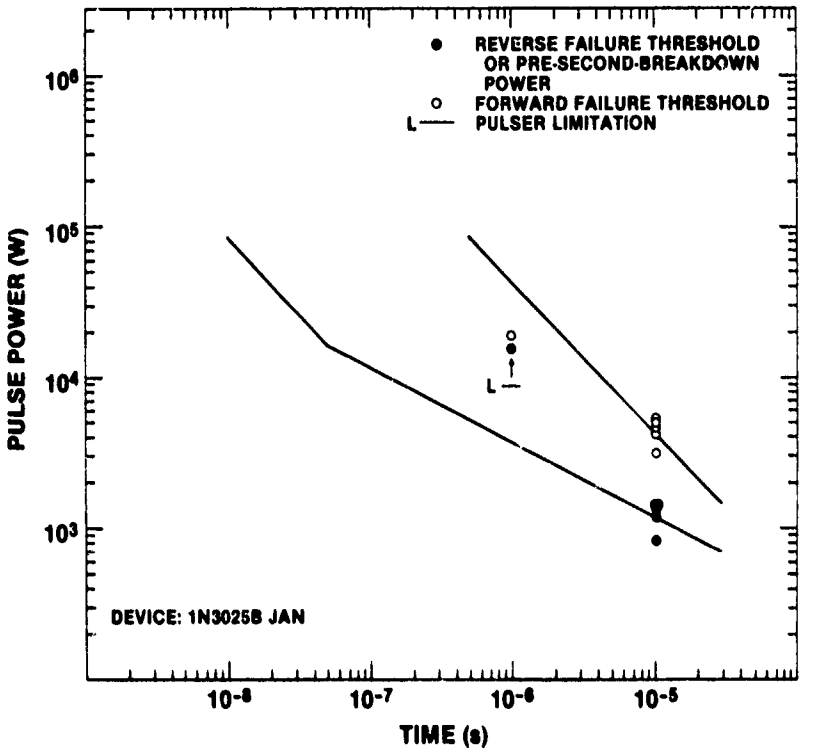

Figure A-12. Damage characteristics of 1N3025B JAN.

TABLE A-12. DAMAGE CHARACTERISTICS OF 1N3025B JAN

Forward						Reverse					
t_o(μs)	t(μs)	P(W)	V(V)	Z(Ω)	Condition	t_o(μs)	t(μs)	P(W)	V(V)	Z(Ω)	Condition
10	-	3100	15	0.07	-	10	-	830	24	0.69	-
10	-	4300	20	0.09	-	10	-	1200	25	0.51	-
10	-	4''00	18	0.06	-	10	-	1300	25	0.48	-
10	-	5100	18	0.06	-	10	-	1400	25	0.45	-
10	-	5200	19	0.07	-	10	-	1400	26	0.48	-

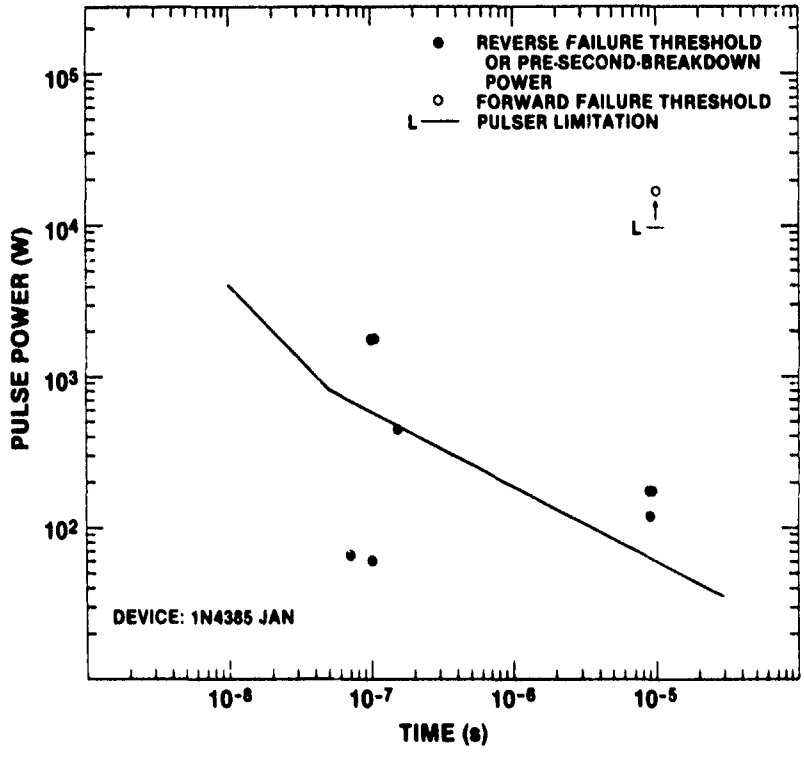

Figure A-13. Damage characteristics of 1N4385 JAN.

TABLE A-13. DAMAGE CHARACTERISTICS OF 1N4385 JAN

Forward						Reverse					
t_o(μs)	t(μs)	P(W)	V(V)	Z(Ω)	Condition	t_o(μs)	t(μs)	P(W)	V(V)	Z(Ω)	Condition
						10	9.0	120	1400	16,000	SBF
						10	9.0	180	1400	11,000	SBD
						10	9.0	180	1600	15,000	SBF
						1.0	0.15	440	1100	2,800	SBF
						1.0	0.10	60	850	12,000	SBF
						1.0	0.07	66	660	6,600	ISBF
						0.20	0.10	1800	1100	680	SBF
						0.20	0.10	1800	1200	870	SBF

APPENDIX A

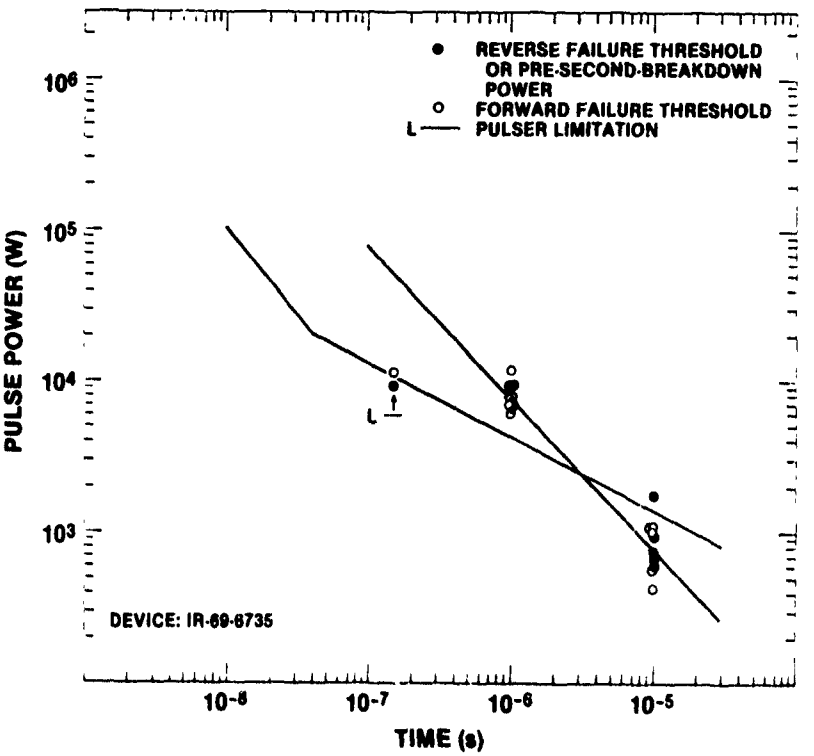

Figure A-14. Damage characteristics of IR-69-6735.

TABLE A-14. DAMAGE CHARACTERISTICS OF IR-69-6735

Forward						Reverse					
t_o(μs)	t(μs)	P(W)	V(V)	Z(Ω)	Condition	t_o(μs)	t(μs)	P(W)	V(V)	Z(Ω)	Condition
10	-	430	23	1.2	-	10	-	590	27	1.2	-
10	-	550	14	0.33	-	10	-	660	28	1.2	-
10	-	1,000	18	0.31	-	10	-	750	29	1.2	-
10	-	1,100	18	0.28	-	10	-	930	30	1.0	-
10	-	1,100	20	0.37	-	10	-	1800	42	0.96	-
1.0	-	5,900	42	0.29	-	1.0	-	6700	90	1.2	-
1.0	-	7,200	41	0.23	-	1.0	-	6900	77	0.86	-
1.0	-	8,000	32	0.13	-	1.0	-	7100	75	0.79	-
1.0	-	8,600	42	0.21	-	1.0	-	9500	90	0.85	-
1.0	-	12,000	50	0.22	-	1.0	-	9500	90	0.85	-

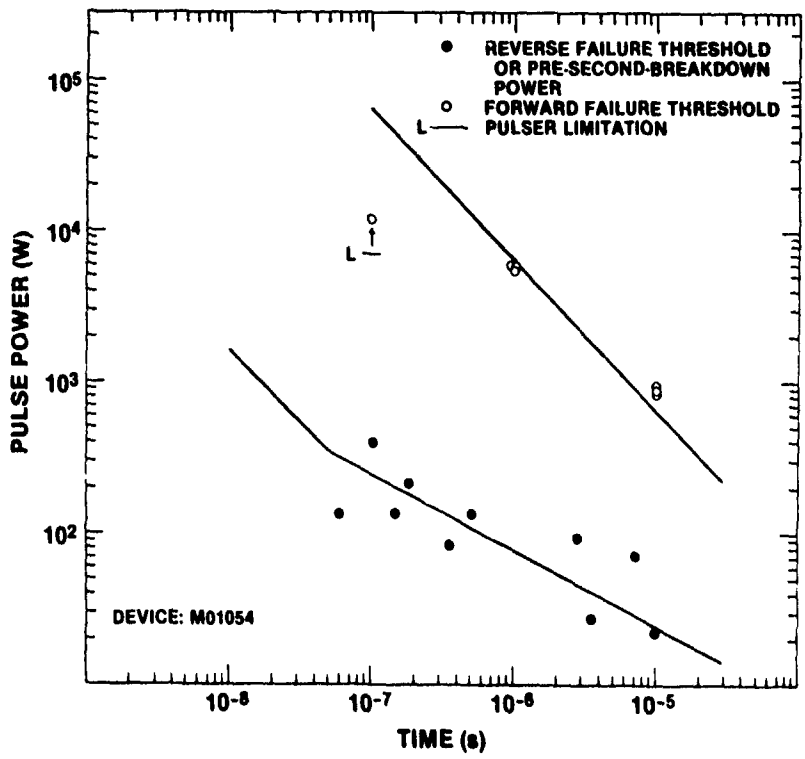

Figure A-15. Damage characteristics of MO1054.

TABLE A-15. DAMAGE CHARACTERISTICS OF MO1054

Forward						Reverse					
t_o(μs)	t(μs)	P(W)	V(V)	Z(Ω)	Condition	t_o(μs)	t(μs)	P(W)	V(V)	Z(Ω)	Condition
10	-	850	9.5	0.11	-	10	-	22	530	13,000	-
10	-	880	11	0.14	-	10	7.0	72	720	7,200	SBF
10	-	950	10	0.11	-	10	3.5	26	650	16,000	SBF
1.0	-	4200	26	0.16	-	10	2.9	95	680	4,900	SB
1.0	-	5600	28	0.15	-	1.0	0.50	130	530	2,100	SB
1.0	-	5900	31	0.16	-	1.0	0.35	84	600	4,300	SB
1.0	-	6000	32	0.17	-	1.0	0.15	130	550	2,300	SB
						0.20	0.18	210	400	780	SB
						0.20	0.10	400	480	570	SBF
						0.20	0.06	130	380	1,100	ISBF

APPENDIX A

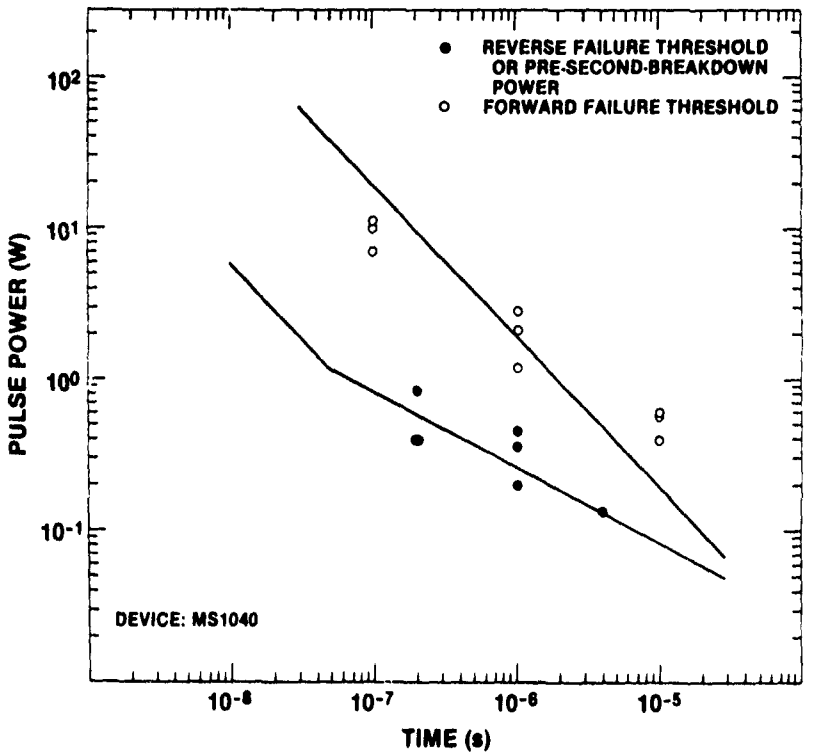

Figure A-16. Damage characteristics of MS1040.

TABLE A-16. DAMAGE CHARACTERISTICS OF MS1040

Forward						Reverse					
t_o(μs)	t(μs)	P(W)	V(V)	Z(Ω)	Condition	t_o(μs)	t(μs)	P(W)	V(V)	Z(Ω)	Condition
10	-	0.40	1.7	7.0	-	10	4.0	0.13	2.4	44	0
10	-	0.60	1.8	5.3	-	1.0	-	0.20	4.0	80	-
10	-	0.60	2.3	8.8	-	1.0	-	0.35	4.3	53	-
1.0	-	1.2	2.9	6.7	-	1.0	-	0.45	4.9	53	-
1.0	-	2.1	3.3	5.2	-	0.20	-	0.40	4.0	40	-
1.0	-	2.8	3.3	4.0	-	0.20	-	0.40	4.9	60	-
0.10	-	6.9	6.0	5.2	-	0.20	-	0.85	5.7	38	-
0.10	-	10	5.8	3.3	-						
0.10	-	11	7.0	4.7	-						

Note: In reverse pulsing, one device open-circuited at 4 μs ("O").

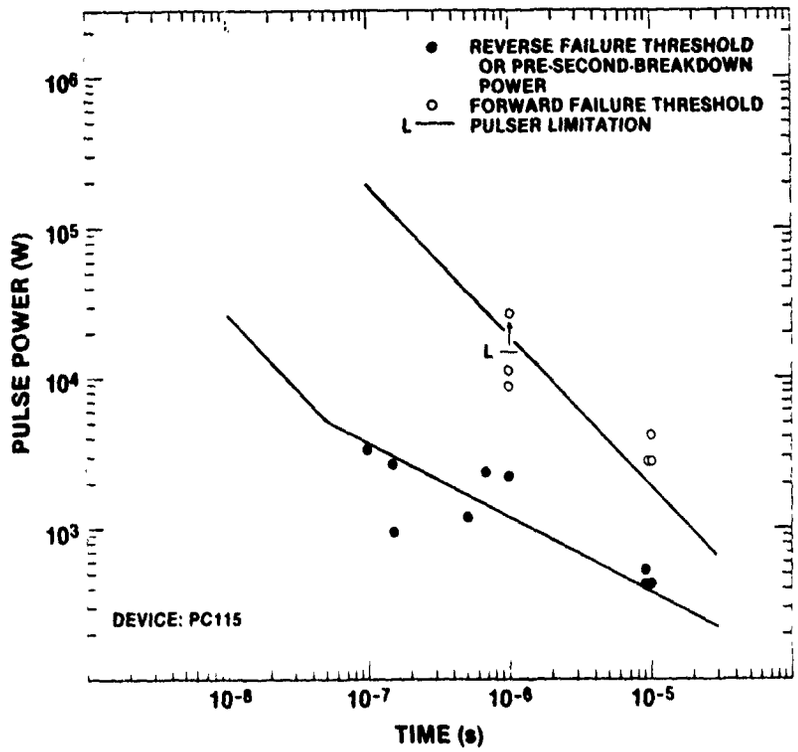

Figure A-17. Damage characteristics of PC115.

TABLE A-17. DAMAGE CHARACTERISTICS OF PC115

Forward						Reverse					
t_o(μs)	t(μs)	P(W)	V(V)	Z(Ω)	Condition	t_o(μs)	t(μs)	P(W)	V(V)	Z(Ω)	Condition
10	-	2,800	15	0.08	-	10	-	430	230	120	-
10	-	2,900	14	0.07	-	10	9.0	430	230	120	SBF
10	-	4,100	17	0.07	-	10	9.0	530	260	120	SBF
1.0	-	8,700	50	0.29	-	1.0	-	2200	290	38	-
1.0	-	11,000	51	0.24	-	1.0	0.65	2400	340	48	SBF
						1.0	0.50	1200	270	62	SBF
						0.15	-	950	180	36	-
						0.15	-	2600	310	36	-
						0.15	0.10	3300	330	33	SBF

APPENDIX A

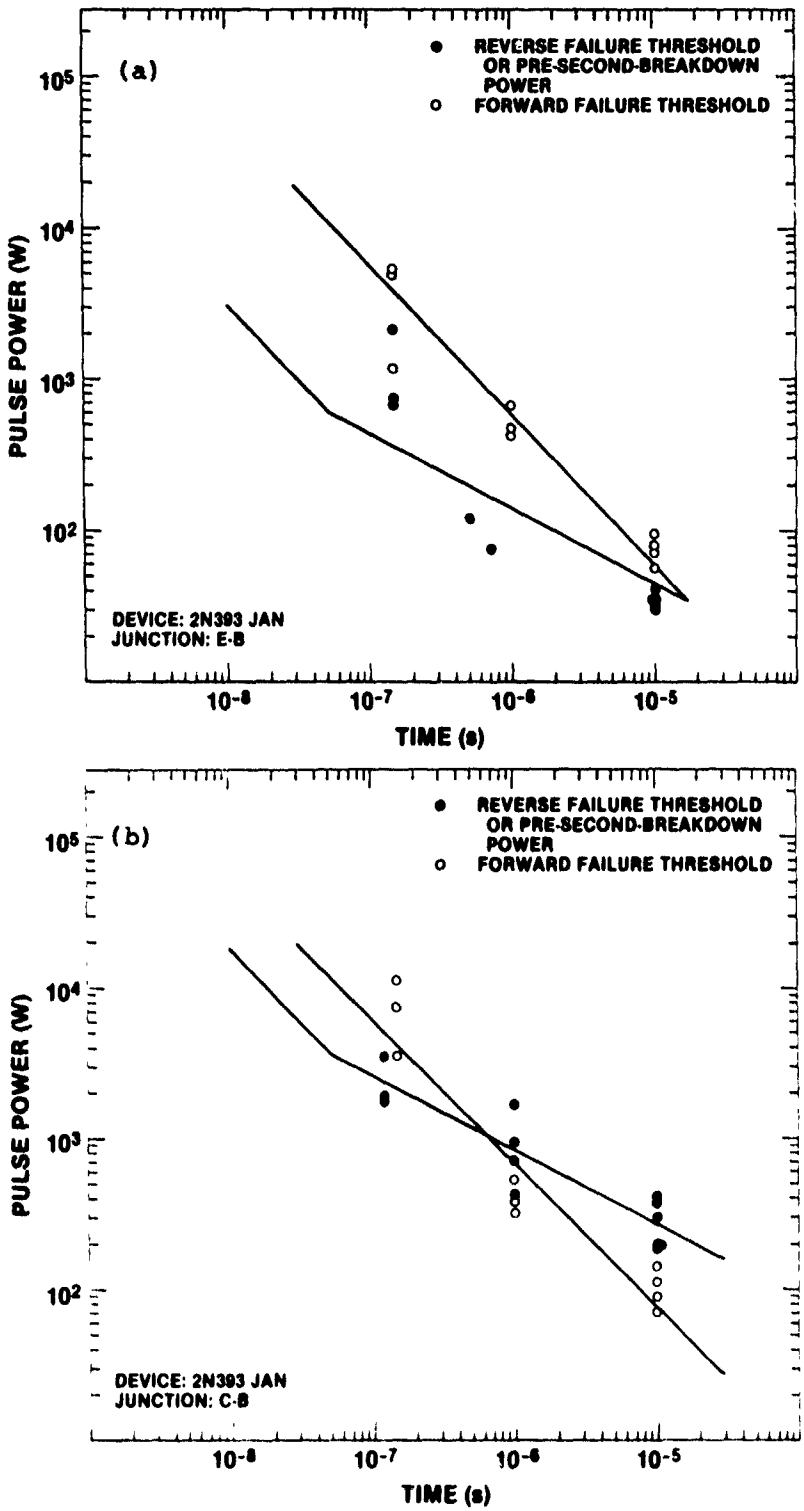

Figure A-18. Damage characteristics of 2N393 JAN: (a) E-B junction and (b) C-B junction.

TABLE A-18. DAMAGE CHARACTERISTICS OF 2N393 JAN

Junction	Forward						Reverse					
	t_o(μs)	t(μs)	P(W)	V(V)	Z(Ω)	Condition	t_o(μs)	t(μs)	P(W)	V(V)	Z(Ω)	Condition
E-B	10	-	57	34	20	-	10	-	30	180	1000	-
	10	-	72	30	12	-	10	-	32	180	1000	-
	10	-	80	34	14	-	10	-	33	170	880	-
	10	-	92	38	16	-	10	-	34	170	890	-
	10	-	97	40	16	-	10	-	39	170	740	-
	1.0	-	410	76	14	-	1.0	0.70	73	350	1700	SBF
	1.0	-	460	80	14	-	1.0	0.60	100	320	1000	SBF
	1.0	-	660	100	16	-	1.0	0.50	120	380	1200	SBF
	0.15	-	1200	210	37	-	0.15	-	650	380	230	-
	0.15	-	5000	550	60	-	0.15	-	690	400	230	-
	0.15	-	5400	580	62	-	0.15	-	2100	580	160	-
C-B	10	-	72	34	16	-	10	-	200	160	120	-
	10	-	89	36	14	-	10	-	200	190	180	-
	10	-	110	40	15	-	10	-	300	140	71	-
	10	-	140	44	14	-	10	-	380	210	120	-
	10	-	200	44	10	-	10	-	400	200	100	-
	1.0	-	320	73	17	-	1.0	-	420	350	290	-
	1.0	-	380	71	13	-	1.0	-	700	340	170	-
	1.0	-	520	76	11	-	1.0	-	930	400	170	-
	0.15	-	3,500	520	77	-	1.0	-	1700	490	140	-
	0.15	-	7,500	750	75	-	0.12	-	1800	500	140	-
	0.15	-	11,000	570	30	-	0.12	-	1900	550	160	-
							0.12	-	3600	550	84	-

Note: A noteworthy feature of the response of both junctions of this device type to forward-biasing pulses is the large increase in device impedance near the damage level at a pulse width approaching 100 ns.

APPENDIX A

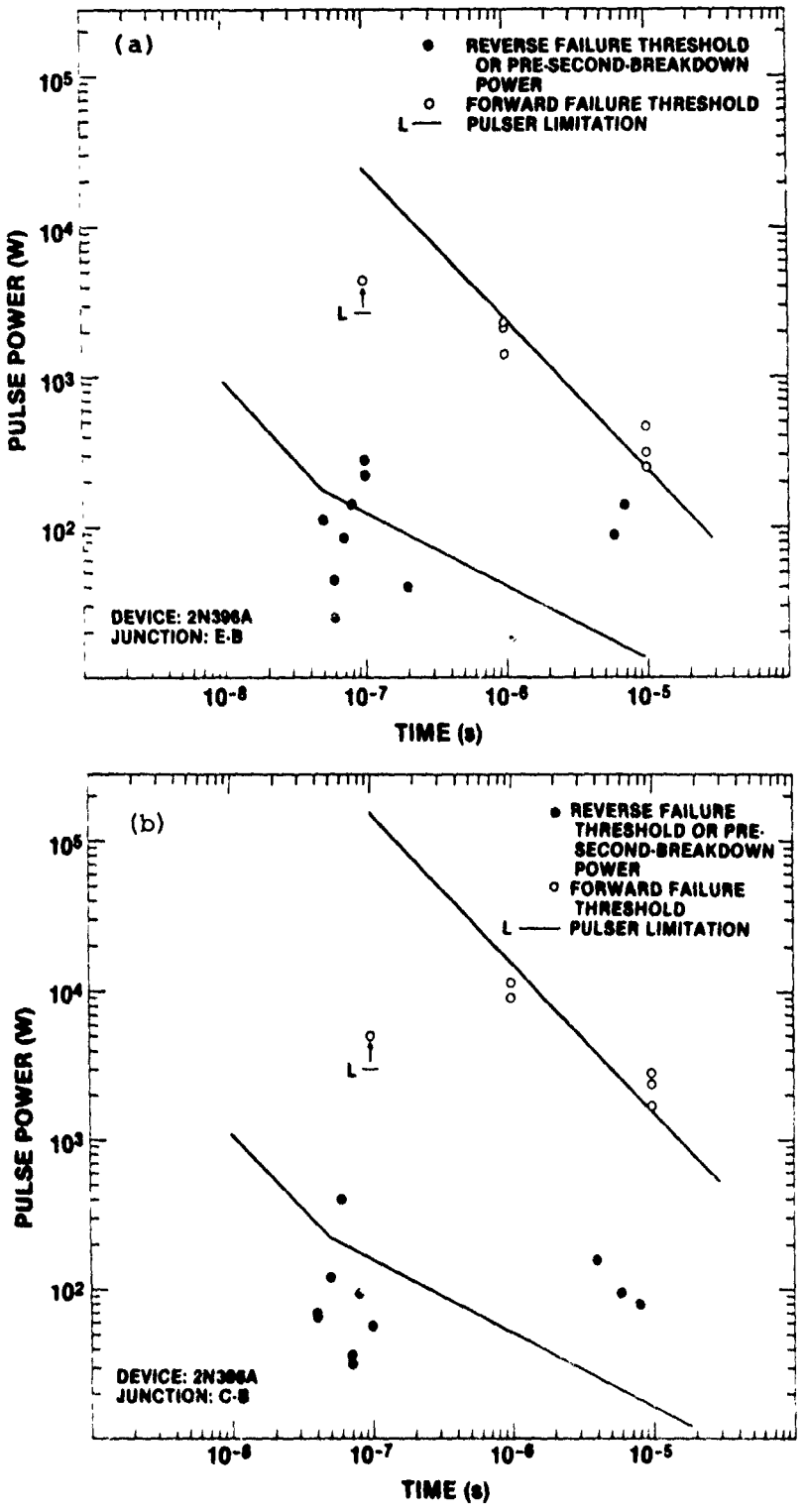

Figure A-19. Damage characteristics of 2N396A: (a) E-B junction and (b) C-B junction.

TABLE A-19. DAMAGE CHARACTERISTICS OF 2N396A

Junction	Forward						Reverse					
	t_o(μs)	t(μs)	P(W)	V(V)	Z(Ω)	Condition	t_o(μs)	t(μs)	P(W)	V(V)	Z(Ω)	Condition
E-B	10	-	250	20	1.6	-	10	7.2	90	320	1200	SB
	10	-	320	21	1.4	-	10	6.0	140	420	1300	SB
	10	-	470	22	1.1	-	10	0.20	39	260	1800	ISB
	1.0	-	1400	45	1.4	-	1.0	0.10	220	500	1100	SB
	1.0	-	2100	51	1.2	-	1.0	0.10	290	500	860	SB
	1.0	-	2200	52	1.2	-	1.0	0.08	140	300	670	ISB
							0.30	0.07	84	280	930	SBD
							0.15	0.06	25	160	1100	ISB
							0.15	0.06	44	200	910	SB
							0.15	0.05	110	200	360	ISB
C-B	10	-	1,700	32	0.60	-	10	8.0	80	310	1200	SB
	10	-	2,400	30	0.38	-	10	6.0	95	380	1500	SB
	10	-	2,800	35	0.43	-	10	4.0	160	350	770	SB
	1.0	-	9,000	65	0.47	-	1.0	0.10	56	200	710	ISB
	1.0	-	11,000	86	0.68	-	1.0	0.08	95	320	1100	ISB
							1.0	0.07	32	190	1100	ISB
							1.0	0.07	35	150	640	ISB
							0.20	0.06	400	450	500	SB
							0.20	0.05	120	260	580	ISB
							0.20	0.04	54	160	440	ISB
							0.20	0.04	75	210	600	ISB

Note: At a 0.15-μs pulse width, the E-B junction exhibited nondegrading SB with the pre-second-breakdown power being lower by a factor of 5 to 20 than the power for failure.

APPENDIX A

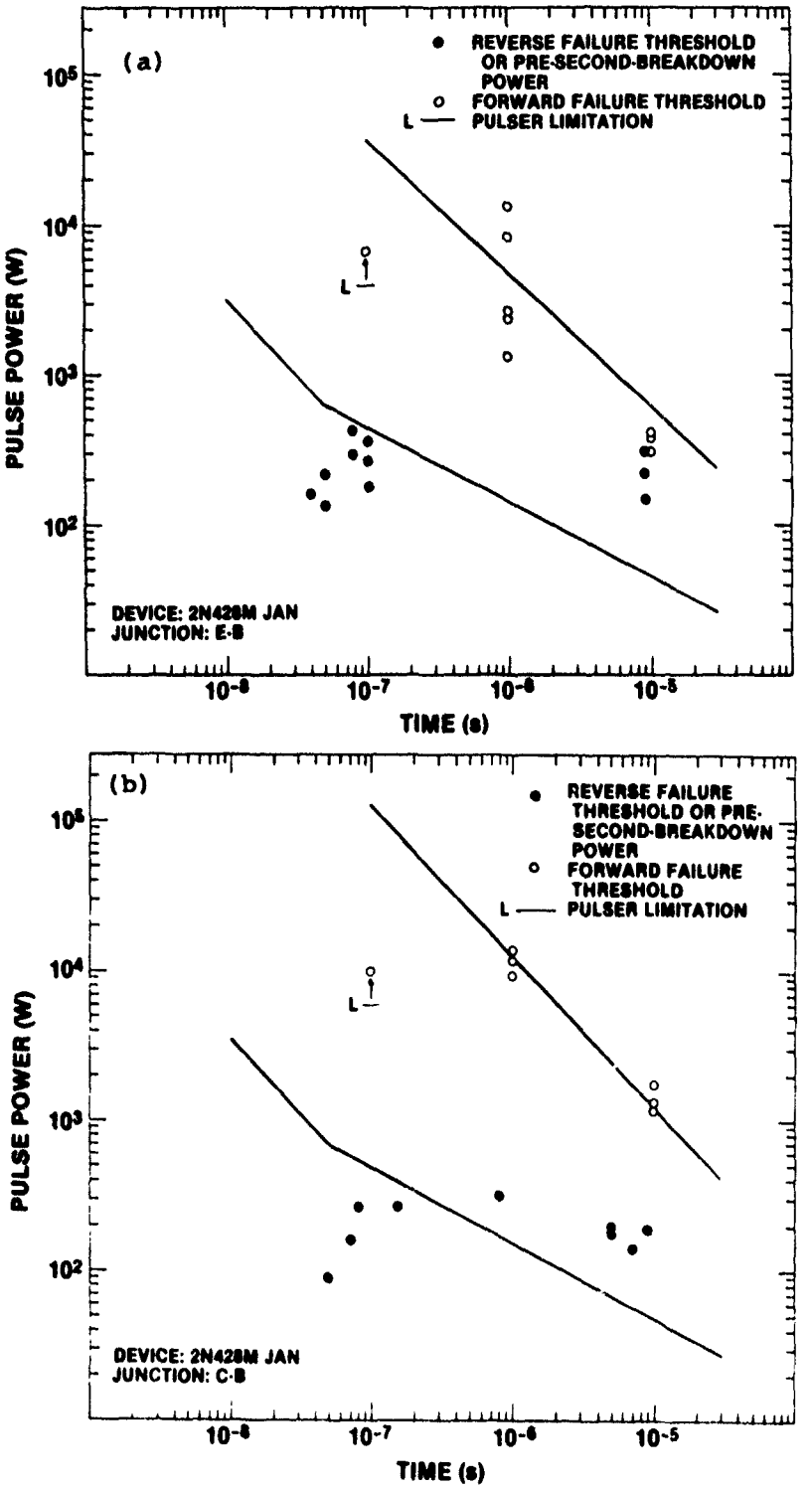

Figure A-20. Damage characteristics of 2N428M JAN: (a) E-B junction and (b) C-B junction.

TABLE A-20. DAMAGE CHARACTERISTICS OF 2N428M JAN

Junction	Forward						Reverse					
	t_o(μs)	t(μs)	P(W)	V(V)	Z(Ω)	Condition	t_o(μs)	t(μs)	P(W)	V(V)	Z(Ω)	Condition
E-B	10	-	320	21	1.4	-	10	9.0	150	270	480	SB
	10	-	380	21	1.2	-	10	9.0	230	270	320	SB
	10	-	400	23	1.3	-	10	9.0	320	380	440	SB
	1.0	-	1,300	59	2.7	-	1.0	0.10	180	410	960	SB
	1.0	-	2,400	51	1.1	-	1.0	0.10	260	290	320	SB
	1.0	-	2,600	60	1.4	-	1.0	0.10	360	750	1500	SB
	1.0	-	8,400	75	0.67	-	0.20	0.08	410	370	330	SB
	1.0	-	13,000	93	0.67	-	0.15	0.08	300	600	1200	SB
							0.15	0.05	130	280	620	ISB
							0.15	0.05	210	260	330	ISB
							0.15	0.04	160	240	380	ISBF
C-B	10	-	1,200	26	0.54	-	10	9.0	140	300	670	SB
	10	-	1,300	26	0.53	-	10	7.0	190	380	760	SB
	10	-	1,700	32	0.59	-	10	5.0	180	350	700	SB
	1.0	-	9,400	82	0.72	-	10	5.0	200	300	450	SB
	1.0	-	12,000	92	0.71	-	1.0	0.80	320	510	820	SB
	1.0	-	14,000	100	0.73	-	1.0	0.15	270	620	1400	SB
							1.0	0.07	160	320	660	ISB
							0.25	0.08	270	400	590	SB
							0.15	0.05	90	260	750	ISB

Note: Cases of multiple breakdown were observed in reverse pulsing of the E-B junction.

APPENDIX A

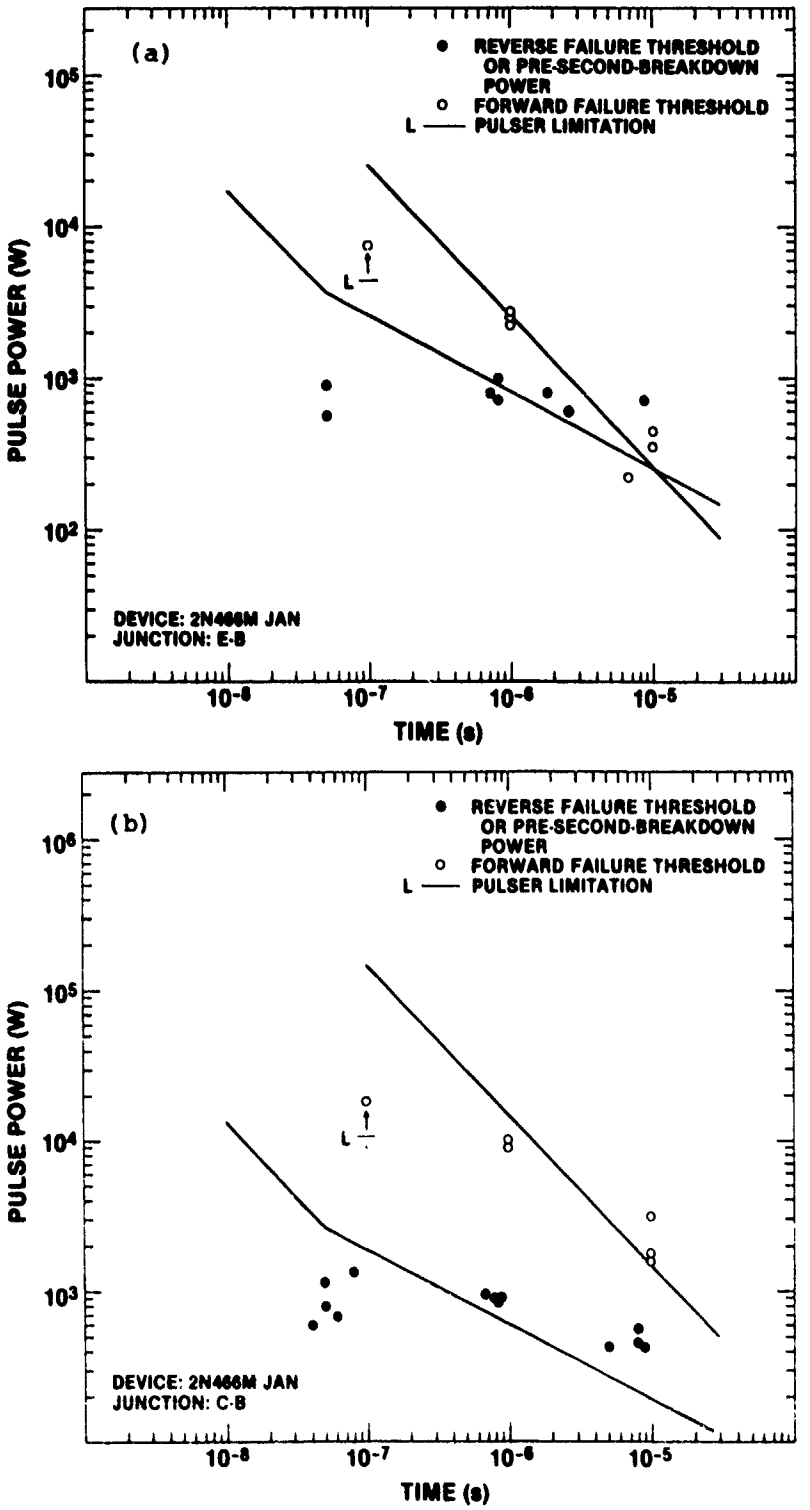

Figure A-21. Damage characteristics of 2N466M JAN: (a) E-B junction and (b) C-B junction.

TABLE A-21. DAMAGE CHARACTERISTICS OF 2N466M JAN

Junction	Forward						Reverse					
	t_o(μs)	t(μs)	P(W)	V(V)	Z(Ω)	Condition	t_o(μs)	t(μs)	P(W)	V(V)	Z(Ω)	Condition
E-B	10	-	360	23	1.5	-	10	8.5	720	360	180	SBD
	10	-	450	25	1.4	-	10	2.5	590	470	370	SB
	10	6.5	220	22	2.2	EVF	10	1.8	800	550	380	SBD
	1.0	-	2200	71	2.2	-	1.0	0.80	690	550	440	SBF
	1.0	-	2500	69	1.9	-	1.0	0.80	1000	750	540	SBF
	1.0	-	2700	75	2.1	-	1.0	0.70	780	620	490	SB
							0.18	0.05	570	480	400	ISBF
							0.18	0.05	910	700	540	ISBF
C-B	10	-	1,600	52	1.7	-	10	9.0	410	320	250	SB
	10	-	1,800	41	0.96	-	10	8.0	450	250	140	SB
	10	-	3,100	46	0.67	-	10	8.0	570	300	160	SB
	1.0	-	8,800	110	1.3	-	10	5.0	410	410	410	SB
	1.0	-	10,000	110	1.2	-	1.0	0.90	870	670	520	SB
							1.0	0.85	820	780	740	SBF
							1.0	0.80	900	750	620	SBF
							1.0	0.65	940	720	550	SBF
							0.40	0.05	800	720	660	ISBF
							0.40	0.05	1100	750	500	ISBF
							0.40	0.04	600	600	600	ISB
							0.20	0.08	1300	850	560	SBF
							0.20	0.06	660	550	460	SB

Note: An event resembling second breakdown occurred in forward pulsing of the E-B junctions; because of a low circuit impedance, the voltage across the device dropped only little, but the current increased significantly. Failure was assumed to have occurred at the beginning of the current increase (6.5 μs, "EVF").

APPENDIX A

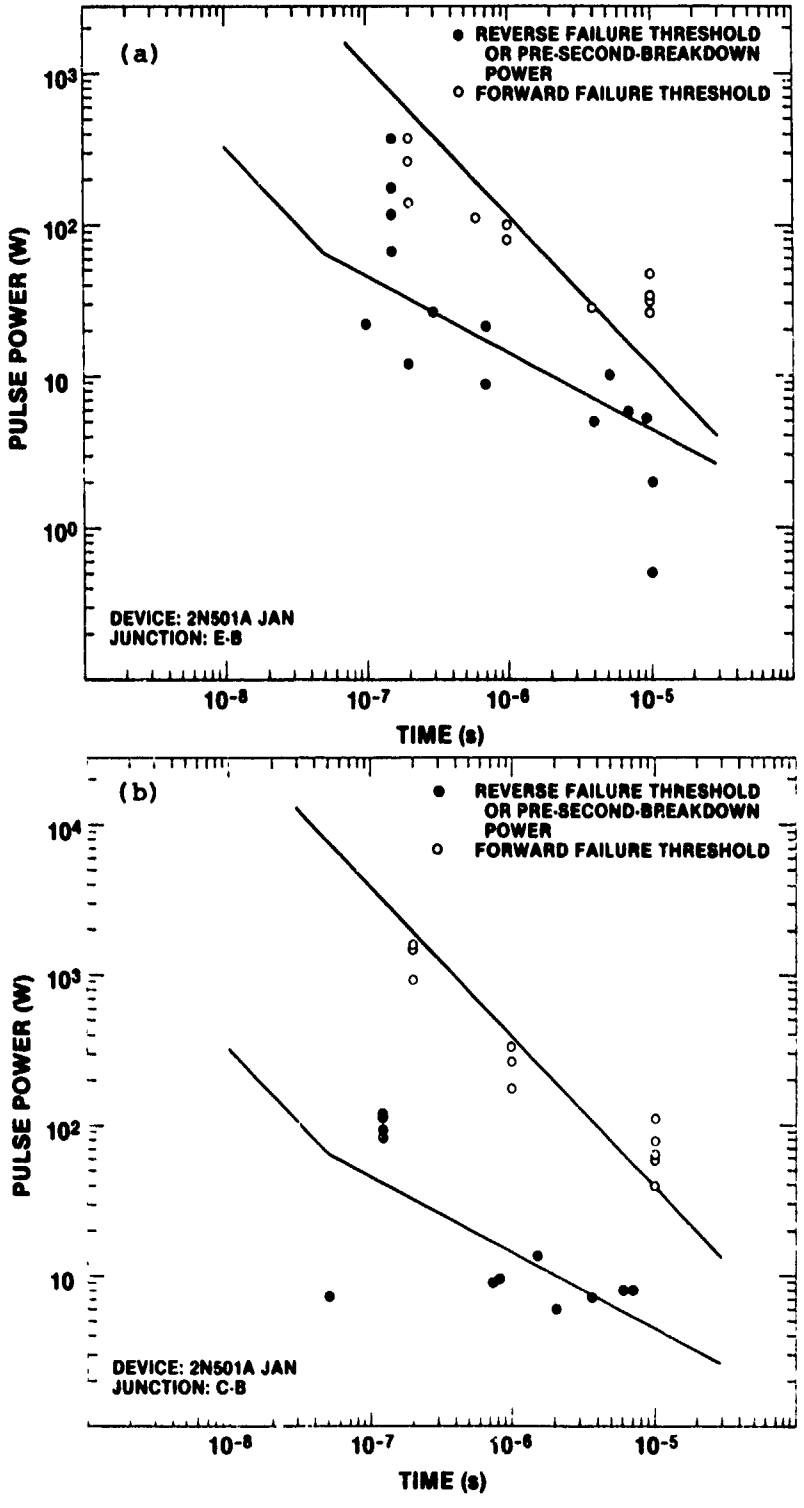

Figure A-22. Damage characteristics of 2N501A JAN: (a) E-B junction and (b) C-B junction.

TABLE A-22. DAMAGE CHARACTERISTICS OF 2N501A JAN

Junction	Forward						Reverse					
	t_o(μs)	t(μs)	P(W)	V(V)	Z(Ω)	Condition	t_o(μs)	t(μs)	P(W)	V(V)	Z(Ω)	Condition
E-B	10	-	26	14	6.9	-	10	-	0.50	14	420	-
	10	-	31	14	6.3	-	10	-	2.0	33	540	-
	10	-	33	18	9.8	-	10	9.7	5.4	72	960	SBD
	10	-	47	16	5.1	-	10	7.0	6.0	67	750	SBF
	10	4.0	28	14	7.0	EVF	10	5.0	10	80	620	SBF
	1.0	-	80	25	7.8	-	10	4.0	5.1	60	710	SBF
	1.0	-	100	22	4.8	-	1.0	0.70	9.0	60	400	SB
	1.0	0.60	110	24	5.1	EVF	1.0	0.70	21	70	230	SB
	0.20	-	140	26	4.8	-	1.0	0.30	26	60	140	SB
	0.20	-	260	34	4.5	-	1.0	0.20	12	65	360	SBF
	0.20	-	380	41	4.4	-	1.0	0.10	22	72	240	SBF
							0.15	-	66	60	54	-
							0.15	-	120	70	39	-
							0.15	-	180	92	46	-
							0.15	-	370	100	30	-
C-B	10	-	39	14	5.4	-	10	7.0	7.8	60	460	SB
	10	-	58	17	5.1	-	10	6.0	7.8	56	400	SB
	10	-	63	16	4.2	-	10	3.5	7.0	62	550	SB
	10	-	80	18	4.1	-	10	2.0	5.9	62	650	SB
	10	-	110	21	4.2	-	10	1.5	13	62	290	SBF
	1.0	-	180	34	6.4	-	1.0	0.80	9.7	65	440	SB
	1.0	-	260	34	4.5	-	1.0	0.70	8.7	46	240	SBD
	1.0	-	330	39	4.6	-	1.0	0.05	7.2	55	420	SB
	0.20	-	940	61	3.9	-	0.12	-	82	58	41	-
	0.20	-	1500	74	3.6	-	0.12		97	52	28	-
	0.20	-	1600	81	4.2	-	0.12		120	52	23	-
							0.12		120	53	22	-

Note: Two second-breakdown-like events occurred in forward pulsing of the E-B junctions: at 4 μs, the voltage dropped from 14 to 10 V with no change in current; at 0.6 μs, the current increased from 4.8 to 6.4 A at practically constant voltage (low impedance pulse source). Failure was assumed to have occurred at these times ("EVF"). One case of multiple breakdown occurred in reverse pulsing of the C-B junctions.

APPENDIX A

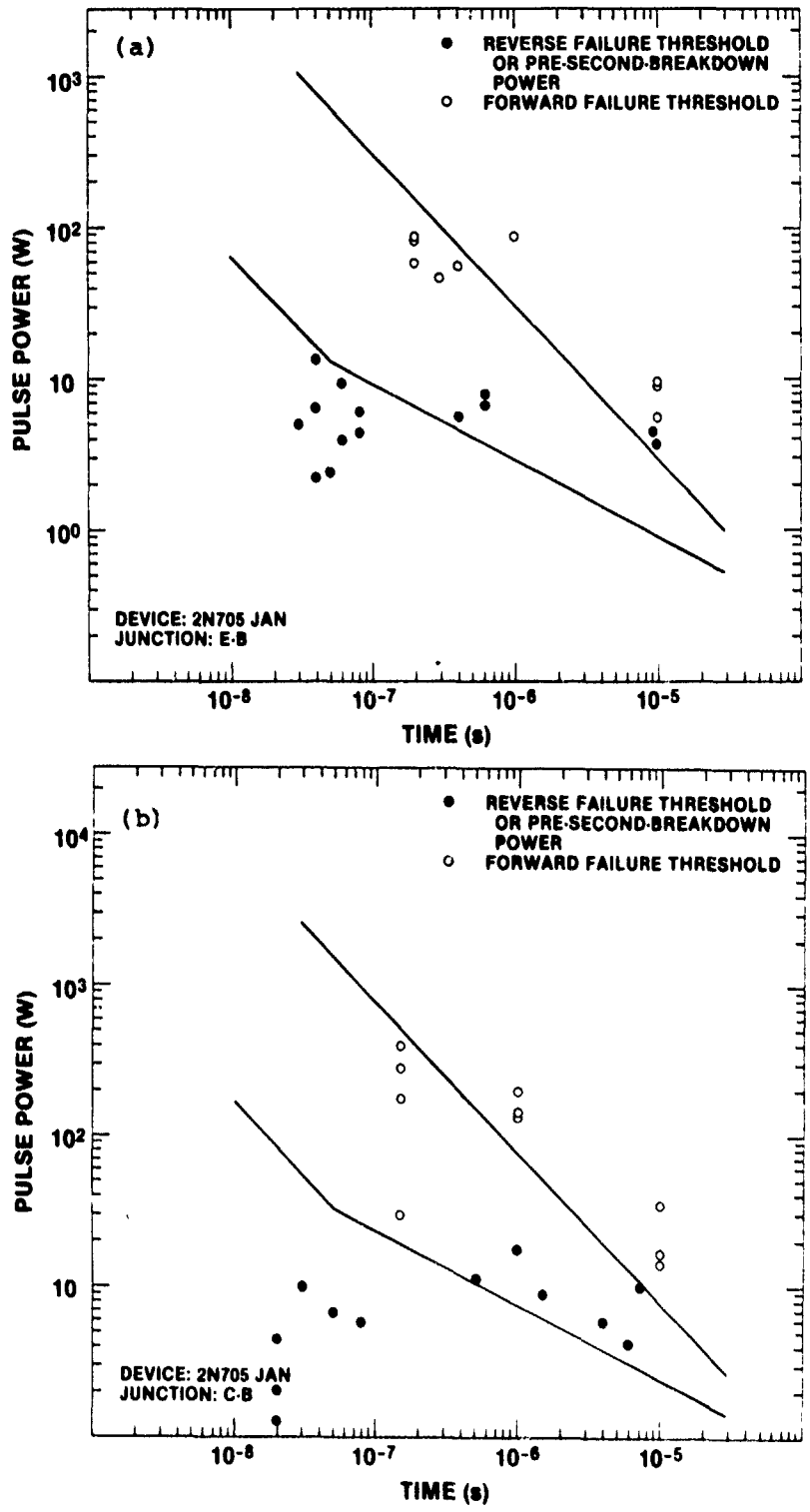

Figure A-23. Damage characteristics of 2N705 JAN: (a) E-B junction and (b) C-B junction.

TABLE A-23. DAMAGE CHARACTERISTICS OF 2N705 JAN

Junction	Forward						Reverse					
	t_o(μs)	t(μs)	P(W)	V(V)	Z(Ω)	Condition	t_o(μs)	t(μs)	P(W)	V(V)	Z(Ω)	Condition
E-B	10	-	5.6	4.1	3.0	-	10	9.5	3.8	48	610	SB
	10	-	9.5	4.0	1.7	-	10	9.0	4.5	50	560	SB
	10	-	9.7	4.6	2.2	-	10	0.08	4.5	28	170	ISBF
	1.0	-	89	9.7	1.1	-	10	0.08	5.8	31	160	ISBF
	1.0	0.40	56	11	2.2	EVF	1.0	0.60	6.8	57	480	SB
	1.0	0.30	47	12	2.8	EVF	1.0	0.60	7.8	32	130	SB
	0.20	-	58	10	1.9	-	1.0	0.40	5.5	55	550	SB
	0.20	-	82	12	1.9	-	0.28	0.05	2.4	30	380	ISB
	0.20	-	84	12	1.7	-	0.18	0.06	4.0	40	400	SBF
							0.13	0.06	9.5	32	110	SB
							0.10	0.04	2.3	16	110	ISB
							0.10	0.03	5.1	32	200	ISB
							0.08	0.04	6.2	28	130	ISB
							0.06	0.04	13	40	120	SB
C-B	10	-	14	3.0	0.65	-	10	7.0	10	64	400	SBF
	10	-	17	4.0	0.93	-	10	6.0	4.3	43	430	SB
	10	-	36	4.1	0.47	-	10	4.0	6.0	45	340	SB
	1.0	-	130	8.3	53	-	10	1.5	8.8	55	340	SBF
	1.0	-	140	8.5	0.52	-	10	1.0	18	50	140	SBF
	1.0	-	200	9.2	0.42	-	1.0	0.50	11	50	230	SB
	0.15	-	30	6.5	1.4	-	1.0	0.08	6.0	30	150	SB
	0.15	-	180	13	0.97	-	1.0	0.05	6.6	30	140	SB
	0.15	-	290	18	1.1	-	1.0	0.03	10	37	130	ISBF
	0.15	-	400	20	1.0	-	0.15	0.02	1.3	10	77	ISBF
							0.13	0.02	4.4	21	100	ISB
							0.10	0.02	2.0	12	72	ISBF

Note: Two second-breakdown-like events (at 0.4 and 0.3 μs) occurred in forward pulsing of the E-B junctions; the voltage dropped little (low impedance pulse source) but the current suddenly increased. Failure was assumed to have occurred at these times ("EVF"). One case of multiple breakdown was observed in reverse pulsing of the E-B junctions.

APPENDIX A

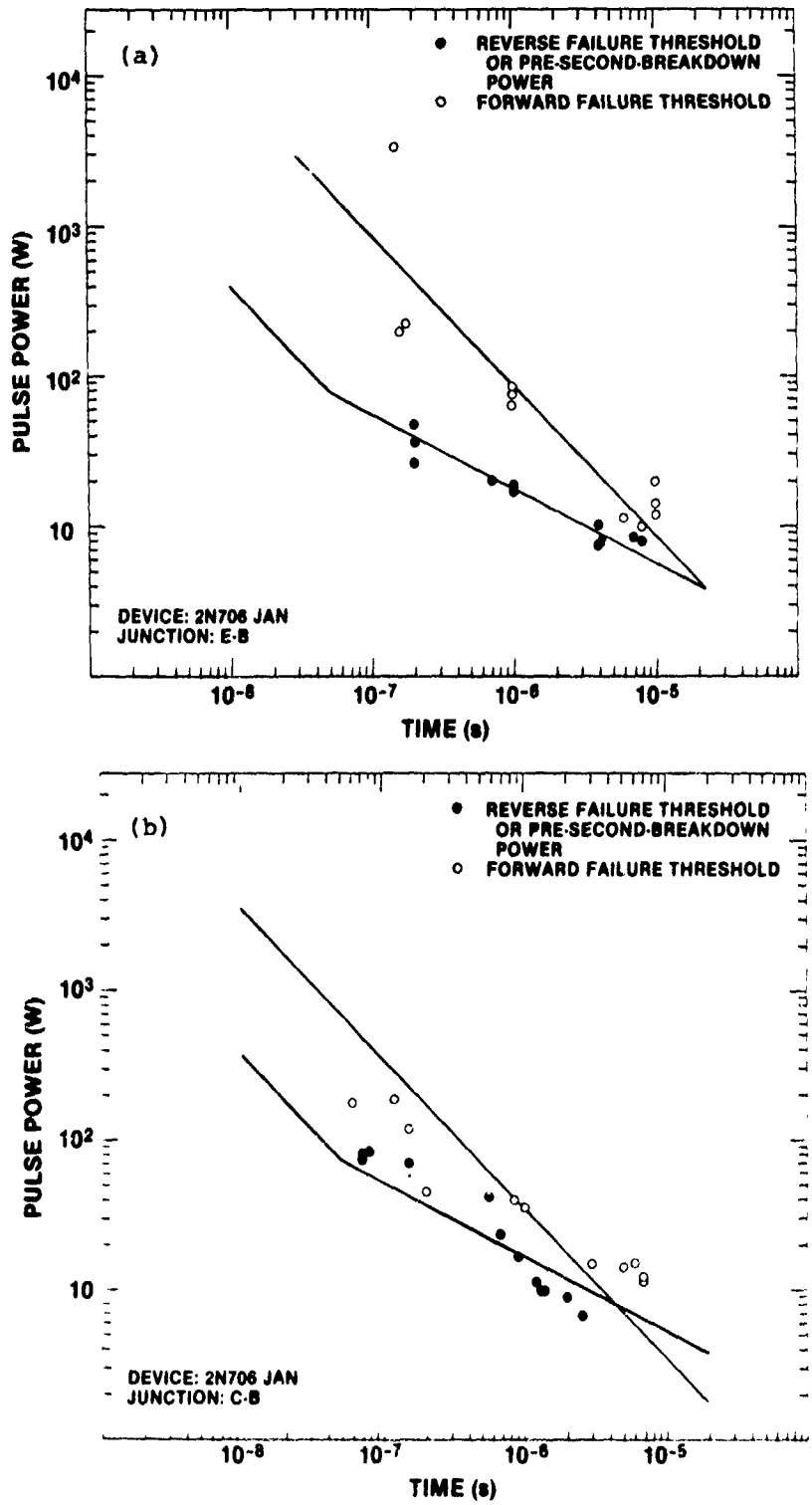

Figure A-24. Damage characteristics of 2N706 JAN: (a) E-B junction and (b) C-B junction.

TABLE A-24. DAMAGE CHARACTERISTICS OF 2N706 JAN

Junction	Forward						Reverse					
	t_o(μs)	t(μs)	P(W)	V(V)	Z(Ω)	Condition	t_o(μs)	t(μs)	P(W)	V(V)	Z(Ω)	Condition
E-B	10	-	12	5.9	3.0	-	10	8.0	7.8	15	29	SBF
	10	-	14	6.0	2.5	-	10	7.0	8.6	18	38	SBF
	10	-	20	7.1	2.5	-	10	4.3	7.8	15	29	SBF
	10	8.0	10	5.1	2.5	O	10	4.0	7.3	15	31	SBF
	10	6.0	11	5.7	2.9	O	10	4.0	10	18	29	SBF
	1.0	-	64	12	2.4	-	1.0	-	17	21	26	-
	1.0	-	76	14	2.8	-	1.0	-	19	22	25	-
	1.0	-	85	20	4.5	-	1.0	0.70	20	24	28	SBF
	0.18	-	220	22	2.2	-	0.20	-	26	22	18	-
	0.16	-	200	22	2.4	-	0.20	-	35	25	18	-
	0.15	-	3400	52	0.80	-	0.20	-	46	31	21	-
C-B	10	6.8	12	5.7	2.6	O	10	2.5	6.7	25	93	SB
	10	6.8	14	6.2	2.7	O	10	2.0	9.0	30	100	SB
	10	6.0	15	6.0	2.4	O	10	1.3	10	28	78	SB
	10	5.0	14	6.0	2.6	O	10	1.3	10	28	75	SB
	10	3.0	15	6.3	2.6	O	10	1.2	11	30	83	SB
	1.0	-	36	8.4	2.0	-	1.0	0.90	17	33	64	SB
	1.0	0.85	40	9.4	2.2	O	1.0	0.65	24	34	48	SBD
	1.0	0.20	44	10	2.5	O	1.0	0.55	41	41	41	SBF
	0.20	0.15	120	15	1.9	O	0.15	-	71	36	19	-
	0.20	0.12	190	19	1.9	O	0.15	0.08	83	46	25	SB
	0.20	0.06	180	18	1.8	O	0.15	0.07	77	43	24	SB
							0.15	0.07	80	44	24	SBF

Note. In forward pulsing, especially of the C-B junctions, sudden increases in voltage across the devices (to about twice the previous value, with no change in current) occurred during the pulses; after these events, the devices exhibited open-circuited terminals ("O"). Failure was assumed to have occurred at the onset of such a voltage increase. Multiple breakdown occurred in several cases of reverse pulsing (both junctions).

APPENDIX A

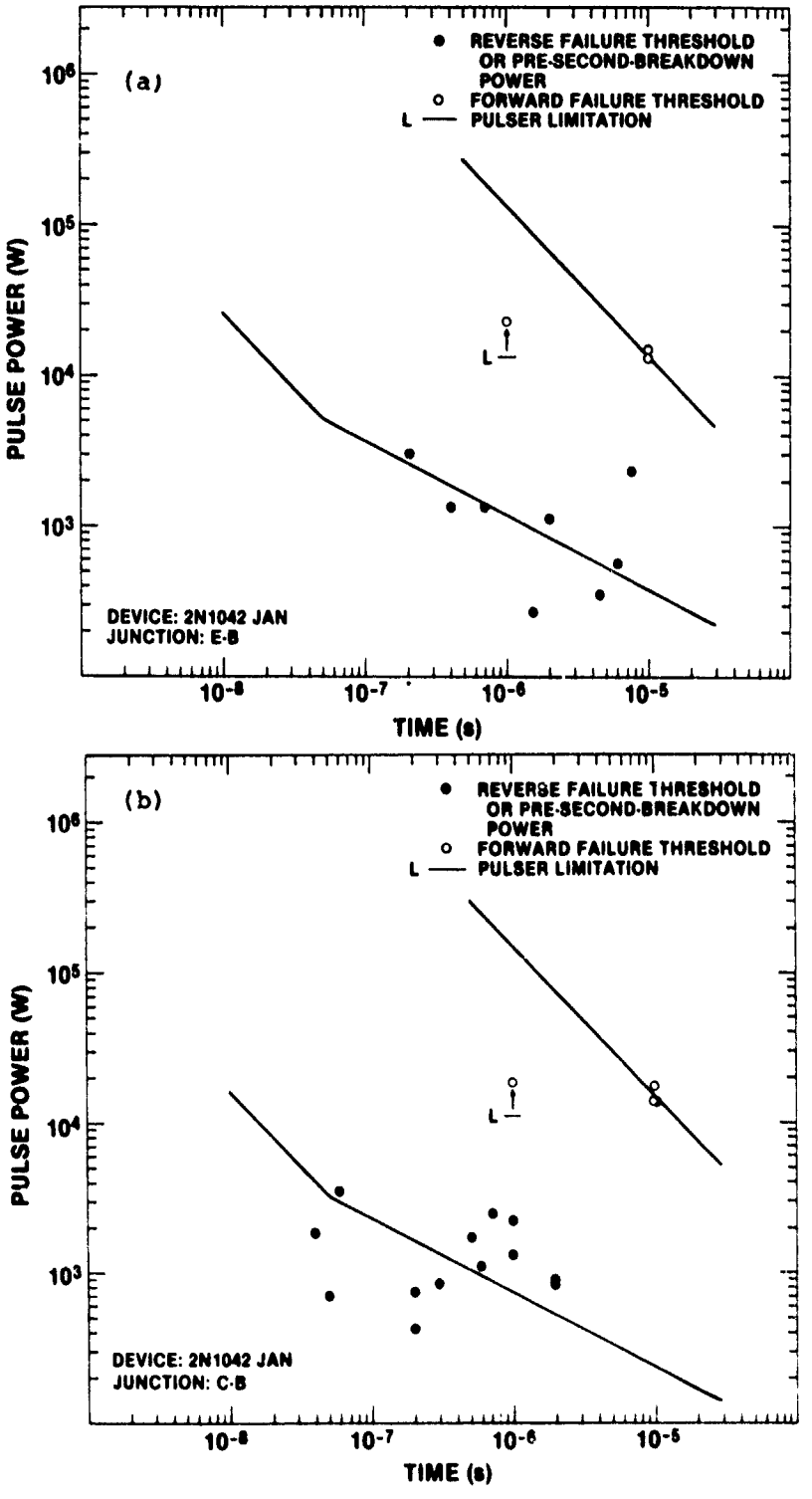

Figure A-25. Damage characteristics of 2N1042 JAN: (a) E-B junction and (b) C-B junction.

TABLE A-25. DAMAGE CHARACTERISTICS OF 2N1042 JAN

Junction	Forward						Reverse					
	t_o(μs)	t(μs)	P(W)	V(V)	Z(Ω)	Condition	t_o(μs)	t(μs)	P(W)	V(V)	Z(Ω)	Condition
E-B	10	-	13,000	72	0.40	-	10	7.5	2400	1100	540	SBF
	10	-	15,000	50	0.17	-	10	6.0	550	460	380	SB
							10	4.5	350	470	630	SBF
							10	2.0	1100	530	260	SB
							10	1.5	270	370	520	SB
							1.0	0.70	1300	700	390	SBF
							1.0	0.40	1300	1000	770	SBF
							1.0	0.20	3000	600	120	SB
C-B	10	-	14,000	53	0.20	-	10	2.0	870	510	300	SB
	10	-	14,000	44	0.13	-	10	2.0	880	380	160	SB
	10	-	18,000	60	0.20	-	10	1.0	1300	470	170	SBF
							10	1.0	2200	670	200	SBF
							10	0.30	850	530	330	ISBF
							10	0.20	420	330	260	ISB
							10	0.20	770	550	390	ISBF
							1.0	0.70	2500	460	85	SBD
							1.0	0.60	1100	1100	1100	SBF
							1.0	0.50	1800	560	170	SB
							1.0	0.05	710	260	100	ISB
							0.15	0.06	3500	500	71	SB
							0.15	0.04	1900	500	130	ISB

Note: Cases of multiple breakdown occurred in reverse pulsing of the E-B junctions.

APPENDIX A

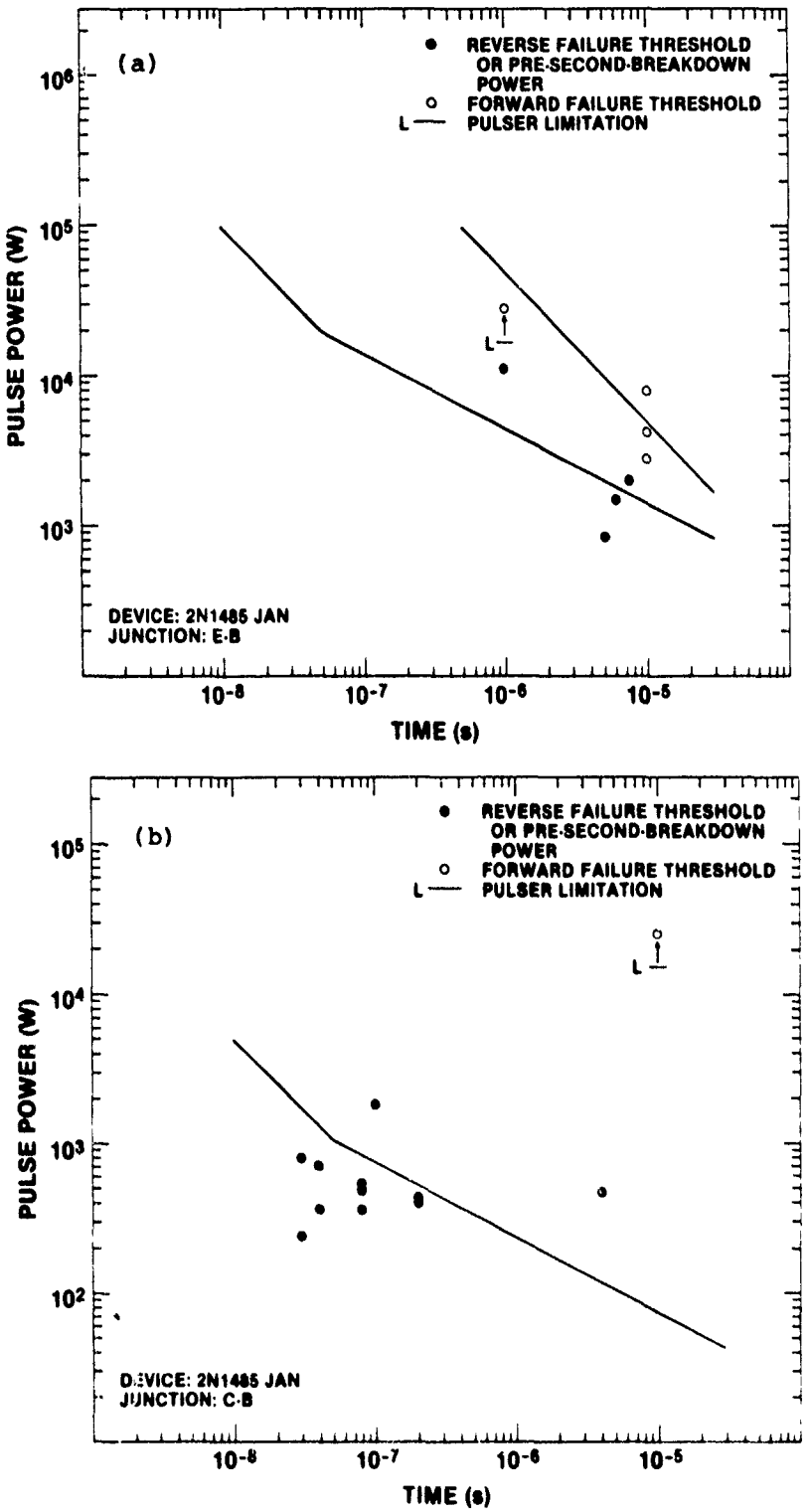

Figure A-26. Damage characteristics of 2N1485 JAN: (a) E-B junction and (b) C-B junction.

TABLE A-26. DAMAGE CHARACTERISTICS OF 2N1485 JAN

Junction	Forward						Reverse					
	t_o(μs)	t(μs)	P(W)	V(V)	Z(Ω)	Condition	t_o(μs)	t(μs)	P(W)	V(V)	Z(Ω)	Condition
E-B	10	-	2800	30	0.32	-	10	7.5	2,000	31	0.48	SBD
	10	-	4100	41	0.45	-	10	6.0	1,500	27	0.50	SBD
	10	-	8000	50	0.31	-	10	5.0	830	26	0.81	SBD
							1.0	-	11,000	71	0.44	-
C-B							10	4.0	460	110	26	SBD
							10	0.20	390	110	32	ISBF
							10	0.20	420	120	37	ISB
							1.0	0.08	360	260	180	SB
							1.0	0.08	460	120	33	ISB
							1.0	0.08	520	130	33	ISB
							0.13	0.04	350	140	56	SB
							0.13	0.04	720	200	56	SBF
							0.13	0.03	240	120	61	ISB
							0.13	0.03	800	160	32	ISB
							0.10	-	1,800	87	4.2	-

Note: The second-breakdown sustaining voltage of the E-B junctions was remarkably high (approximately 70% of the pre-second-breakdown voltage) despite a high impedance pulse source. At a 0.13-μs pulse width, three C-B junctions exhibited nondegrading SB with the pre-second-breakdown power being lower by a factor of 5 to 10 than the power for failure. Multiple breakdown occurred in reverse pulsing of several C-B junctions.

APPENDIX A

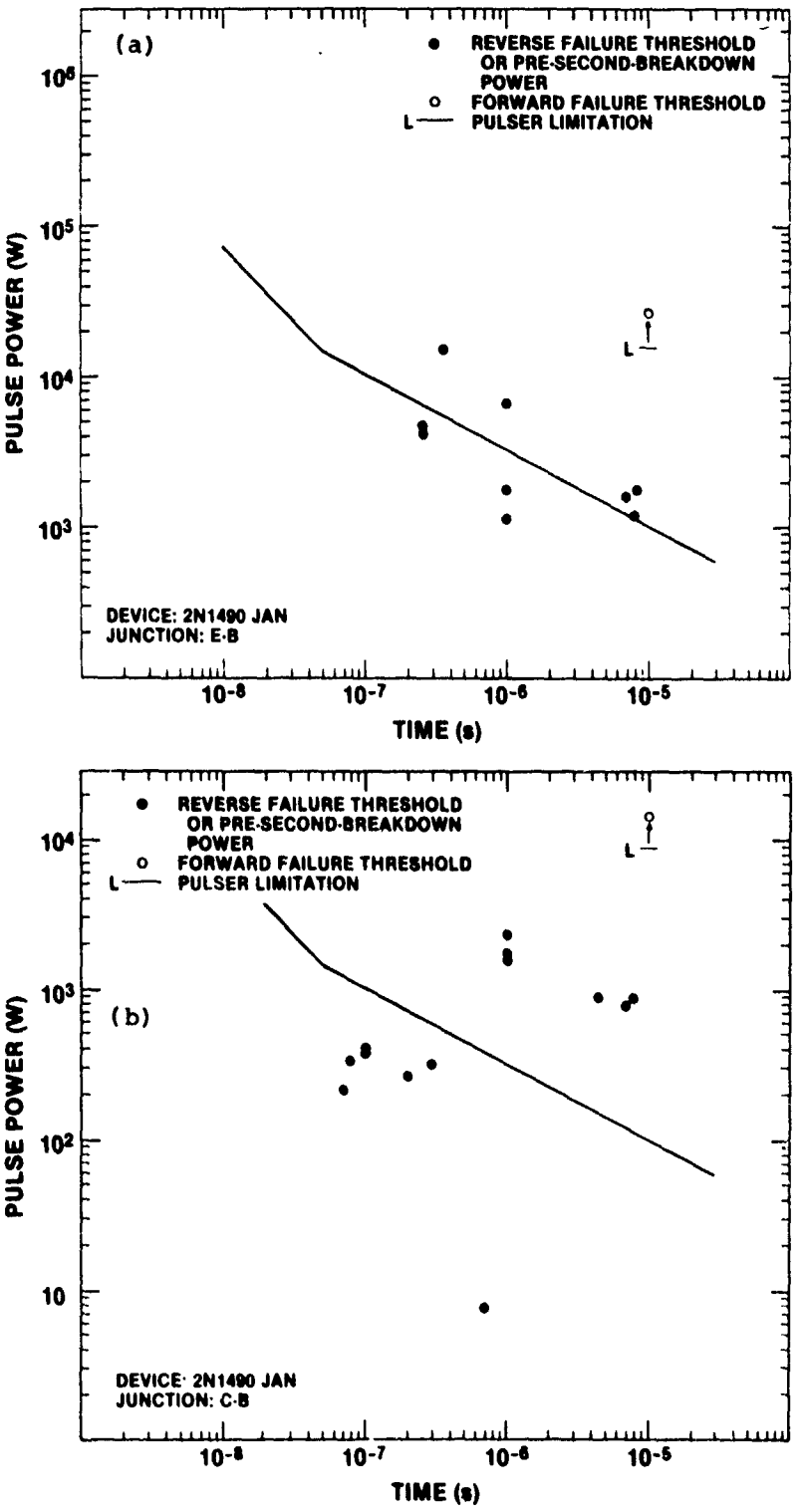

Figure A-27. Damage characteristics of 2N1490 JAN: (a) E-B junction and (b) C-B junction.

TABLE A-27. DAMAGE CHARACTERISTICS OF 2N1490 JAN

Junction	Forward						Reverse					
	t_o(μs)	t(μs)	P(W)	V(V)	Z(Ω)	Condition	t_o(μs)	t(μs)	P(W)	V(V)	Z(Ω)	Condition
E-B							10	8.3	1,800	46	1.2	SB
							10	8.0	1,200	54	2.5	SBD
							10	7.0	1,600	58	2.1	SBF
							1.0	-	1,100	34	1.1	-
							1.0	-	1,800	36	0.7	-
							1.0	-	6,700	82	1.0	-
							0.35	-	15,000	140	1.3	-
							0.25	-	4,100	130	4.1	-
							0.25	-	4,800	120	2.8	-
C-B							10	8.0	880	120	16	SB
							10	7.0	790	120	18	SB
							10	4.5	900	120	16	SB
							1.0	-	1,600	50	1.6	-
							1.0	-	1,800	60	1.9	-
							1.0	-	2,400	75	2.4	-
							1.0	0.70	7.3	140	2900	SBD
							1.0	0.30	310	130	53	SBD
							1.0	0.20	270	140	58	SB
							1.0	0.10	380	100	26	ISB
							0.12	0.10	390	150	58	SB
							0.12	0.08	330	150	58	SB
							0.12	0.07	210	140	93	SB

Note: One case of multiple breakdown was observed in reverse pulsing of the E-B junctions (10 μs). At a 0.12-μs pulse width, the C-B junctions exhibited nondegrading SB with the pre-second-breakdown power a factor of 8 to 20 lower than the power for failure.

APPENDIX A

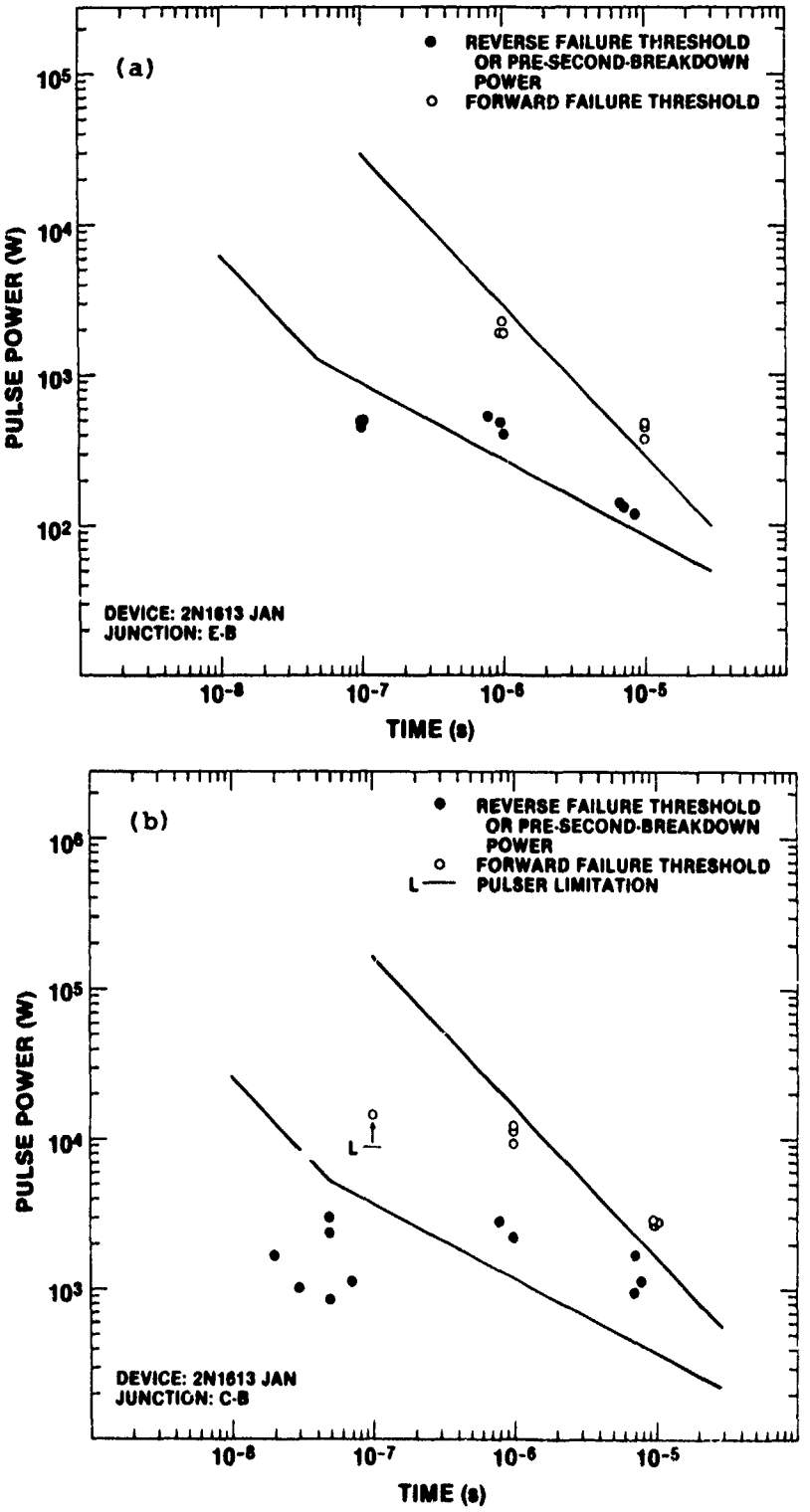

Figure A-28. Damage characteristics of 2N1613 JAN: (a) E-B junction and (b) C-B junction.

Table A-28. Damage Characteristics of 2N1613 JAN

Junction	Forward						Reverse					
	t_o(μs)	t(μs)	P(W)	V(V)	Z(Ω)	Condition	t_o(μs)	t(μs)	P(W)	V(V)	Z(Ω)	Condition
E-B	10	-	380	17	0.73	-	10	8.5	120	31	7.8	SBF
	10	-	450	16	0.55	-	10	7.0	130	32	8.1	SBF
	10	-	470	16	0.58	-	10	6.5	140	36	9.5	SBF
	1.0	-	1900	39	0.81	-	1.0	-	400	52	6.8	-
	1.0	-	1900	39	0.80	-	1.0	0.90	460	56	6.8	SBF
	1.0	-	2300	42	0.78	-	1.0	0.80	520	68	8.9	SBF
							0.10	-	440	50	5.7	-
							0.10	-	500	52	5.4	-
							0.10	-	500	55	6.1	-
C-B	10	-	2,800	38	0.51	-	10	8.0	1100	280	74	SBF
	10	-	2,800	37	0.49	-	10	7.0	960	310	100	SB
	10	-	2,900	40	0.57	-	10	7.0	1700	320	60	SB
	1.0	-	9,200	74	0.60	-	1.0	-	2200	240	26	-
	1.0	-	11,000	83	0.61	-	1.0	0.80	2800	340	42	SB
	1.0	-	12,000	85	0.60	-	1.0	0.07	1100	220	41	ISBF
							1.0	0.05	820	280	92	ISBF
							0.12	0.05	3000	340	38	ISBF
							0.10	0.05	2400	350	50	ISBF
							0.10	0.03	1000	160	25	ISBF
							0.10	0.02	1700	190	21	ISBF

APPENDIX A

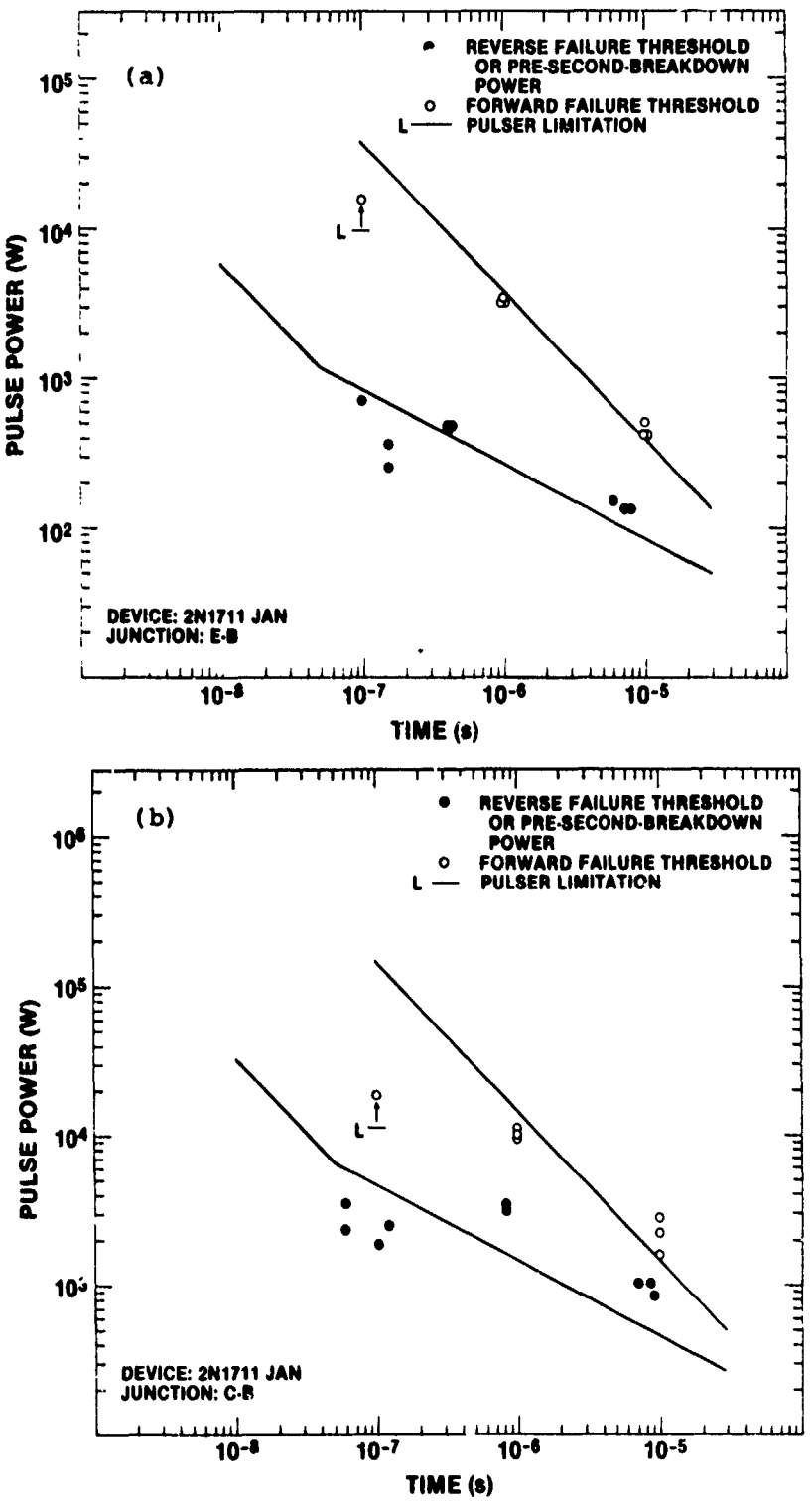

Figure A-29. Damage characteristics of 2N1711 JAN: (a) E-B junction and (b) C-B junction.

TABLE A-29. DAMAGE CHARACTERISTICS OF 2N1711 JAN

Junction	Forward						Reverse					
	t_o(μs)	t(μs)	P(W)	V(V)	Z(Ω)	Condition	t_o(μs)	t(μs)	P(W)	V(V)	Z(Ω)	Condition
E-B	10	-	420	15	0.56	-	10	8.0	130	35	9.7	SBF
	10	-	420	15	0.54	-	10	7.0	130	36	10	SBF
	10	-	500	16	0.51	-	10	6.0	150	38	9.5	SBF
	1.0	-	3200	47	0.70	-	1.0	0.75	460	62	8.4	SBF
	1.0	-	3200	50	0.77	-	1.0	0.70	440	55	6.9	SBF
	1.0	-	3400	52	0.78	-	1.0	0.70	470	57	6.9	SBF
							0.15	-	250	43	7.4	-
							0.15	-	360	47	6.1	-
							0.10	-	720	60	5.0	-
C-B	10	-	1,600	26	0.41	-	10	9.0	830	280	98	SBF
	10	-	2,200	31	0.43	-	10	8.5	1000	300	88	SB
	10	-	2,800	36	0.47	-	10	7.0	1000	350	120	SB
	1.0	-	9,700	80	0.66	-	1.0	0.80	3200	360	41	SB
	1.0	-	10,000	80	0.62	-	1.0	0.80	3400	360	38	SBD
	1.0	-	11,000	80	0.60	-	1.0	0.10	1900	260	38	SB
							0.12	-	2500	310	38	-
							0.12	0.06	2400	340	48	SBF
							0.12	0.06	3600	400	44	SBF

Note: Multiple breakdown was observed in reverse pulsing of one C-B junction (1-μs pulse width).

APPENDIX A

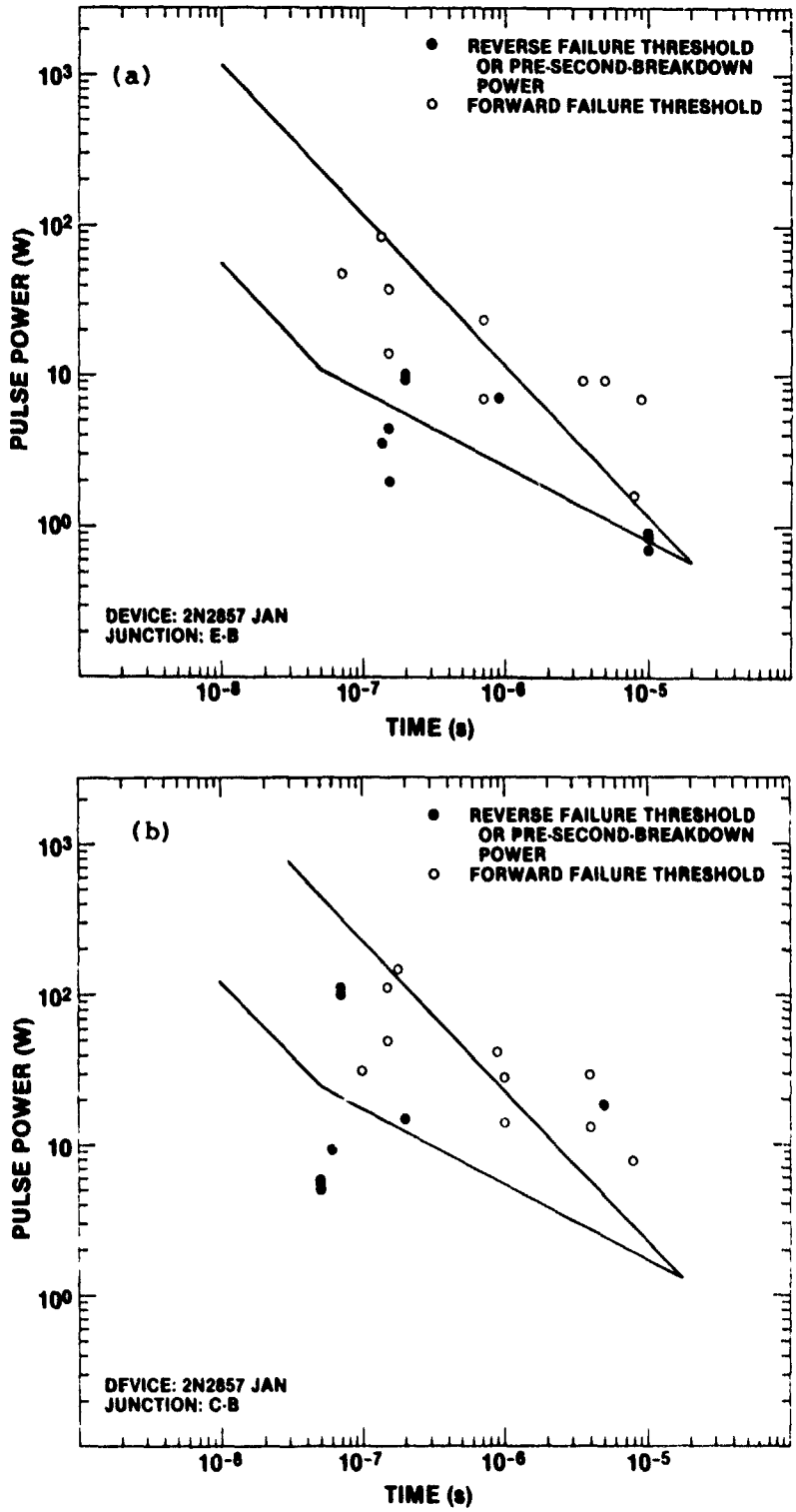

Figure A-30. Damage characteristics of 2N2857 JAN: (a) E-B junction and (b) C-B junction.

TABLE A-30. DAMAGE CHARACTERISTICS OF 2N2857 JAN

Junction	Forward						Reverse					
	t_o(μs)	t(μs)	P(W)	V(V)	Z(Ω)	Condition	t_o(μs)	t(μs)	P(W)	V(V)	Z(Ω)	Condition
E-B	10	9.0	7.2	3.8	2.0	O	10	-	0.70	6.7	64	-
	10	8.0	1.6	2.6	4.2	O	10	-	0.82	6.9	58	-
	10	5.0	9.7	4.3	1.9	O	10	-	0.87	6.8	53	-
	10	3.5	9.7	4.2	1.8	O	1.0	0.90	6.9	8.6	11	SBF
	1.0	0.70	7.0	5.0	3.5	O	1.0	0.20	9.5	9.5	9.5	SBF
	1.0	0.70	24	6.7	1.9	O	1.0	0.20	9.8	9.8	9.8	SBF
	1.0	0.15	14	7.0	3.6	O	0.15	-	2.0	7.8	30	-
	0.15	-	38	9.8	2.5	O	0.15	-	4.5	7.0	11	-
	0.15	0.07	46	12	2.9	O	0.13	-	3.5	7.2	15	-
	0.13	-	84	14	2.3	O						
C-B	10	8.0	7.8	4.1	2.2	O	10	5.0	19	95	480	SBF
	10	4.0	13	5.3	2.2	O	10	0.20	15	18	22	ISBF
	10	4.0	30	7.1	1.7	O	1.0	0.06	9.5	47	230	ISBF
	1.0	-	14	7.0	3.5	O	1.0	0.05	5.0	37	270	ISBF
	1.0	-	28	7.0	1.8	O	1.0	0.05	5.7	42	310	ISBF
	1.0	0.90	41	9.0	2.0	O	1.0	0.05	6.0	40	270	ISBF
	0.19	-	150	19	2.4	O	0.10	0.07	100	87	76	SB
	0.18	0.10	32	10	3.1	O	0.10	0.07	110	82	59	SB
	0.15	-	50	10	2.0	O						
	0.15	-	110	18	3.0	O						

Note: All forward-pulsed E-B and C-B junctions open-circuited ("O"). Multiple breakdown occurred in reverse pulsing of the C-B junctions (all devices at a 1-μs pulse width).

APPENDIX A

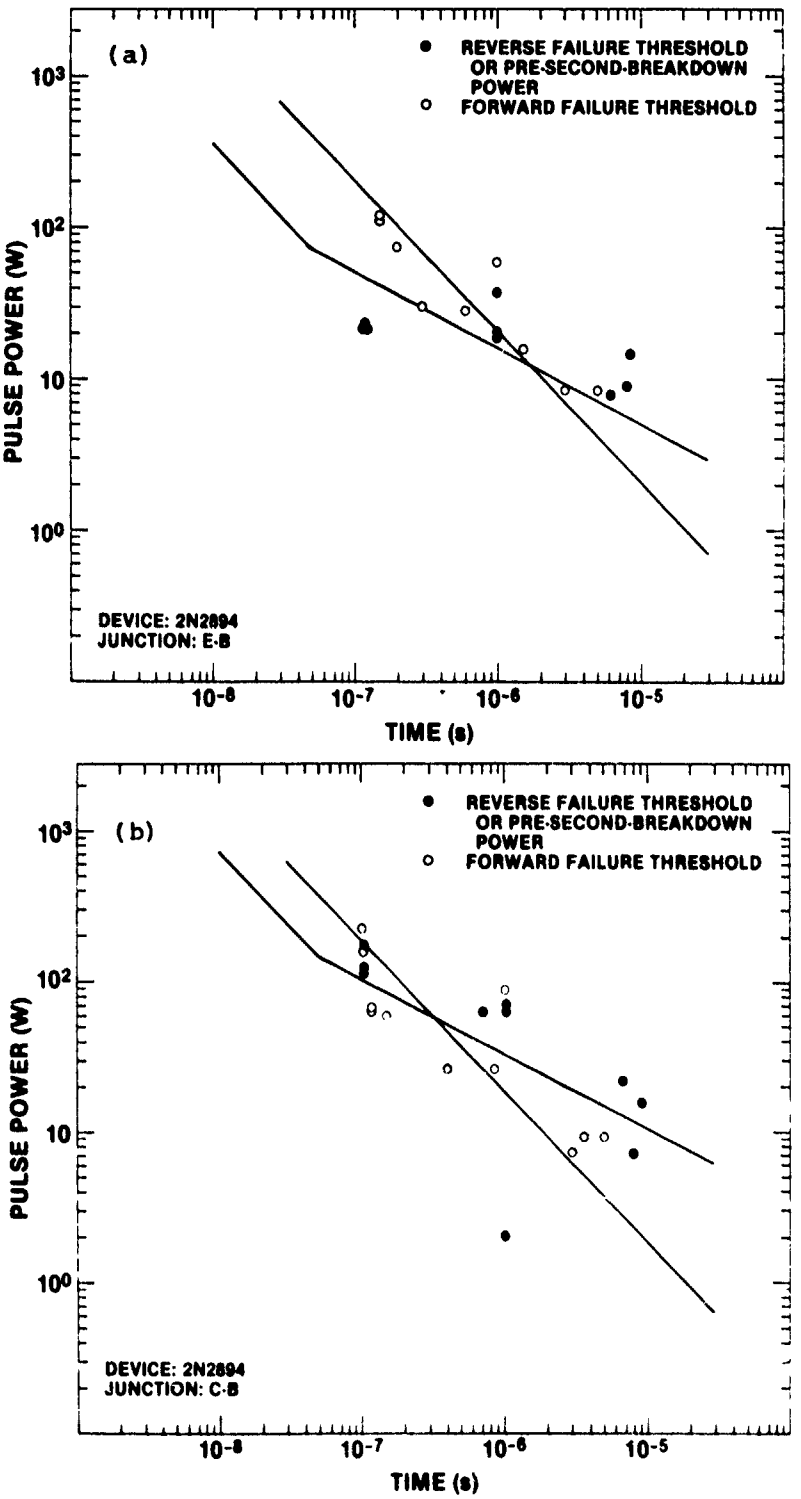

Figure A-31. Damage characteristics of 2N2894: (a) E-B junction and (b) C-B junction.

TABLE A-31. DAMAGE CHARACTERISTICS OF 2N2894

Junction	Forward						Reverse					
	t_o(μs)	t(μs)	P(W)	V(V)	Z(Ω)	Condition	t_o(μs)	t(μs)	P(W)	V(V)	Z(Ω)	Condition
E-B	10	5.0	8.4	4.4	2.3	O	10	8.3	15	10	6.7	SBF
	10	3.0	8.2	4.1	2.1	O	10	8.0	8.8	16	29	SBF
	10	1.5	16	4.6	1.4	O	10	6.3	8.1	14	23	SBF
	1.0	-	61	10	1.8	O	1.0	-	19	19	19	-
	1.0	0.60	28	7.5	2.0	O	1.0	-	20	20	20	-
	1.0	0.30	30	7.5	1.9	O	1.0	-	38	13	4.4	-
	0.20	-	74	16	3.2	O	0.12	-	23	20	17	-
	0.15	-	110	13	1.5	O	0.12	-	23	20	17	-
	0.15	-	120	14	1.6	O	0.12	-	24	18	14	-
C-B	10	5.0	9.2	4.2	1.9	O	10	9.0	16	60	230	SB
	10	3.5	9.7	4.4	2.0	O	10	8.0	7.7	45	260	SB
	10	3.0	7.6	4.2	2.3	O	10	6.5	23	62	170	SBF
	1.0	-	90	12	1.6	-	10	1.0	2.1	60	1700	SB
	1.0	0.85	26	6.8	1.8	O	1.0	-	63	57	52	-
	1.0	0.40	26	6.5	1.6	O	1.0	-	69	55	44	-
	0.15	-	60	12	2.2	O	1.0	0.70	64	53	44	SBF
	0.15	0.10	220	20	1.8	O	0.15	0.10	110	60	32	SBF
	0.12	-	65	10	1.5	O	0.15	0.10	120	58	29	SBF
	0.12	-	66	12	2.2	O	0.15	0.10	180	75	31	SBF
	0.12	0.10	160	17	1.8	O						

Note: With one exception, all forward-pulsed E-B and C-B junctions open-circuited ("O"). One case of multiple breakdown occurred in reverse pulsing of the C-B junctions.

APPENDIX A

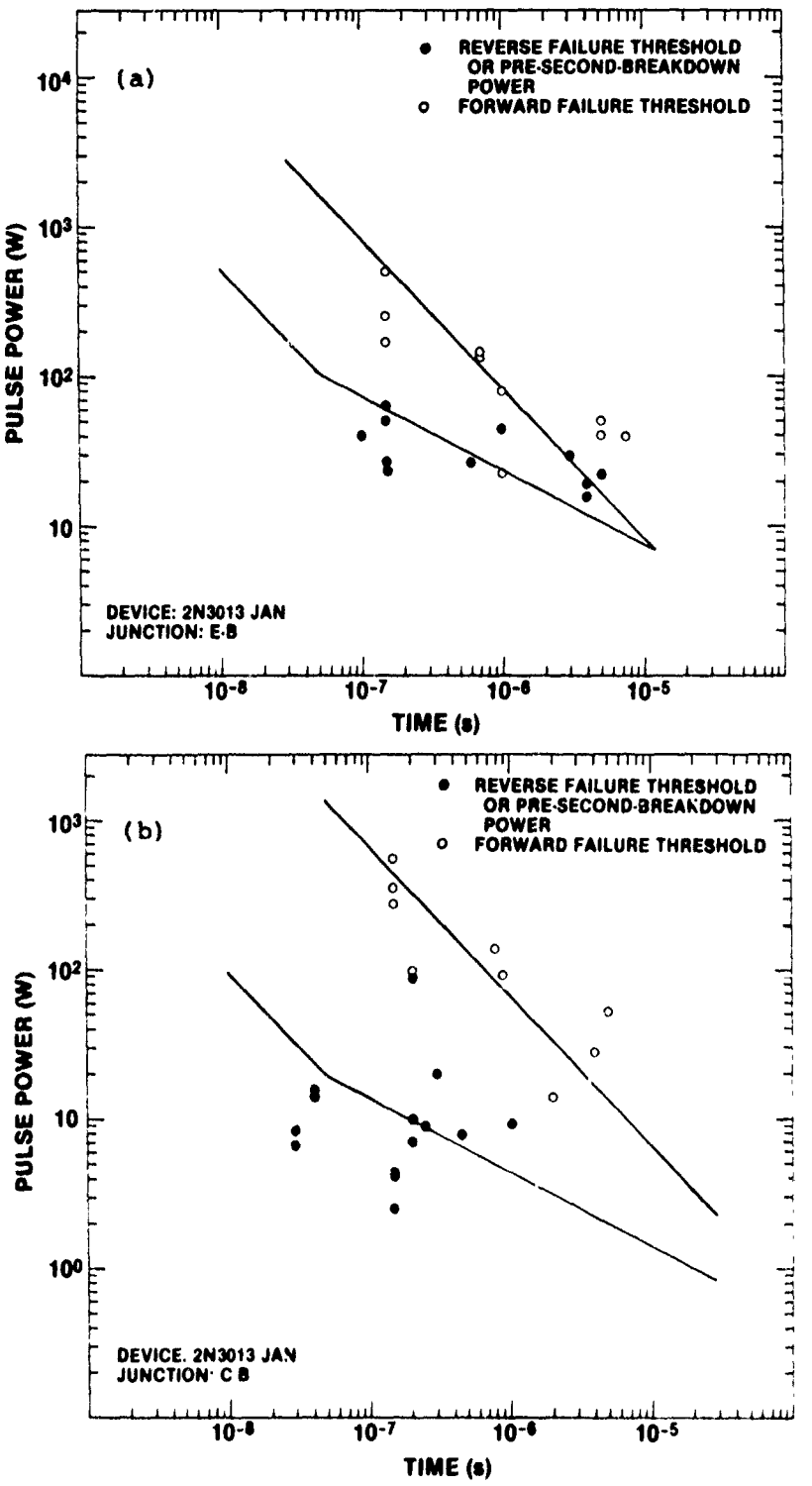

Figure A-32. Damage characteristics of 2N3013 JAN: (a) E-B junction and (b) C-B junction.

TABLE A-32. DAMAGE CHARACTERISTICS OF 2N3013 JAN

Junction	Forward						Reverse					
	t_o(μs)	t(μs)	P(W)	V(V)	Z(Ω)	Condition	t_o(μs)	t(μs)	P(W)	V(V)	Z(Ω)	Condition
E-B	10	7.5	40	6.0	0.9	O	10	5.0	22	15	10	SBF
	10	5.0	40	6.0	0.9	O	10	4.0	16	13	11	SBF
	10	5.0	50	6.5	0.8	O	10	4.0	19	12	7.6	SBF
	10	1.0	22	5.5	1.4	O	10	3.0	30	20	13	SBF
	1.0	-	80	8.4	0.9	O	1.0	-	44	22	11	-
	1.0	0.70	130	12	1.0	O	1.0	0.60	26	12	6.0	SBF
	1.0	0.70	140	12	1.0	O	1.0	0.10	39	14	5.4	SBF
	0.15	-	170	16	1.5	-	0.15	-	24	12	6.0	-
	0.15	-	250	25	2.5	-	0.15	-	27	15	8.3	-
	0.15	-	500	22	1.0	O	0.15	-	50	20	8.0	-
							0.15	-	63	25	10	-
C-B	10	5.0	52	7.5	1.1	O	10	1.0	9.7	70	500	SBD
	10	4.0	29	5.8	1.2	O	10	0.30	20	75	290	SBF
	10	2.0	14	5.5	2.2	O	10	0.15	2.5	36	520	ISBF
	1.0	0.90	95	10	1.1	O	10	0.15	4.2	34	280	ISBF
	1.0	0.80	140	12	3.3	O	10	0.15	4.3	37	320	ISBF
	1.0	0.20	100	11	1.3	O	1.0	0.45	8.0	80	800	SB
	0.15	-	290	21	1.5	O	1.0	0.25	9.0	80	710	SB
	0.15	-	360	24	1.5	O	1.0	0.20	7.0	70	700	SB
	0.15	-	550	26	1.2	O	1.0	0.20	10	82	670	SB
							1.0	0.20	90	77	66	SBF
							0.15	0.04	16	70	310	SB
							0.10	0.04	14	70	350	SB
							0.10	0.03	6.5	36	200	ISB
							0.10	0.03	8.2	39	180	ISB

Note. With the two exceptions indicated (E-B), all forward-pulsed E-B and C-B junctions open-circuited ("O"). Besides the (instantaneous) SB step observed in reverse pulsing of the C-B junctions at a 10-μs pulse width, there occurred two more breakdown steps in these specimens. Multiple breakdown (one additional step besides SB) occurred in other C-B junctions.

APPENDIX A

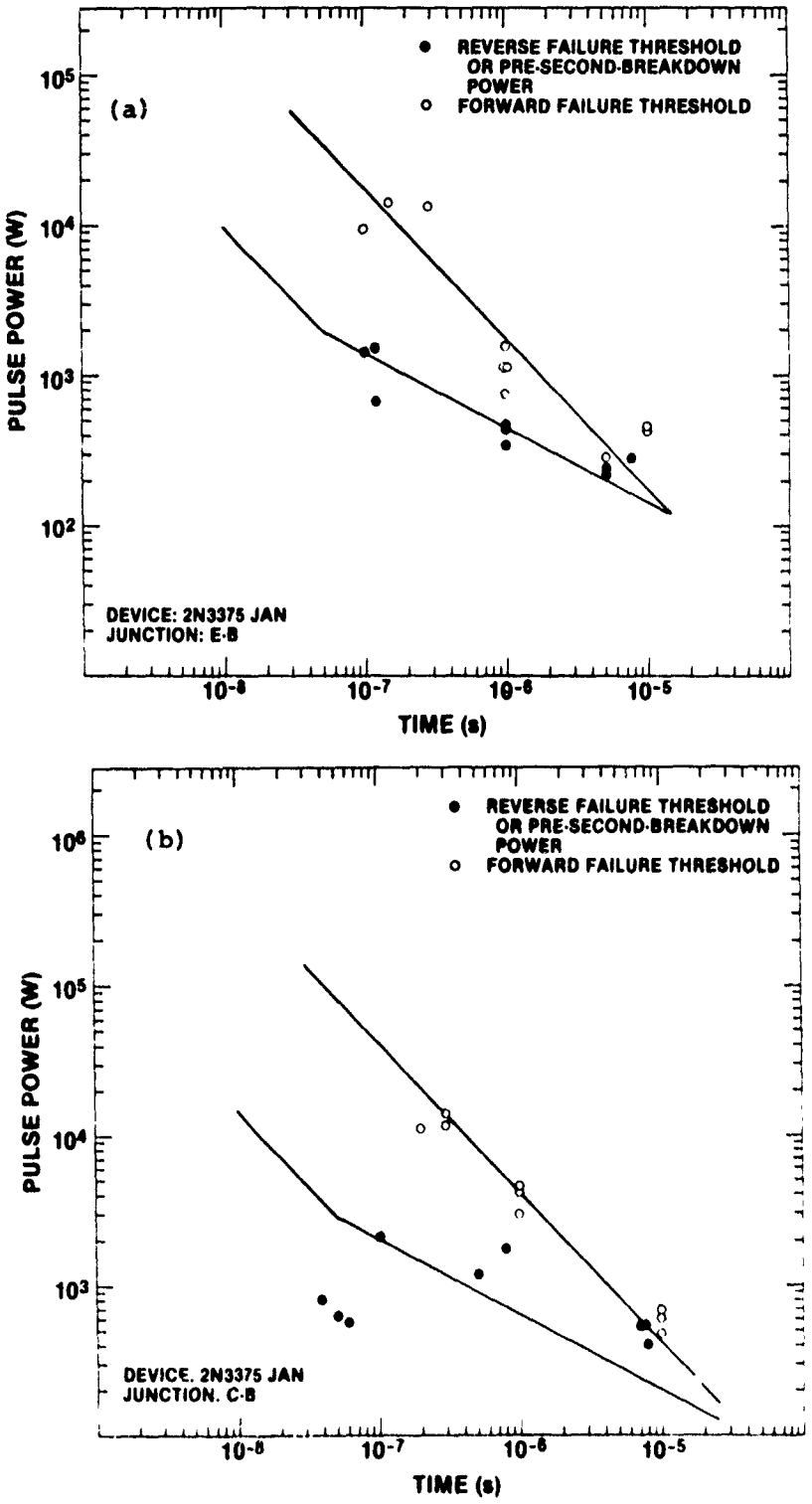

Figure A-33. Damage characteristics of 2N3375 JAN: (a) E-B junction and (b) C-B junction.

TABLE A-33. DAMAGE CHARACTERISTICS OF 2N3375 JAN

Junction	Forward						Reverse					
	t_o(μs)	t(μs)	P(W)	V(V)	Z(Ω)	Condition	t_o(μs)	t(μs)	P(W)	V(V)	Z(Ω)	Condition
E-B	10	-	420	9.5	0.21	-	10	7.5	230	12	0.58	EVF
	10	-	440	9.5	0.20	-	10	5.0	240	11	0.52	EVF
	10	5.0	280	10	0.36	EVF	10	5.0	280	12	0.55	EVF
	1.0	-	740	12	0.19	-	1.0	-	340	16	0.71	-
	1.0	-	1,100	14	0.17	-	1.0	-	440	14	0.42	-
	1.0	-	1,100	18	0.28	-	1.0	-	440	14	0.44	-
	1.0	-	1,600	16	0.15	-	0.12	-	660	25	0.94	-
	0.28	-	13,000	72	0.39	-	0.12	-	1500	35	0.82	-
	0.15	-	14,000	73	0.39	-	0.10	-	1400	39	1.1	-
	0.10	-	9,300	82	0.72	-						
C-B	10	-	460	13	0.38	-	10	8.0	400	190	90	SBD
	10	-	600	10	0.17	-	10	8.0	530	190	68	SBF
	10	-	660	11	0.19	-	10	7.0	540	210	82	SB
	1.0	-	3,000	24	0.18	-	1.0	0.80	1800	260	38	SBF
	1.0	-	4,300	26	0.16	-	1.0	0.50	1200	220	42	SB
	1.0	-	4,400	35	0.28	-	1.0	0.10	2100	260	33	SBF
	0.30	-	12,000	73	0.45	-	0.10	0.06	550	180	62	SBD
	0.30	-	14,000	74	0.40	-	0.10	0.05	630	180	51	SB
	0.20	-	11,000	68	0.43	-	0.10	0.04	800	200	50	SBF

Note: In forward pulsing of the E-B junctions, a sudden drop in current occurred in one specimen at 5 μs ("EVF"); failure was assumed to have occurred at that moment. The events ("EVF") in reverse pulsing of the E-B junctions at a 10-μs pulse width are the beginnings of oscillations. Spikes of current, to about 1.1 times the starting value and about 1 μs apart, occurred (the associated fluctuations in voltage were very small because of a low source impedance); they can be interpreted as periodic transitions into SB. Device failure was assumed to have occurred at the onset of these oscillations.

APPENDIX A

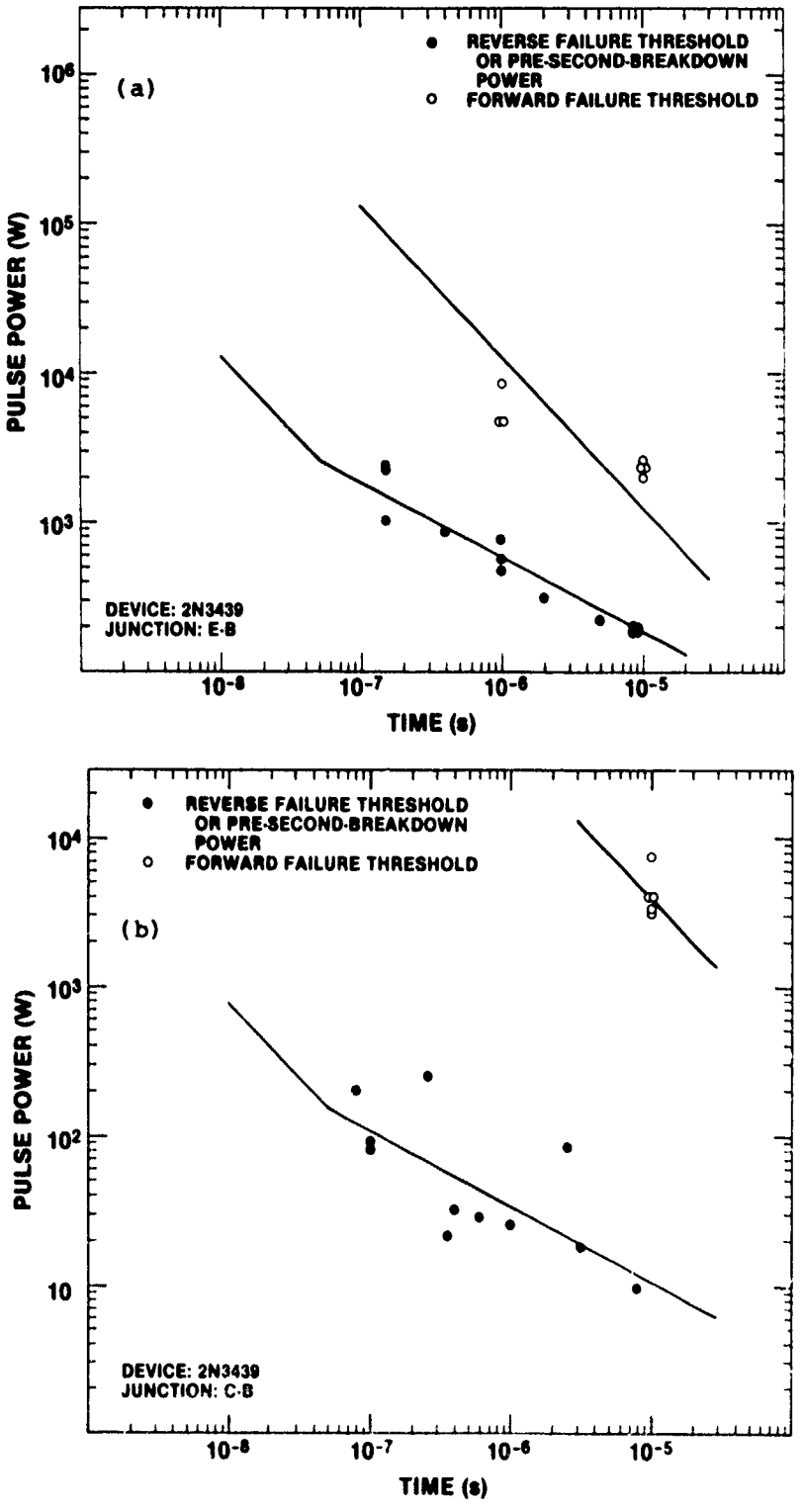

Figure A-34. Damage characteristics of 2N3439: (a) E-B junction and (b) C-B junction.

TABLE A-34. DAMAGE CHARACTERISTICS OF 2N3439

Junction	Forward						Reverse					
	t_o(μs)	t(μs)	P(W)	V(V)	Z(Ω)	Condition	t_o(μs)	t(μs)	P(W)	V(V)	Z(Ω)	Condition
E-B	10	-	2000	24	0.28	-	10	9.0	190	19	1.9	SBF
	10	-	2400	25	0.27	-	10	9.0	190	19	1.9	SBF
	10	-	2400	28	0.32	-	10	8.5	200	19	1.8	SBF
	10	-	2600	28	0.29	-	10	8.3	190	19	1.9	SBF
	1.0	-	4700	38	0.30	-	10	5.0	220	20	1.8	SBF
	1.0	-	4800	42	0.36	-	10	2.0	310	21	1.4	SBF
	1.0	-	8300	52	0.33	-	1.0	-	460	24	1.2	-
							1.0	-	570	26	1.2	-
							1.0	-	760	27	1.0	-
							0.40	-	850	30	1.0	-
							0.15	-	1000	36	1.3	-
							0.15	-	2300	54	1.3	-
							0.15	-	2400	56	1.3	-
C-B	10	-	3100	28	0.25	-	10	8.0	9.5	640	42,000	SB
	10	-	3400	30	0.27	-	10	3.2	18	700	28,000	SB
	10	-	3900	30	0.24	-	10	2.5	82	680	5,600	SB
	10	-	4000	33	0.27	-	10	1.0	25	720	21,000	SB
	10	-	4200	34	0.27	-	1.1	0.60	29	480	7,900	SB
							1.0	0.40	31	600	12,000	SB
							1.0	0.35	21	630	19,000	SB
							1.0	0.25	12	660	36,000	SB
							0.20	0.10	80	670	5,600	SBF
							0.20	0.10	90	700	5,400	SBF
							0.20	0.08	200	770	3,000	SBF

Note: Multiple breakdown occurred in one C-B junction reverse pulsed at a 10-μs pulse width.

APPENDIX A

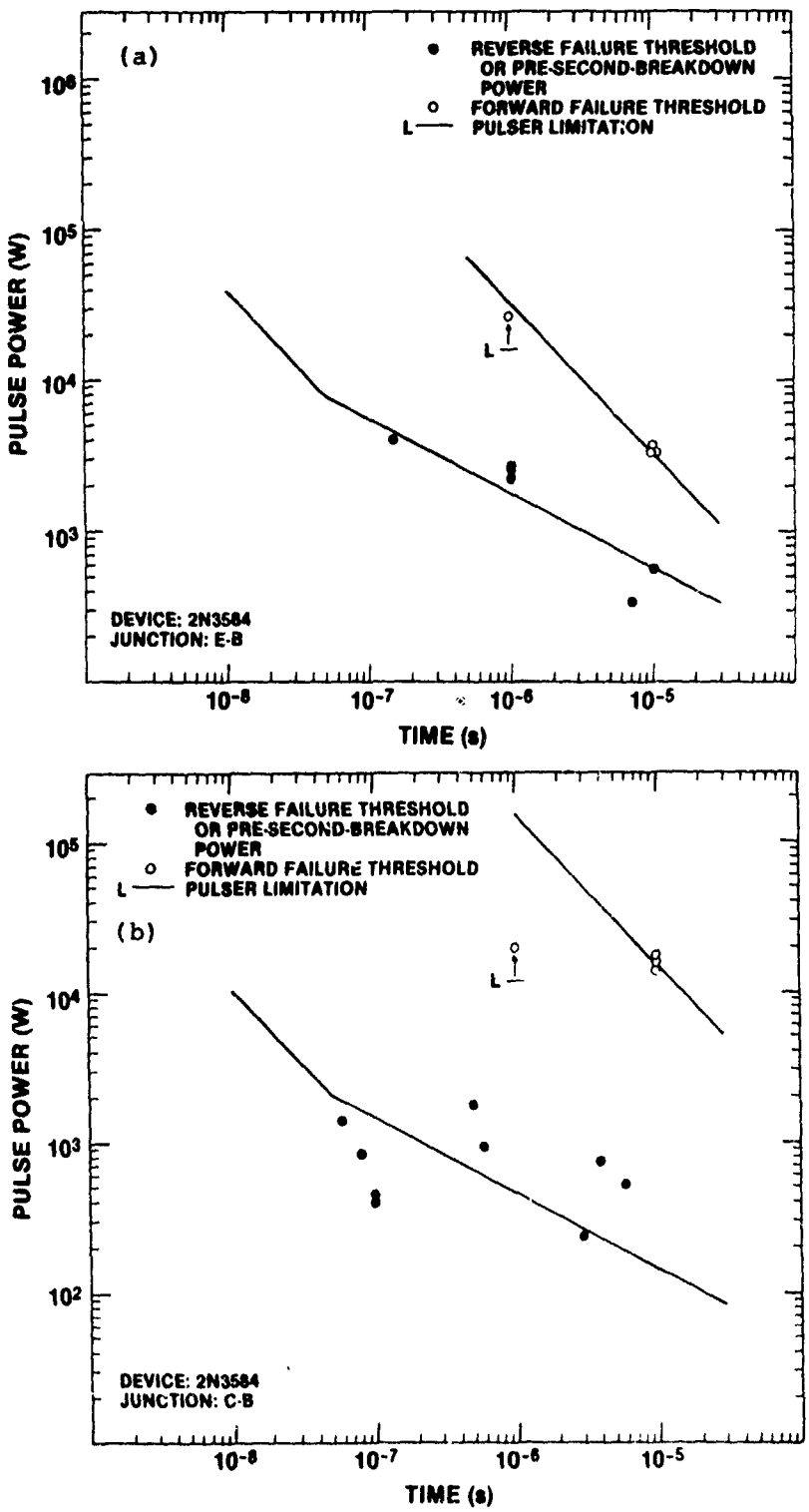

Figure A-35. Damage characteristics of 2N3584: (a) E-B junction and (b) C-B junction.

APPENDIX A

TABLE A-35. DAMAGE CHARACTERISTICS OF 2N3584

Junction	Forward						Reverse					
	t_o(μs)	t(μs)	P(W)	V(V)	Z(Ω)	Condition	t_o(μs)	t(μs)	P(W)	V(V)	Z(Ω)	Condition
E-B	10	-	3300	22	0.15	-	10	-	340	34	3.4	-
	10	-	3300	22	0.15	-	10	7.0	570	40	2.8	SBF
	10	-	3700	37	0.37	-	1.0	-	2200	55	1.4	-
							1.0	-	2500	50	1.0	-
							1.0	-	2600	40	0.63	-
							0.15	-	4000	80	1.6	-
C-B	10	-	14,000	29	0.06	-	10	6.0	530	820	1300	SB
	10	-	16,000	28	0.05	-	10	4.0	730	860	1000	SB
	10	-	18,000	31	0.05	-	10	3.0	240	620	1900	SB
							1.0	0.60	960	740	570	SB
							1.0	0.50	1800	820	370	SB
							1.0	0.10	400	580	830	SB
							0.27	0.10	440	550	690	SB
							0.27	0.08	820	750	680	SB
							0.27	0.06	1400	830	500	SB

APPENDIX A

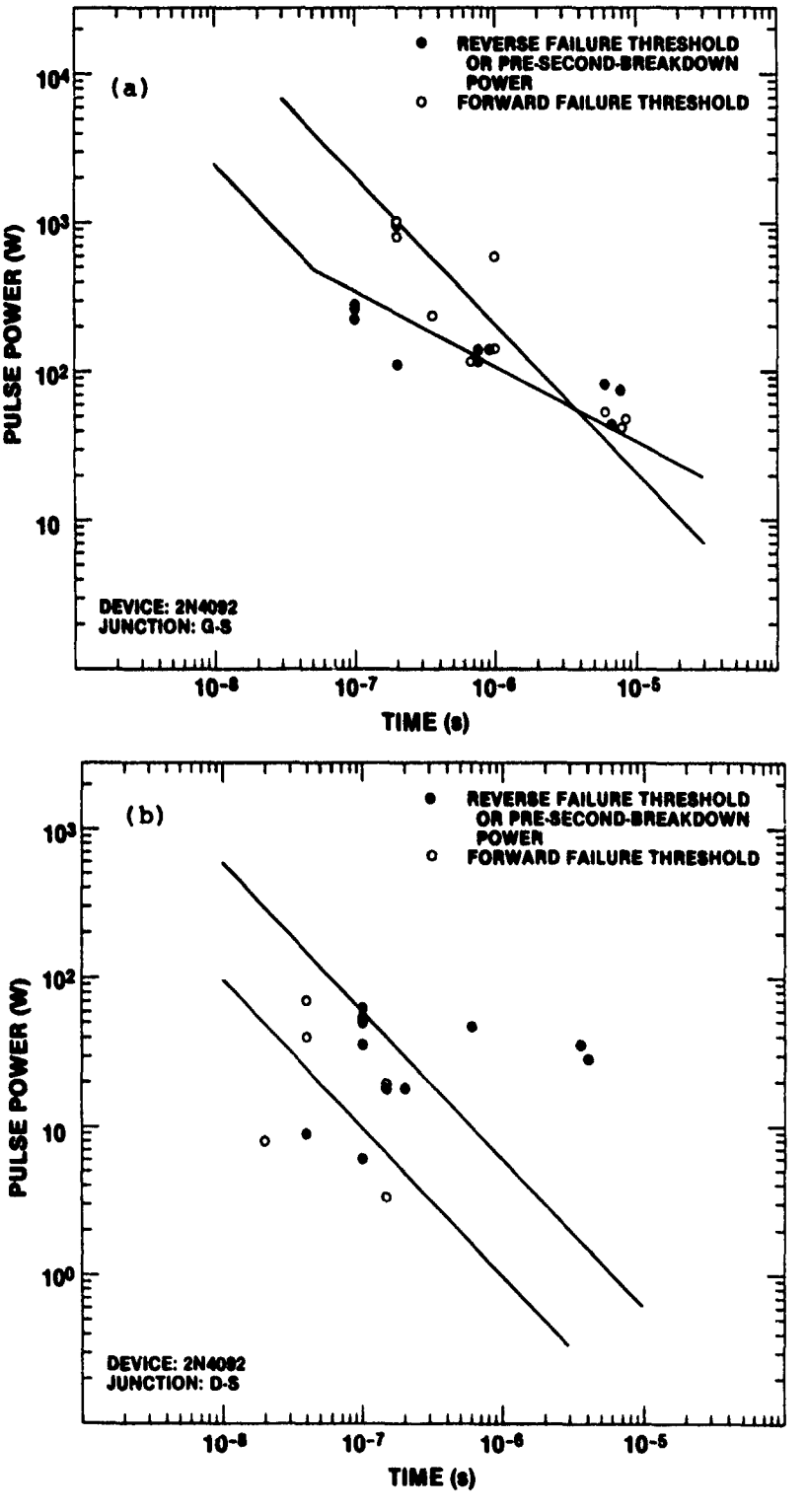

Figure A-36. Damage characteristics of 2N4092: (a) G-S junction and (b) D-S junction.

TABLE A-36. DAMAGE CHARACTERISTICS OF 2N4092

Junction	Forward						Reverse					
	t_o(μs)	t(μs)	P(W)	V(V)	Z(Ω)	Condition	t_o(μs)	t(μs)	P(W)	V(V)	Z(Ω)	Condition
G-S	10	8.5	46	6.2	0.84	O	10	7.5	75	75	75	SBF
	10	8.0	41	5.1	0.63	O	10	6.5	44	71	120	SBD
	10	6.0	52	6.2	0.74	O	10	6.0	84	77	71	SBF
	1.0	-	140	10	0.74	O	1.0	0.90	140	80	44	SB
	1.0	-	610	23	0.88	O	1.0	0.75	120	66	35	SB
	1.0	0.65	120	22	4.2	O	1.0	0.75	140	70	35	SB
	1.0	0.35	240	25	2.6	O	1.0	0.20	110	72	45	SB
	0.20	-	780	25	0.80	O	0.18	0.10	220	77	27	SB
	0.20	-	940	40	1.7	O	0.18	0.10	270	80	24	SB
	0.20	-	1000	30	0.87	O	0.10	-	290	77	20	-
D-S	10	0.15	3.3	27	220	ISB	10	4.0	28	60	130	SBF
	1.0	0.15	19	54	150	SB	10	3.5	36	60	100	SBF
	1.0	0.10	53	55	57	SB	10	0.10	5.8	24	99	ISBF
	1.0	0.02	8	32	130	ISB	1.0	0.60	43	63	83	SBF
	0.10	0.04	39	65	110	SB	1.0	0.20	18	44	110	SB
	0.10	0.04	72	65	59	SB	1.0	0.15	1.8	54	170	SB
							1.0	0.04	9	33	120	ISBF
							0.10	-	36	34	32	-
							0.10	-	51	32	20	-
							0.10	-	62	50	40	-

Note: The G-S junction open-circuited in all cases of forward pulsing ("O"). Second breakdown was observed in pulsing of the D-S terminal pair in both the D^-S^+ ("forward") and D^+S^- ("reverse") condition. (Not enough devices were available for obtaining more data on the D^-S^+ condition.)

APPENDIX A

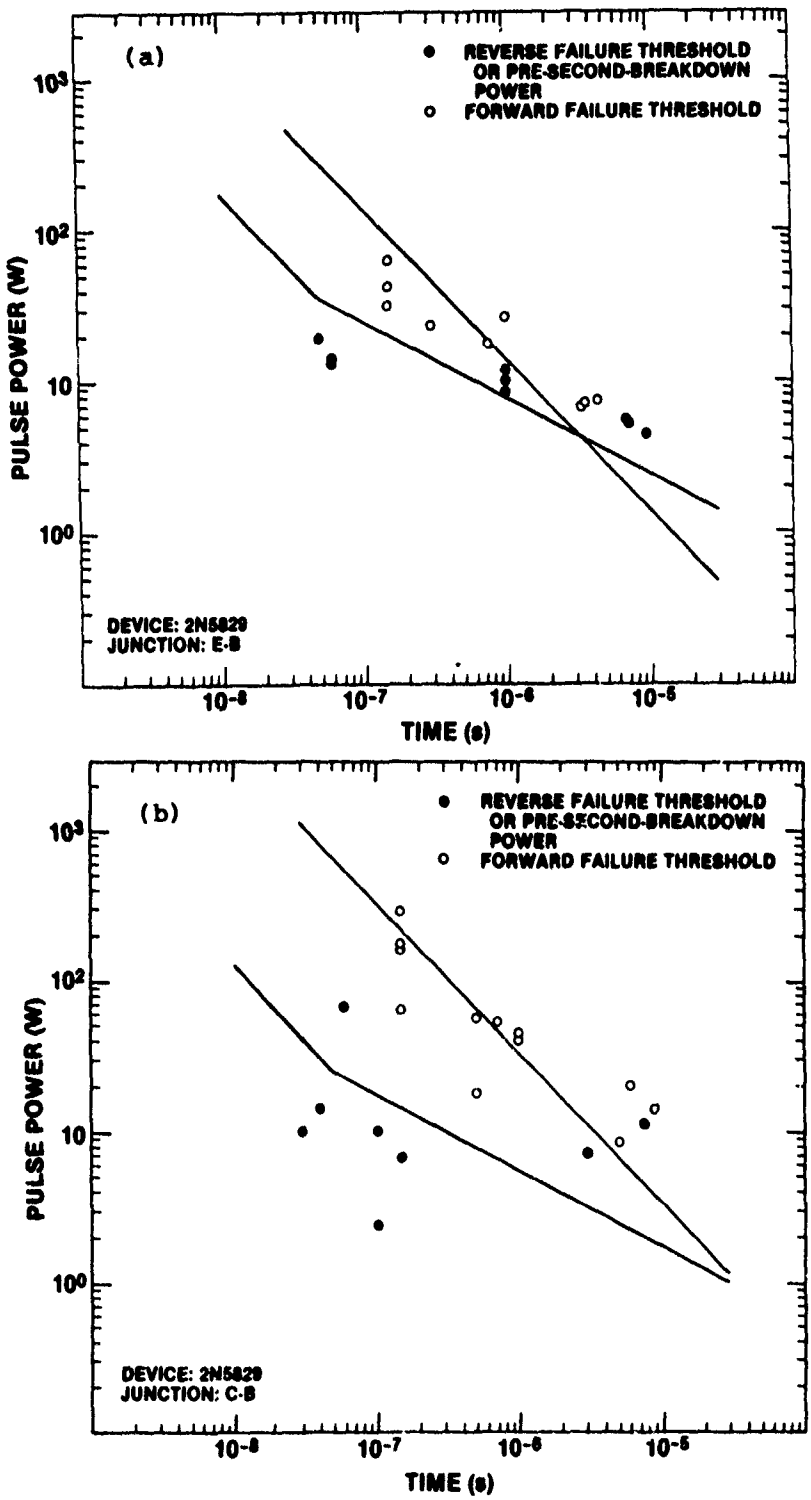

Figure A-37. Damage characteristics of 2N5829: (a) E-B junction and (b) C-B junction.

TABLE A-37. DAMAGE CHARACTERISTICS OF 2N5829

Junction	Forward						Reverse					
	t_o(μs)	t(μs)	P(W)	V(V)	Z(Ω)	Condition	t_o(μs)	t(μs)	P(W)	V(V)	Z(Ω)	Condition
E-B	10	5.5	7.7	4.0	2.1	O	10	9.5	4.4	10	25	SBF
	10	3.5	7.2	3.6	1.8	O	10	7.0	5.2	11	24	SBF
	10	3.3	6.6	3.5	1.9	O	10	6.5	5.5	11	22	SBF
	1.0	-	26	6.5	1.6	-	1.0	-	8.4	12	17	-
	1.0	0.75	18	5.2	1.5	O	1.0	-	10	14	18	-
	1.0	0.30	24	6.2	1.6	O	1.0	-	12	15	19	-
	0.15	-	31	7.1	1.6	O	0.10	0.06	13	14	14	ISBF
	0.15	-	42	8.0	1.5	O	0.10	0.06	14	14	14	ISBF
	0.15	-	64	9.2	1.3	-	0.10	0.05	19	18	17	ISBF
C-B	10	9.0	14	5.0	1.8	O	10	7.5	11	140	1900	SBF
	10	6.0	20	6.2	1.9	O	10	3.0	7.2	90	1100	SBF
	10	5.0	8.4	5.4	3.5	O	10	0.10	2.4	42	730	ISBF
	10	0.50	18	5.7	1.8	O	1.0	0.15	6.5	82	1000	SBD
	1.0	-	40	8.0	1.6	O	1.0	0.10	10	100	1000	SB
	1.0	-	44	8.6	1.7	O	0.10	0.06	65	100	170	SBD
	1.0	0.70	54	9.0	1.5	O	0.10	0.04	14	43	130	ISBF
	1.0	0.50	57	10	1.8	O	0.10	0.03	10	37	140	ISBD
	1.0	0.15	63	11	1.9	O						
	0.15	-	160	17	1.8	O						
	0.15	-	170	18	2.0	O						
	0.15	-	280	21	1.6	O						

Note: In forward pulsing, most E-B terminals and all C-B terminals open-circuited ("O"). Multiple breakdown was frequently observed in reverse pulsing of the C-B junctions.

APPENDIX A

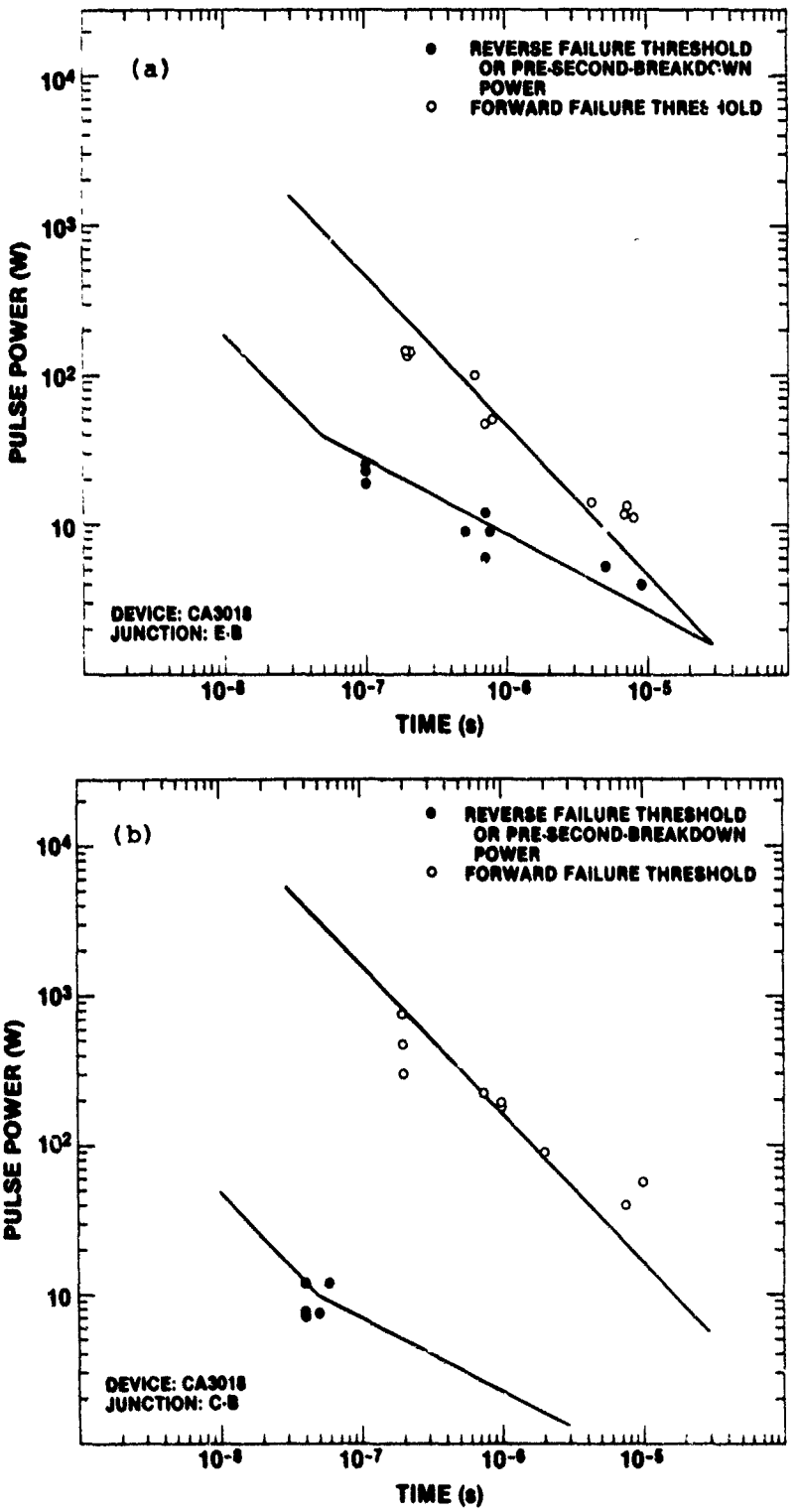

Figure A-38. Damage characteristics of CA3018: (a) E-B junction and (b) C-B junction.

TABLE A-38. DAMAGE CHARACTERISTICS OF CA 3018

Junction	Forward						Reverse					
	t_o(μs)	t(μs)	P(W)	V(V)	Z(Ω)	Condition	t_o(μs)	t(μs)	P(W)	V(V)	Z(Ω)	Condition
E-B	10	8.0	11	10	9.7	EVF	10	9.0	3.9	26	170	SBF
	10	7.0	13	12	10	EVF	10	5.0	5.3	33	200	SBF
	10	6.5	12	11	9.4	EVF	10	4.0	6.1	35	200	SBF
	10	4.0	14	12	11	EVF	1.0	0.75	9.0	31	110	SBF
	1.0	0.80	50	20	8.0	EVF	1.0	0.70	12	41	140	SBF
	1.0	0.70	48	19	7.7	EVF	1.0	0.50	8.7	30	100	SBF
	1.0	0.60	100	37	13	EVF	0.10	-	19	45	110	-
	0.20	-	130	25	4.8	-	0.10	-	22	45	94	-
	0.20	-	140	26	5.1	-	0.10	-	27	45	76	-
	0.20	-	140	26	5.0	-						
C-B	10	-	55	16	4.7	O	1.0	0.05	7.5	40	210	ISB
	10	7.5	39	11	3.1	O	1.0	0.04	7.0	40	230	ISBD
	10	2.0	88	20	4.5	O	1.0	0.04	7.5	40	210	ISBD
	1.0	-	180	22	2.7	O	0.10	0.06	12	60	290	ISB
	1.0	-	190	28	4.2	O	0.10	0.04	12	59	220	ISB
	1.0	0.75	220	23	2.4	O						
	0.20	-	300	43	6.2	-						
	0.20	-	460	45	4.4	-						
	0.20	-	730	44	2.7	-						

Note: Events resembling SB (sudden increase in current at practically constant voltage) occurred in forward pulsing of the E-B junction; failure was assumed to have occurred at the beginning of the current increase ("EVF"). In forward pulsing of the C-B junction at 10 and 1 μs, the devices open-circuited ("O"). Multiple breakdown, up to two breakdown steps after SB, occurred frequently in reverse pulsing of the C-B junctions. SB at a 10-μs pulse width (C-B) was in all cases instantaneous without making it possible to determine a pre-second-breakdown power.

APPENDIX A

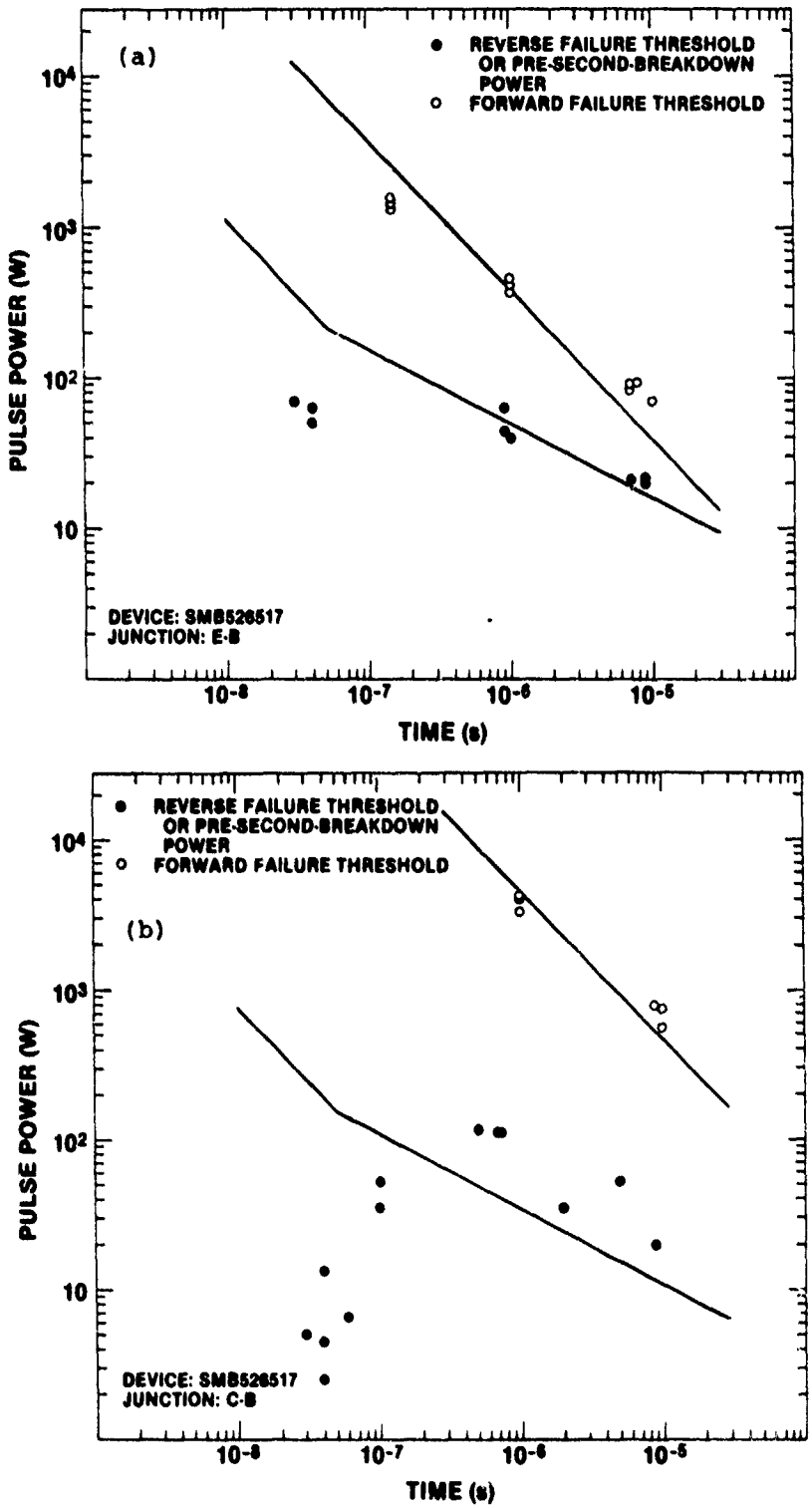

Figure A-39. Damage characteristics of SMB526517: (a) E-B junction and (b) C-B junction.

TABLE A-39. DAMAGE CHARACTERISTICS OF SMB526517

Junction	Forward						Reverse					
	t_o(μs)	t(μs)	P(W)	V(V)	Z(Ω)	Condition	t_o(μs)	t(μs)	P(W)	V(V)	Z(Ω)	Condition
E-B	10	-	71	5.5	0.43	-	10	9.0	20	38	72	SBF
	10	8.0	94	12	1.7	EVF	10	9.0	21	38	69	SBF
	10	7.0	86	12	1.5	EVF	10	7.0	21	37	65	SBF
	10	7.0	90	12	1.6	EVF	1.0	-	39	33	28	-
	1.0	-	370	22	1.3	-	1.0	0.90	44	34	26	SBF
	1.0	-	420	23	1.3	-	1.0	0.90	62	55	49	SBF
	1.0	-	440	22	1.2	-	0.10	0.04	50	38	29	ISBF
	0.15	-	1300	50	2.0	-	0.10	0.04	62	63	64	ISBF
	0.15	-	1400	52	2.0	-	0.10	0.03	71	55	43	ISBF
	0.15	-	1600	52	1.7	-						
C-B	10	-	560	24	1.1	-	10	9.0	20	67	220	SB
	10	-	730	28	1.0	-	10	5.0	53	240	1100	SBF
	10	9.0	790	28	1.0	O	10	2.0	35	220	1400	SBF
	1.0	-	3300	55	0.9	-	1.0	0.70	110	240	540	SB
	1.0	-	4100	62	0.9	-	1.0	0.70	110	270	640	SB
	1.0	-	4200	62	0.9	-	1.0	0.50	120	260	580	SBF
							0.20	0.10	36	240	1600	SB
							0.20	0.10	53	240	1100	SB
							0.20	0.06	6.7	180	4600	SB
							0.20	0.03	4.3	120	3000	ISB
							0.15	0.04	2.5	110	4700	ISB
							0.15	0.04	4.5	110	2800	ISB
							0.10	0.04	13	130	1300	ISB

Note: Events resembling SB were observed in forward pulsing of the E-B junctions at a 10-μs pulse width; failure was assumed to have occurred at the beginning of the current increase ("EVF"). One C-B junction open-circuited in forward pulsing ("O"). Two cases of multiple breakdown, up to two breakdown steps after SB, occurred in reverse pulsing of the C-B junctions at a 10-μs pulse width.

DISTRIBUTION

DEFENSE TECHNICAL INFORMATION CENTER
CAMERON STATION, BUILDING 5
ATTN DTIC-DDA (12 COPIES)
ALEXANDRIA, VA 22314

COMMANDER
US ARMY RSCH & STD GP (EUR)
BOX 65
ATTN CHIEF, PHYSICS & MATH BRANCH
FPO NEW YORK 09510

COMMANDER
US ARMY ARMAMENT MATERIEL
READINESS COMMAND
ATTN DRSAR-LEP-L, TECHNICAL LIBRARY
ATTN DRSAR-ASF, FUZE & MUNITIONG
SUPPORT DIVISION
ROCK ISLAND, IL 61299

COMMANDER
US ARMY MISSILE & MUNITIONS
CENTER & SCHOOL
ATTN ATSK-CTD-F
REDSTONE ARSENAL, AL 35809

DIRECTOR
US ARMY MATERIEL SYSTEMS
ANALYSIS ACTIVITY
ATTN DRXSY-MP
ATTN DRXSY-CC, COMM & ELECTRONICS
ABERDEEN PROVING GROUND, MD 21005

DIRECTOR
US ARMY BALLISTIC RESEARCH LABORATORY
ATTN DRDAR-TSB-S (STINFO)
ATTN DRDAR-BLV, VULNERABILITY/
LETHALITY DIV
ABERDEEN PROVING GROUND, MD 21005

TELEDYNE BROWN ENGINEERING
CUMMINGS RESEARCH PARK
ATTN DR. MELVIN L. PRICE, MS-44
HUNTSVILLE, AL 35807

ENGINEERING SOCIETIES LIBRARY
345 EAST 47TH STREET
ATTN ACQUISITIONS DEPARTMENT
NEW YORK, NY 10017

US ARMY ELECTRONICS TECHNOLOGY
AND DEVICES LABORATORY
ATTN DELET-DD
FORT MONMOUTH, NJ 07703

HQ USAF/SAMI
WASHINGTON, DC 20330

DEPARTMENT OF COMMERCE
NATIONAL BUREAU OF STANDARDS
ATTN ELECTR DEV DIV, K. GALLOWAY
ATTN ELECTR TECHNOLOGY DIV, D. L. BLACKBURN
WASHINGTON, DC 20234

US DEPT OF ENERGY
ATTN ASST ADMIN FOR NUCLEAR ENERGY
ATTN OFFICE OF TECHNICAL INFORMATION
WASHINGTON, DC 20585

DIRECTOR
DEFENSE ADVANCED RESEARCH
PROJECT AGENCY
ARCHITECT BLDG
1400 WILSON BLVD
ATTN DR, TACTICAL TECHNOLOGY OFFICE
ARLINGTON, VA 22209

DIRECTOR
DEFENSE COMMUNICATIONS AGENCY
ATTN TECH LIBRARY
WASHINGTON, DC 20305

DIRECTOR
DEFENSE COMMUNICATIONS AGENCY
COMMAND & CONTROL TECHNICAL CENTER
ATTN TECHNICAL DIRECTOR
WASHINGTON, DC 20301

DIRECTOR
DEFENSE COMMUNICATIONS ENGINEERING CENTER
1860 WIEHLE AVE
ATTN RES & DEV
RESTON, VA 22090

COMMANDER-IN-CHIEF
CONTINENTAL AIR DEFENSE COMMAND, JCS
ENT AFB
ATTN TECHNICAL LIB
COLORADO SPRINGS, CO 80912

DIRECTOR
DEFENSE INTELLIGENCE AGENCY
ATTN DT-1, NUCLEAR & APPLIED
SCIENCES DIV
WASHINGTON, DC 20301

CHAIRMAN
OFFICE OF THE JOINT CHIEFS OF STAFF
ATTN J-6, COMMUNICATIONS-ELECTRONICS
WASHINGTON, DC 20301

DIRECTOR
NATIONAL SECURITY AGENCY
ATTN TECHNICAL LIBRARY
FORT GEORGE G. MEADE, MD 20755

DISTRIBUTION (Cont'd)

DIRECTOR
DEFENSE NUCLEAR AGENCY
ATTN DDST, E. E. CONRAD,
DEP DIR SCIENCE & TECHNOLOGY
ATTN RAEE, EMP EFFECTS DIV
ATTN RAEV, ELECTRONICS VULNERABILITY
DIV (2 COPIES)
ATTN STNA, NUCLEAR ASSESSMENT DIRECTORATE
ATTN BLIS, CAPT M. A. KING
WASHINGTON, DC 20305

UNDER SECRETARY OF DEFENSE
FOR RESEARCH & ENGINEERING
ATTN DEP DIR (RESEARCH &
ADVANCED TECH)
ATTN ELECTRONICS & PHYSICAL SCIENCE
ATTN DEFENSE SCIENCE BOARD
WASHINGTON, DC 20301

ASSISTANT SECRETARY OF THE ARMY (DRA)
ATTN DEP FOR SCI & TECH
WASHINGTON, DC 20310

OFFICE, DEPUTY CHIEF OF STAFF
FOR OPERATIONS & PLANS
ATTN DAMO-SSN, NUCLEAR DIV
WASHINGTON, DC 20310

OFFICE OF THE DEPUTY CHIEF OF STAFF
FOR RESEARCH, DEVELOPMENT,
& ACQUISITION
ATTN DIR OF ARMY RESEARCH,
DR. M. E. LASSER
ATTN DAMA-RA, SYSTEMS REVIEW
& ANALYSIS OFFICE
ATTN DAMA-CSC, COMMAND, CONTROL,
SURVEILLANCE SYS DIV
WASHINGTON, DC 20310

COMMANDER
US ARMY ARMAMENT RESEARCH AND
DEVELOPMENT COMMAND
ATTN DRDAR-TDR, RES & TECHNOLOGY
DOVER, NJ 07801

COMMANDER
US ARMY BALLISTIC MISSILE
DEFENSE SYSTEMS COMMAND
ATTN R. W. DEKALB
HUNTSVILLE, AL 35807

COMMANDER
US ARMY COMMUNICATIONS COMMAND
ATTN EMP STUDY GP
FORT HUACHUCA, AZ 85613

COMMANDER
US ARMY COMMUNICATIONS RESEARCH AND
DEVELOPMENT COMMAND
ATTN DRCPM-ATC, OFFICE OF
THE PM ARMY TACTICAL
COMMUNICATIONS SYS (ATACS)
FT MONMOUTH, NJ 07703

US ARMY ENGINEER DIVISION
ATTN A. T. BOLT
HUNTSVILLE, AL 35807

COMMANDER
US ARMY MATERIEL DEVELOPMENT
& READINESS COMMAND
5001 EISENHOWER AVE
ATTN DRCCE, DIR FOR COMMUNICATIONS-
ELECTRONICS
ALEXANDRIA, VA 22333

DEPT OF THE ARMY
MICHIGAN ARMY MISSILE PLANT
38111 VAN DYKE
ATTN DRCPM-GCM-SW, R. SLAUGHTER
WARREN, MI 48090

PROJECT MANAGER, LANCE
DRCPM-LC
REDSTONE ARSENAL, AL 35809

PROJECT MANAGER
PATRIOT MISSILE SYSTEM, USADARCOM
DRCPM-MD-T-E
REDSTONE ARSENAL, AL 35809

PROJECT MANAGER
PERSHING WEAPONS SYSTEM
REDSTONE ARSENAL, AL 35809

COMMANDER
US ARMY MISSILE COMMAND
ATTN DRSMI-ET, MFG TECH DIV
ATTN DRSMI-EA, DAVID MATTHEWS
REDSTONE ARSENAL, AL 35809

COMMANDER
US ARMY MOBILITY EQUIPMENT R&D COMMAND
ATTN TECH LIB DIV
FORT BELVOIR, VA 22060

COMMANDER
US ARMY NUCLEAR & CHEMICAL AGENCY
7500 BACKLICK RD
BUILDING 2073
ATTN COL A. LOWREY
ATTN TECH LIB
SPRINGFIELD, VA 22150

DISTRIBUTION (Cont'd)

ARMY RESEARCH OFFICE (DURHAM)
P.O. BOX 12211
ATTN TECH LIBRARY
RESEARCH TRIANGLE PARK, NC 27709

COMMANDER
WHITE SANDS MISSILE RANGE
DEPT OF THE ARMY
ATTN STEWS-TE, ARMY MAT TEST
& EVALUATION DIR, MR. DELAPAZ
WHITE SANDS MISSILE RANGE, NM 88002

COMMANDER
US ARMY ELECTRONICS PROVING GROUND
ATTN STEEP-MT-M, ELECTROMAGNETIC BR
FORT HUACHUCA, AZ 85613

CHIEF OF NAVAL OPERATIONS
DEPT OF THE NAVY
ATTN DIR, RDT&E
ATTN G. J. SHARP
WASHINGTON, DC 20350

CHIEF OF NAVAL RESEARCH
DEPT OF THE NAVY
ATTN TECHNICAL LIBRARY
ARLINGTON, VA 22217

COMMANDER
NAVAL AIR DEVELOPMENT CENTER
ATTN P. YOUNG
WARMINSTER, PA 18974

COMMANDER
NAVAL AIR SYSTEMS COMMAND HQ
DEPT OF THE NAVY
ATTN R. E. DAVIS
ATTN H. P. FLEMING
WASHINGTON, DC 20361

COMMANDER
NAVAL OCEAN SYSTEMS CENTER
ATTN RESEARCH & TECH OFFICE
ATTN W. F. MOLER (2 COPIES)
SAN DIEGO, CA 92152

DIRECTOR
NAVAL RESEARCH LABORATORY
ATTN 2600, TECHNICAL INFO DIV
ATTN H. L. HUGHES
WASHINGTON, DC 20375

COMMANDER
NAVAL SEA SYSTEMS COMMAND HQ
DEPT OF THE NAVY
ATTN R. E. BOWSER
WASHINGTON, DC 20362

COMMANDER
NAVAL SURFACE WEAPONS CENTER
ATTN DX-21, LIBRARY DIV
DAHLGREN, VA 22448

COMMANDER
NAVAL SURFACE WEAPONS CENTER
ATTN WA-50, NUCLEAR WEAPONS
EFFECTS DIV
ATTN WA-51, ELECTROMAGNETIC PULSE
TECHNOLOGY BR
ATTN WX-40, TECHNICAL LIB
ATTN F-32, D. C. KOURY
WHITE OAK, MD 20910

COMMANDER OFFICER
NAVAL WEAPONS EVALUATION FACILITY
KIRTLAND AIR FORCE BASE
ATTN R. CARROLL
ALBUQUERQUE, NM 87117

COMMANDER
NAVAL ELECTRONIC SYSTEMS COMMAND
2511 JEFFERSON DAVIS HIGHWAY
ATTN G. BRUNHART
ATTN B. KRUGER
ATTN F. D. RICHARDSON
ARLINGTON, VA 20360

ASSISTANT SECRETARY OF THE AIR FORCE
(RESEARCH & DEVELOPMENT)
WASHINGTON, DC 20330

SAMSO
P.O. BOX 92960
WORLDWAY POSTAL CENTER
ATTN YAS, SURVIVABILITY OFC
ATTN P. STADLER
LOS ANGELES, CA 90009

COMMANDER
HQ STRATEGIC AIR COMMAND
ATTN XPFS, R. E. LEWIS
ATTN LT COL B. STEPHAN
OFFUTT AFB, NE 68113

COMMANDER
AF WEAPONS LAB, AFSC
ATTN EL, ELECTRONICS DIV, J. DARRAH, (3 COPIES)
ATTN EL, B. SINGARAJU
ATTN DYVM, C. ASHLEY (2 COPIES)
ATTN NSR, G. FIRSTENBURG
ATTN NXS, W. BRUMMER
ATTN B. CIKOTAS
KIRTLAND AFB, NM 87117

AEROSPACE CORPORATION
2350 E. EL SEGUNDO BLVD
ATTN S. P. BOWER
ATTN I. M. GARUNKEL
EL SEGUNDO, CA 90245

DISTRIBUTION (Cont'd)

ANALYTICAL SYSTEMS ENGINEERING CORP
OLD CONCORD ROAD
ATTN RAYNA LEE NORSTER, LIBRARIAN
BURLINGTON, MA 01803

BDM CORPORATION
P.O. BOX 9274
ATTN D. ALEXANDER
ATTN R. L. HUTCHINS
ATTN J. J. SCHWARZ
ALBUQUERQUE, NM 87119

BDM CORPORATION
7915 JONES BRANCH DRIVE
ATTN TECH LIBRARY (2 COPIES)
MCLEAN, VA 22102

BOEING CO
P.O. BOX 3707
ATTN R. CARNEY
ATTN D. N. EGELKROUT, M/S 2R-00
ATTN TECH LIBRARY
SEATTLE, WA 98124

BOOZ-ALLEN & HAMILTON, INC
4330 EAST WEST HIGHWAY
ATTN D. L. DURGIN
BETHESDA, MD 20014

BOOZ-ALLEN & HAMILTON, INC
106 APPLE STREET
ATTN R. J. CHRISNER
TINTON FALLS, NJ 07724

EG&G/KIRTLAND
P.O. BOX 4339
ATTN TECH LIBRARY
ALBUQUERQUE, NM 87196

ELECTRO-MAGNETIC APPLICATIONS, INC.
P.O. BOX 8482
ATTN D. E. MEREWETHER
ALBUQUERQUE, NM 87198

GENERAL ELECTRIC COMPANY
SPACE DIVISION
VALLEYFORGE SPACE CENTER
P.O. BOX 8555
ATTN H. B. O'DONNELL
ATTN J. C. PEDEN
ATTN TECH LIBRARY
PHILADELPHIA, PA 19101

GENERAL ELECTRIC CO.-TEMPO
816 STATE STREET (PO DRAWER QQ)
ATTN R. E. CRONK
ATTN DASIAC
SANTA BARBARA, CA 93102

GTE SYLVANIA, INC
COMMUNICATIONS SYSTEMS DIVISION
189 B. STREET
ATTN D. BLOOD
ATTN R. PERILLI
ATTN D. H. RICE
ATTN E. MOTCHOK
NEEDHAM, MA 02194

HARRIS CORPORATION
SEMICONDUCTOR PROGRAMS DIVISION
P.O. BOX 37
ATTN TECH LIBRARY
MELBOURNE, FL 32901

HUGHES AIRCRAFT CO
CENTINELA & TEALE STREETS
ATTN D. BINDER
ATTN TECH LIBRARY
CULVER CITY, CA 90230

IIT RESEARCH INSTITUTE
10 WEST 35TH STREET
ATTN J. E. BRIDGES
ATTN J. J. KRSTANSKY
ATTN I. N. MINDEL
CHICAGO, IL 60616

INTEL CORPORATION
3065 BOWERS AVENUE
MAIL STOP 1-156
ATTN R. N. NOYCE
SANTA CLARA, CA 95051

IRT CORPORATION
P.O. BOX 81087
ATTN A. H. KALMA
ATTN J. A. RUTHERFORD
ATTN TECH LIBRARY
SAN DIEGO, CA 92138

ITT AVIONICS
390 WASHINGTON AVENUE
ATTN J. TANNER
NUTLEY, NJ 07110

JAYCOR
1401 CAMINO DEL MAR
ATTN R. E. LEADON
ATTN E. P. WEENAS
ATTN A. J. WOODS
DEL MAR, CA 92014

KAMAN SCIENCES CORPORATION
P.O. BOX 7463
ATTN J. LUBELL
ATTN W. STARK
ATTN R. THOMAS
COLORADO SPRINGS, CO 80933

DISTRIBUTION (Cont'd)

LAWRENCE LIVERMORE NATIONAL LABORATORY
P.O. BOX 808
ATTN H. CABAYAN
ATTN L. C. MARTIN
ATTN E. K. MILLER
ATTN R. WAGNER, JR.
LIVERMORE, CA 94550

LITTON SYSTEMS, INC
GUIDANCE & CONTROL SYSTEMS DIV
5500 CANOGA AVENUE
ATTN TECH LIBRARY
WOODLAND HILLS, CA 91364

LOCKHEED MISSILES & SPACE COMPANY, INC
PALO ALTO RESEARCH LABORATORY
3251 HANOVER ST
ATTN TECH LIBRARY
PALO ALTO, CA 94304

MAGNAVOX GOVT & INDUS ELECTRONICS CO
1313 PRODUCTION ROAD
ATTN L. W. RICKETTS
FORT WAYNE, IN 46808

MARTIN MARIETTA CORP
ORLANDO DIVISION
P.O. BOX 5837
ATTN G. FREYER
ATTN R. A. KIRCHOFER
ATTN C. D. WHITESCARVER
ORLANDO, FL 32855

MCDONNELL DOUGLAS CORP
5301 BOLSA AVENUE
ATTN G. R. REYNOLDS
ATTN G. L. WEINSTOCK
HUNTINGTON BEACH, CA 92647

MISSION RESEARCH CORP--SAN DIEGO
P.O. BOX 1209
ATTN V. VANLINT
LA JOLLA, CA 92038

MISSION RESEARCH CORPORATION
P.O. DRAWER 719
ATTN C. LONGMIRE
SANTA BARBARA, CA 93102

MISSION RESEARCH CORPORATION
1400 SAN MATEO BLVD, SE
ATTN A. CHODOROW
ALBUQUERQUE, NM 87108

MITRE CORPORATION
P.O. BOX 208
ATTN G. KRANTWEISS
BEDFORD, MA 01730

NATIONAL SEMICONDUCTOR CORPORATION
2900 SEMICONDUCTOR DRIVE
ATTN TECH LIBRARY
SANTA CLARA, CA 95051

NORTHROP CORPORATION
NORTHROP RESEARCH & TECHNOLOGY CENTER
1 RESEARCH PARK
ATTN TECH LIBRARY
PALOS VERDES PENINSULA, CA 90274

PALMER-SMITH CORPORATION
418 PACIFIC AVENUE
ATTN H. P. SMITH
PIEDMONT, CA 94611

R&D ASSOCIATES
P.O. BOX 9695
ATTN B. P. GAGE
ATTN W. GRAHAM
ATTN W. KARZAS
ATTN J. D. PENAR
ATTN S. C. ROGERS
MARINA DEL REY, CA 90291

R&D ASSOCIATES
1401 WILSON BLVD
SUITE 500
ATTN J. BOMBARDT
ARLINGTON, VA 22209

RAYTHEON COMPANY
MISSILE SYSTEMS DIVISION
HARTWELL ROAD
ATTN G. H. JOSHI
BEDFORD, MA 01730

ROCKWELL INTERNATIONAL CORPORATION
P.O. BOX 3105
ATTN G. E. MORGAN
ATTN D. A. STILL
ANAHEIM, CA 92803

SANDIA NATIONAL LABORATORIES
P.O. BOX 5800
ATTN R. J. CHAFFIN
ATTN B. L. GREGORY
ATTN C. N. VITTITOE
ALBUQUERQUE, NM 87185

SCIENCE APPLICATIONS, INC.
RADIATION AND ELECTROMAGNETIC DIVISION
P.O. BOX 1303
ATTN B. L. BEERS
MCLEAN, VA 22102

STANFORD RESEARCH INSTITUTE
3980 EL CAMINO REAL
ATTN E. F. VANCE
ATTN A. L. WHITSON
PALO ALTO, CA 94306

DISTRIBUTION (Cont'd)

TELEDYNE BROWN ENGINEERING
CUMMINGS RESEARCH PARK
ATTN J. M. MCSWAIN
HUNTSVILLE, AL 35807

TEXAS INSTRUMENTS, INC
P.O. BOX 6015
ATTN W. SLAUSON
DALLAS, TX 75265

TRW DEFENSE & SPACE SYSTEMS GROUP
P.O. BOX 1310
ATTN R. A. KITTER
ATTN TECH LIBRARY
SAN BERNARDINO, CA 92402

TRW DEFENSE & SPACE SYSTEMS GROUP
ONE SPACE PARK
ATTN P. CHIVINGTON
ATTN C. W. LEAR
ATTN W. H. ROWAN
ATTN TECH LIBRARY
REDONDO BEACH, CA 90278

WESTINGHOUSE ELECTRIC CORPORATION
DEFENSE AND ELECTRONIC SYSTEMS CTR
P.O. BOX 1693
BALTIMORE-WASHINGTON INTL AIRPORT
ATTN D. E. JOHNSON
BALTIMORE, MD 21203

AUBURN UNIVERSITY
PHYSICS DEPT
ATTN P. BUDENSTEIN
AUBURN, AL 35830

CLARKSON COLLEGE OF TECHNOLOGY
ATTN H. DOMINGOS
POTSDAM, NY 13676

GEORGIA INSTITUTE OF TECHNOLOGY
ENGINEERING EXPERIMENT STATION
ATTN J. A. WOODY
ATLANTA, GA 30332

PURDUE UNIVERSITY
ATTN G. W. NEUDECK
WEST LAFAYETTE, IN 47907

US ARMY ELECTRONICS RESEARCH
& DEVELOPMENT COMMAND
ATTN TECHNICAL DIRECTOR, DRDEL-CT

HARRY DIAMOND LABORATORIES
ATTN CO/TD/TSO/DIVISION DIRECTORS
ATTN RECORD COPY, 81200
ATTN HDL LIBRARY, 81100 (3 COPIES)
ATTN HDL LIBRARY, 81100 (WOODBRIDGE)
ATTN TECHNICAL REPORTS BRANCH, 81300
ATTN CHAIRMAN, EDITORIAL COMMITTEE
ATTN LEGAL OFFICE, 97000
ATTN CHIEF, 21000
ATTN CHIEF, 21100
ATTN CHIEF, 21200
ATTN CHIEF, 21300 (2 COPIES)
ATTN CHIEF, 21400
ATTN CHIEF, 21500 (2 COPIES)
ATTN CHIEF, 22000
ATTN CHIEF, 22100
ATTN CHIEF, 22300 (2 COPIES)
ATTN CHIEF, 22800
ATTN CHIEF, 22900
ATTN CHIEF, 20240
ATTN BALICKI, F., 20240
ATTN CORRIGAN, J., 20240
ATTN BASSETT, D., 21100
ATTN FAZI, C., 21100
ATTN GAUL, E., 21100
ATTN MILETTA, J., 21100
ATTN WARD, A., 21100
ATTN MAK, T., 21300
ATTN VRABEL, M., 21300
ATTN BEILFUSS, J., 21400
ATTN DAVIS, D., 22100
ATTN LEPOER, K., 22100
ATTN POLIMADEI, R., 22100
ATTN VALLIN, J., 22100
ATTN KLEBERS, J., 22300
ATTN EISEN, H., 22800
ATTN MCGARRITY, J., 22800
ATTN SCHALLHORN, D., 22900
ATTN SEBOL, E., 36200
ATTN MCLEAN, F., 22800
ATTN ROFFMAN, G., 11400
ATTN KALAB, B., 21400 (12 COPIES)

END

DATE
FILMED

3-81

DTIC